NTNU

Norwegian University of
Science and Technology

Stability of Synchronous Generators

Stability analysis of synchronous generators
connected to rectifiers

Jarle Kirkeluten

Master of Energy Use and Energy Planning
Submission date: June 2016
Supervisor: Trond Toftevaag, ELKRAFT

Norwegian University of Science and Technology
Department of Electric Power Engineering

Problem Description

This master's thesis examines stability problems related to a synchronous generator connected to a rectifier. This kind of power systems has been addressed with instability problems in different papers and reports but the cause of this instability is not well explained.

Unstable operation in a diesel-electric propulsion system on a tugboat is the reason why this problem is examined at NTNU. The diesel-electric system in question is loaded through a diode-bridge rectifier and instability is observed in the system during normal operation. The present thesis constitutes a continuation of a master's thesis (2015) and two specialization projects (2014, 2015) at NTNU.

The scope of work for the master's thesis is:

- Study the literature related to these kinds of instability problems.
- Establish models for the unstable system in proper simulation tool.
- Further investigate the instability problem of the system.
- Analyze how the damping of the generators influences the observed instability.
- Analyze the influence of the type and control of the rectifier.
- If time permits, investigate whether introduction of a PSS might contribute to enhanced system damping or not.

The results should yield a conclusion to why the instability problem arises in the system and how it is possible to make the system stable during operation.

Project time-period: January-June 2016

Supervisor: Trond Toftevaag

Preface

This master's thesis marks the end of my 2-year master's degree in "Energy Use and Energy Planning" with "Energy Supply" as orientation at the Norwegian University of Science and Technology in Trondheim. It also marks the end of a total six-year education in engineering. It has been a challenging but also quite amusing ride where I have met many great people, gotten a lot of great memories and learned very much.

I hope the readers of this master's thesis find the problem and findings interesting. It has been a challenging task with a fair amount of frustration related to the simulation programs and some extremely happy moments when things sometimes finally did work out.

I want to thank my supervisor, Trond Toftevaag for guidance and always having time for questions in a busy schedule.

In addition, a huge thanks to my family and friends for support, motivation and getting my mind onto something else when it all has felt difficult. Most important of all the people around me, Ingvild. You have always been there supporting me through ups and downs during my master's degree, I'm forever grateful for that.

Jarle Kirkeluten

Oslo, June 2016

Abstract

This master's thesis constitutes a continuation of a master's thesis (2015) and two specialization projects (2014, 2015) at NTNU. The basis for the work presented in this thesis is an islanded power system onboard a tug-boat. This is a power system where the load is supplied through a rectifier / inverter. This design is used in order to allow the diesel engine in the system operate at an optimum speed at any given time. The power system is experienced to be unstable during normal operation. The instability is reflected in oscillations in the output power, voltages and speed. The cause of the instability is not yet found and the literature regarding these kinds of problems does not yield any defined answers to why instability occurs in such systems.

The thesis presents two models, one in PSCAD and one in DigSILENT Powerfactory. Both models are able to recreate the instability problem. Based on literature and previous work, it is believed that the oscillations can be related to a poorly damped synchronous generator. Investigation of the inertia constant of the synchronous generator supports this theory. It is further tried to enhance the damping by installing an additional damper winding on the rotor which also yields a positive result. Based on these findings is it plausible to connect the cause of the instability problem to the synchronous generator and its poorly damping.

The constant switching caused by the diode rectifier in the system is observed to be a factor that might contribute to amplify the instability problem. The synchronous generator is operating in the transient state due to these small disturbances by the rectifier. This theory is also supported by literature found about the problem. It was tested to change the rectifier from a diode rectifier to a thyristor rectifier, this was found to not enhance the stability of the system. By reducing the DC voltage at the DC terminal of the thyristor rectifier in addition to reduce the gain of the AVR is it possible to make the system stable.

A PSS is also introduced to the system in an attempt to provide an additional damping torque to the synchronous generator during this transient state of operation. The result of these simulations has not provided any satisfactory result. Whether this is because of poorly chosen parameters of the PSS or because of other factors is not known. The time did not allow for any further investigation of this solution.

Sammendrag

Denne masteroppgaven er en videreføring av en masteroppgave (2015) og to fordypningsprosjekter (2014, 2015) ved NTNU. Grunnlaget for arbeidet som presenteres i denne avhandlingen er et isolert kraftsystem ombord i en slepebåt. Dette er et kraftsystem hvor lasten blir forsynt gjennom en likeretter/vekselretter. Grunnen for denne designen av systemet er for å kunne la dieselmotoren i systemet operere på et optimalt turtall på ethvert tidspunkt. Kraftsystemet oppleves å være ustabilt under normal drift. Ustabiliteten er reflektert i svingninger i den aktive effekten, spenningen og hastigheten til synkrongeneratoren. Årsaken til ustabilitet er ennå ikke funnet, og litteraturen som omhandler denne typen problemer gir ikke noen definerte gode svar på hvorfor ustabilitet er observert i denne typen kraftsystemer.

Avhandlingen presenterer to modeller, en i PSCAD og en i DigSILENT Powerfactory. Begge modellene er i stand til å gjenskape den observerte ustabiliteten som er funnet i systemet. Basert på litteraturen som er funnet og tidligere arbeid er det antatt at svingningene kan være relatert til en dårlig dempet synkrongenerator. Undersøkelse av treghetskonstanten til synkrongeneratoren understøtter denne teorien. Det er videre forsøkt å forbedre dempningen ved å installere en dempervikling på rotoren til synkrongeneratoren. Dette gir også et positivt resultat for å forbedre stabiliteten i systemet. Basert på disse funnene er det sannsynlig å koble årsaken til ustabilitetsproblemet til synkrongeneratoren og dens dårlige demping.

Den stadige forstyrrelsen i systemet på grunn av diodelikeretteren er observert å være en faktor som kan bidra til å forsterke stabilitetsproblemet. Synkrongeneratoren observeres å operere i en transient driftstilstand på grunn av disse små forstyrrelser fra likeretteren. Denne teorien støttes også av litteratur funnet om problemet. Det utført simuleringer av stabiliteten ved å skifte likeretteren fra en diodelikeretter til en tyristorlikeretter basert på observert forbedring av stabiliteten ombord på Slepebåten. Simuleringene viser at å kun skifte likeretter forbedrer ikke stabiliteten i systemet. Ved å redusere DC-spenning på DC-terminalen av tyristorlikeretteren i tillegg til å redusere forsterkningen i spenningsregulatoren er det mulig å gjøre systemet permanent stabilt.

En dempetilsats er også testet på systemet i et forsøk på å gi en ekstra demping til synkrongeneratoren i løpet av den transiente driftstilstanden. Resultatet av disse simuleringene har ikke gitt noen tilfredsstillende resultat. Hvorvidt dette er på grunn av dårlig valgte parametere av dempetilsatsen eller på grunn av andre faktorer er ikke kjent. Tiden tillot ikke videre undersøkelser av denne løsningen.

Content

1 Introduction 1

1.1 Objective 1

1.2 Scope of Work 1

1.3 Limitations 1

1.4 Simplifications and Assumptions 2

1.5 Software 2

1.6 Report Structure 3

2 System Description 4

2.1 System topology 4

2.2 Problem 5

2.3 Measurements 5

3 Summary of previous work at NTNU 10

3.1 Specialization project (2015) 10

3.2 Specialization project (2014) 11

3.3 Master's thesis (2015) 11

4 Theory 12

5 Basic theory 15

5.1 Synchronous generators 15

5.2 Power electronics 18

5.3 PSS 22

5.4 Modal analysis 24

6 Simulations in PSCAD 26

6.1 Description of the model 26

6.2 Increasing the load 30

6.3 Increasing the load with a battery connected 32

6.4 Inertia constant 36

6.5 Q-axis damper winding 41

6.6 Changing the synchronous generator parameters 42

6.7 Transient disturbances 43

7 Simulations in DigSILENT PowerFactory 44

7.1 Description of the model 44

7.2 Loading of the synchronous generator 48

7.3 Impact of AVR 49

7.4 Impact of rectifier 51
7.5 Power System Stabilizer 56
8 Discussion 59
9 Conclusion 61
10 Further work 62
11 Bibliography 63
12 Appendices 65
12.1 Appendix A 65
12.2 Appendix B 66
12.3 Appendix C 67
12.4 Appendix D 69
12.5 Appendix E 70
12.6 Appendix F 73
12.7 Appendix G 74
12.8 Appendix H 77
12.9 Appendix I 78
12.10 Appendix J 81
12.11 Appendix K 83

Figures:

Figure 1: One-line diagram of the diesel-electric system [1] 4
Figure 2: Measurements of the RMS voltage, current and the excitation voltage at engine speed = 750 RPM and AVR gain = 40 for the 1940 kVA synchronous generator (G1) and the 3333 kVA synchronous generator (G2) [3]. 6
Figure 3: Measurements of the RMS voltage, current and the excitation voltage at engine speed = 750 RPM and AVR gain = 1 for the 1940 kVA synchronous generator (G1) and the 3333 kVA synchronous generator (G2) [3]. 7
Figure 4: Measurements of the RMS voltage, current and the excitation voltage at engine speed = 1000 RPM and AVR gain = 40 for the 1940 kVA synchronous generator (G1) and the 3333 kVA synchronous generator (G2) [3]. 8
Figure 5: Voltage U, the current from the synchronous generator, I, the speed of the synchronous generator, and the current through the rectifier, Ig. Time steps of 0.1 seconds [6]. 12
Figure 6: Synchronous generator design A) round rotor. B) Salient rotor [8] 15
Figure 7: DC excitation of a synchronous generator [10] 16
Figure 8:Brushless excitation of a synchronous generator [10] 17
Figure 9: a) Diode, b) I-V characteristic, c) Idealized characteristic [11] 18
Figure 10: Three-phase, full-bridge rectifier [11] 18
Figure 11: The Ac voltages and the DC voltage for the diode rectifier [11] 19
Figure 12: a) Thyristor diagram, b) I-V characteristic for the thyristor [11] 20
Figure 13: Full-bridge, thyristor rectifier [11] 20
Figure 14: Waveforms for the thyristor rectifier 21
Figure 15: Common used structure in a PSS [12] 23
Figure 16: Effect of damping ratio on oscillatory modes [15] 25
Figure 17: Simulation model in PSCAD 26
Figure 18: Prime mower and governor 27
Figure 19: Initial condition of the system supplying a load of ca. 1 MW. Voltage at AC side of rectifier, voltage at DC side of rectifier, exciter voltage, active power from the synchronous generator and the speed of the synchronous generator. 28
Figure 20:Detailed plot of the oscillation in the active power from the generator 28
Figure 21: Switching frequency of the full-bridge diode rectifier 29
Figure 22: Synchronous generator supplying a load of 1 MW through a rectifier and no battery connected. Voltage at AC side of rectifier, voltage at DC side of rectifier, exciter voltage, active power from the synchronous generator and the speed of the synchronous generator. 30
Figure 23: Synchronous generator supplying a load of 1.9 MW through a rectifier and no battery connected. Voltage at AC side of rectifier, voltage at DC side of rectifier, exciter voltage, active power from the synchronous generator and the speed of the synchronous generator. 31
Figure 24: PSCAD model with a battery connected to the DC side of the rectifier. 32
Figure 25: Synchronous generator supplying a load of 1 MW through a rectifier and a battery connected. Voltage at AC side of rectifier, voltage at DC side of rectifier, exciter voltage, active power from the synchronous generator and the speed of the synchronous generator. 33
Figure 26: Synchronous generator supplying a load of 1.9 MW through a rectifier and a battery connected. Voltage at AC side of rectifier, voltage at DC side of rectifier, exciter voltage, active power from the synchronous generator and the speed of the synchronous 34

Figure 27:Synchronous generator supplying a load of 1 MW through with H = 0.1 s. Voltage at AC side of rectifier, voltage at DC side of rectifier, exciter voltage, active power from the synchronous generator and the speed of the synchronous generator. 37
Figure 28:Synchronous generator supplying a load of 1 MW through with H = 1 s. Voltage at AC side of rectifier, voltage at DC side of rectifier, exciter voltage, active power from the synchronous generator and the speed of the synchronous generator. 38
Figure 29: Synchronous generator supplying a load of 1 MW through with H = 2 s. Voltage at AC side of rectifier, voltage at DC side of rectifier, exciter voltage, active power from the synchronous generator and the speed of the synchronous generator. 39
Figure 30: Synchronous generator supplying a load of 1 MW through with H = 5 s. Voltage at AC side of rectifier, voltage at DC side of rectifier, exciter voltage, active power from the synchronous generator and the speed of the synchronous generator. 40
Figure 31.Simulation of an extra q-axis damper winding. Voltage at AC side of rectifier, voltage at DC side of rectifier and the exciter voltage, active power from the synchronous generator and the speed of the synchronous generator. 41
Figure 32: Synchronous generator with other internal parameters supplying a load of 1 MW. Voltage at AC side of rectifier, voltage at DC side of rectifier, exciter voltage, active power from the synchronous generator and the speed of the synchronous generator. 42
Figure 33: a) Currents without a rectifier, b) Currents with a rectifier 43
Figure 34: Simulation model in DigSILENT PowerFactory 44
Figure 35: Observed oscillation in the active power from the synchronous generator 45
Figure 36: Eigenvalues for the initial state of the synchronous generator 46
Figure 37: Eigenvalues of the system under different loads 48
Figure 38: Eigenvalues when changing the AVR gain Ka. 49
Figure 39: Active power from the synchronous generator with the AVR gain set to 1 50
Figure 40: Eigenvalues for the system with diode-bridge rectifier and for a system with a thyristor-bridge rectifier 51
Figure 41: Eigenvalues for the system with the DC voltage of the rectifier set to 1 p.u. and 0.5 p.u. . 52
Figure 42: Active power from the synchronous generator with the DC voltage of the thyristor rectifier set to 0.5 p.u. 53
Figure 43: Eigenvalues for the thyristor rectifier with Vdc = 0.5 p.u., Vdc= 1 p.u. and Vdc = 0.5 p.u. and Ka = 20 54
Figure 44: Active power from the synchronous generator with reduced DC voltage of the rectifier. The scale is 5.72*10^(-01), or 0.572 p.u. 54
Figure 45: Currents in the system with the diode rectifier 55
Figure 46: Currents in the system with the thyristor rectifier with the voltage at the DC terminal set to 0.5 p.u. 55
Figure 47: Eigenvalues for the instable system with a PSS added 57
Figure 48: Eigenvalues for the instable system during increase in the washout time constant 57
Figure 49: Effect of changing the PSS gain 58
Figure 50: Block diagram AC1A AVR 65
Figure 51: Synchronous generator supplying a load of 1 MW through a rectifier. Voltage at AC side of rectifier, voltage at DC side of rectifier, exciter voltage, active power from the synchronous generator and the speed of the synchronous generator. 67

Figure 52: Synchronous generator supplying a load of 1.9 MW through a rectifier with a load of 1.9 MW. Voltage at AC side of rectifier, voltage at DC side of rectifier, exciter voltage, active power from the synchronous generator and the speed of the synchronous generator. 68
Figure 53: Synchronous generator supplying a load of 1 MW through a rectifier with a battery connected at the DC terminal.. Voltage at AC side of rectifier, voltage at DC side of rectifier, exciter voltage, active power from the synchronous generator and the speed of the synchronous generator. 69
Figure 54: Synchronous generator supplying a load of 1 MW through a rectifier with H = 0.1 s. Voltage at AC side of rectifier, voltage at DC side of rectifier, exciter voltage, active power from the synchronous generator and the speed of the synchronous generator 70
Figure 55: Synchronous generator supplying a load of 1 MW through a rectifier with H = 1 s. Voltage at AC side of rectifier, voltage at DC side of rectifier, exciter voltage, active power from the synchronous generator and the speed of the synchronous generator 71
Figure 56: Synchronous generator supplying a load of 1 MW through a rectifier with H = 2 s. Voltage at AC side of rectifier, voltage at DC side of rectifier, exciter voltage, active power from the synchronous generator and the speed of the synchronous generator 72
Figure 57: Block diagram for the governor 74
Figure 58: BLock diagram for the PID AVR ESAC8B 75
Figure 59: Block diagram for the power system stabilizer 76
Figure 60: Initial oscillations observed in the Powerfactory model 77
Figure 61: Oscillations with the rectifiers DC voltage reduced to 0.5 p.u. 81
Figure 62: Oscillations with the rectifiers DC voltage reduced to 0.5 p.u. and the AVR gain set to 20 82

Tables:

Table 1: AVR gain test results [3] 8
Table 2:DC loads for the PSCAD model 27
Table 3: Initial eigenvalues of the system 46
Table 4: The changes of the oscillatory eigenvalues when decreasing the gain of the AVR 49
Table 5: Eigenvalues for the system with the diode-bridge rectifier and for the thyristor-bridge rectifier 51
Table 6: Eigenvalue for the system with the DC voltage at the thyristor-bridge rectifier set to 0.5 p.u. 52
Table 7:Eigenvalues for the thyristor rectifier with Vdc = 0.5 p.u. and Ka = 20 54
Table 8: Instable oscillatory eigenvalue used for design of the PSS 56
Table 9: AVR AC1A parameters: 65
Table 10: Diesel engine parameters 66
Table 11: Governor parameters 66
Table 12: New generator parameters 73
Table 13: Diesel governor parameters 74
Table 14: EASC8B AVR parameters 75
Table 15: Initial eigenvalues for the instable system 77
Table 16: Eigenvalues for the system with the AVR gain, Kg, equal to 40 78
Table 17: Eigenvalues for the system with the AVR gain, Kg, equal to 30 78
Table 18: Eigenvalues for the system with the AVR gain, Kg, equal to 20 79

Table 19: Eigenvalues for the system with the AVR gain, Kg, equal to 10 79
Table 20: Eigenvalues for the system with the AVR gain, Kg, equal to 1 80
Table 21: Eigenvalues for the situatuion with the thyristors rectifier voltage equal to 0.5 p.u. 81
Table 22: Eigenvalues for the situatuion with the thyristors rectifier voltage equal to 0.5 p.u. and the AVR gain set to 20 82
Table 23: Eigenvalues for the system without a PSS added 83
Table 24: Eigenvalues for the system with a PSS added 83

1 Introduction

1.1 Objective

The main objective for the work undertaken in this master's thesis is to understand why power systems with a synchronous generator where the load is connected via a rectifier seem to be more likely to become unstable. The problem is addressed in some literature but a defined answer to why this phenomenon with instability in such systems is observed is not found.

1.2 Scope of Work

- Study the literature related to these kinds of instability problems.
- Establish models for the unstable system in a proper simulation tool.
- Further investigate the instability problem of the system.
- Analyze how the damping of the generators influences the observed instability.
- Analyze the influence of the type and control of the rectifier.
- If time permits, investigate whether introduction of a PSS might contribute to enhanced system damping or not.

The results should yield a conclusion to why the instability problem arises in the system and how it is possible to make the system stable during operation.

1.3 Limitations

The real-life system onboard the tugboat where the instability problem is observed is quite large and extensive. The cause of the problem is believed to be related to the interaction between the synchronous generator and the rectifier based on literature and tests conducted on the tugboat. During modelling of the system in this master's thesis only these main components of the system in question is considered. This means that this thesis will try to find the solution to the instability problem on the tugboat through a simplified model rather than model the whole electric system for the tugboat.

1.4 Simplifications and Assumptions

During the modelling of the power system in question some simplifications and assumptions are made:

- In both simulation models, all components are assumed ideal, hence no losses.
- The simulation models are simplified compared to the real-life system and only the main components are included in the simulation models.
- The loads are connected directly to the DC-bus and the inverters are therefore not considered in this study.
- In the simulations where the battery is considered, it is modelled as a small resistance in series with a large capacitor.
- The diesel engine in the real-life system has the opportunity to operate on different speeds according to various load profiles on the tugboat. This means that the frequency of the synchronous generators can vary. In the simulation models all the generators are operating on a fixed frequency.
- The effect of the harmonic components created by the rectifiers is not taken in to account during this study.

1.5 Software

Two different simulation softwares are used in this master's thesis. The first one is "Power System Computer Aided Design", normally abbreviated to PSCAD which is a time-domain simulation tool. PSCAD has a large library of components and systems can easily be built up from scratch. This gives an opportunity to examine the power system in question on a very detailed level. The other simulation tool, DIgSILENT PowerFactory, is a more component-based simulation tool where larger power systems is easier to be examined. It also has some more functions to observe the stability aspect of the simulation model, like eigenvalue analysis.

Matlab is used for root locus plots and this master's thesis is written in Microsoft Word.

1.6 Report Structure

Chapter 2 presents the system which is under study, the instability problem observed in the system and a summary of the tests that is conducted of the system by the company that delivered the automatic voltage regulator.

Chapter 3 presents summaries of the previous work at NTNU in relation to the problem under consideration.

Chapter 4 consists of the basic theory of the components used in the models. This is underlying theory to understand how the components work alone and together.

Chapter 5 is a section dedicated to the theory of instability in islanded systems with generators and rectifiers.

Chapter 6 presents the PSCAD model and the simulations related to:

- Stability with/without battery
- Increase of the inertia constant
- Extra damper windings
- Changing the synchronous generators internal parameters

Chapter 7 presents the DigSILENT Powerfactory model and eigenvalue analysis of the following aspects

- The initial state of the synchronous generator.
- Different load situations.
- Impact of the AVR gain.
- Impact of the rectifier type.
- Effect of a PSS added to the system.

Chapter 8 is a discussion section for the results of the simulations.

Chapter 9 consists of a conclusion and recommendations.

2 System Description

2.1 System topology

The system where the problem disussed in this master's thesis was discovered is a power system onboard a tugboat. Two designs of the system with different ratings of the synchronous generators is used on these types of tugboats. One is operated with synchronous generators with a rated capacity of 1940 kVA and others with synchronous generators with a rated capacity of 3333 kVA. Common to both systems is that there is experienced instability during normal operation.

This is a variable speed diesel-electric power system. The variable speed gives the system the ability to operate at an optimal speed for the diesel engine at all time. The postive sides to having a system with variable speed is that the fuel consumption is reduced and hence, the emittion of greenhouse gases is reduced.

The one-line diagram for the design of the diesel-electric system is shown in Figure 1.

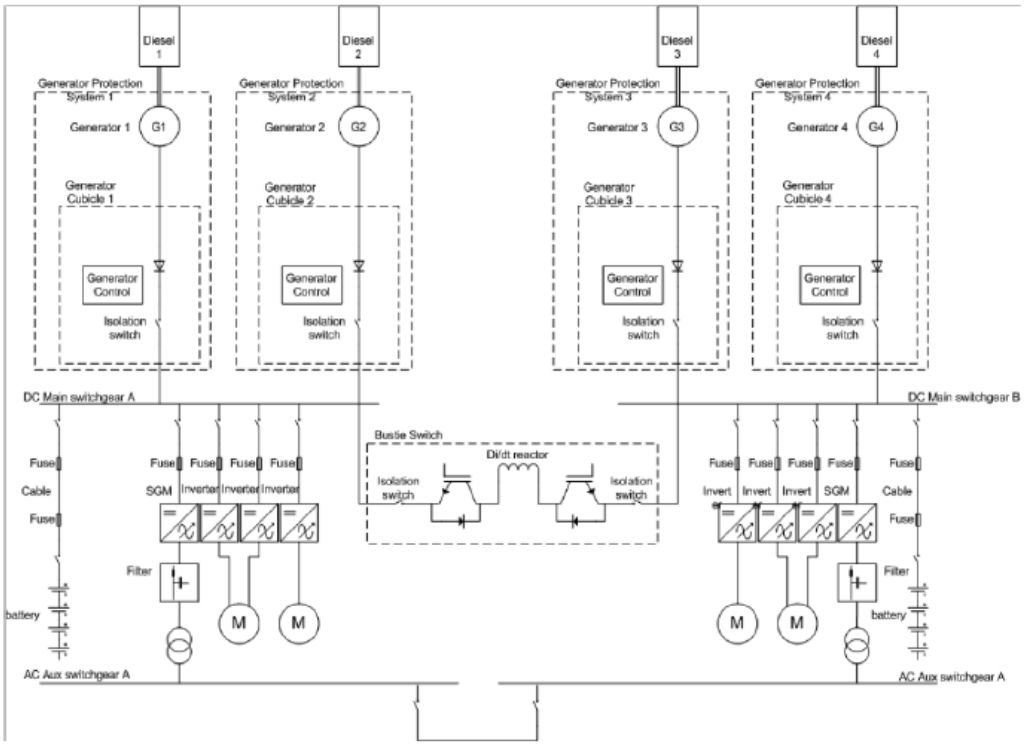

Figure 1: One-line diagram of the diesel-electric system [1]

The prime movers in the system is diesel engines. These are named diesel 1, 2, 3 and 4 in the one-line diagram. The synchronous generators driven by the diesel engines are connected to 6-pulse diode rectifiers which is rectifying the voltage. The following DC-bridge behind the rectifier named DC main A and DC main B in the one-line diagram has batteries connected to

give the system the ability to receive power during short high-demand loads. The batteries also serve as a redundancy security if the system should lose power for a short time. At the end of the DC-bridge an inverter converts the voltage back to a desired amplitude and frequency demanded by the connected loads.

2.2 Problem

The stability problem observed in the system is standing oscillations in the output power, currents and voltages of the synchronous generator. The system therefore has an undesirable operation where the instability is best observed by oscillations in the power supplying the thrusters and other critical loads of the tug-boat. All the instable parameters that is mentioned oscillates around the frequency of 2 Hz and is detected during normal operation. The cause of the instability problem is not detected, but measurements have confirmed the instability problem. The synchronous generators in question has got internal synchronous reactances that are quite large compared to more “normal” values found in other synchronous generators. This is an intentional design to prevent large short-circuit currents from flowing in the system which may cause severe damage to delicate components like the rectifiers and inverters. The large values of the internal synchronous reactances has been mentioned as a possible cause of the observed instability problem [2], in addition to the rectifier, which may also be a contributory factor to the instability.

2.3 Measurements

The supplier of the automatic voltage regulator (AVR) to the synchronous generators has conducted some tests when the instability problem was discovered in August 2014 [3]. The tests were taken at the shipyard where the tug-boats were built. The tests are mainly based on the AVR’s influence on the system instability. During the discussion and presentation of the results from the tests in this chapter, the 1940 kVA synchronous generator will be named G1 and the 3333 kVA synchronous generator will be named G2.

During the test, G1 and G2 were working in parallel with a test load of about 0.5 MW. The battery at the DC-link was not connected during the test. The droop of the generator was set to 10 % and the generator was running at a fixed frequency. The initial PID settings on the AVR were believed to be good enough by the company that delivered the AVR and were used throughout the tests [3].

During the test the sensing voltage transformer (VT) was connected between phase B-C and the voltage ratio of the VT is 690/110 V. The sensing current transformer was connected on

phase B on both of the synchronous generators and the current ratio on the primary side was 1800/1A [3] [1].

The engine is set to run at a speed of 750 RPM and the two generators are supplying the test load of 0.5 MW. The gain of the AVR in this situation is set to Kg = 40. The results are shown in Figure 2 and show the RMS voltage measured by the voltage transformer, the current measured by the current transformer and the direct voltage measured over the exciter.

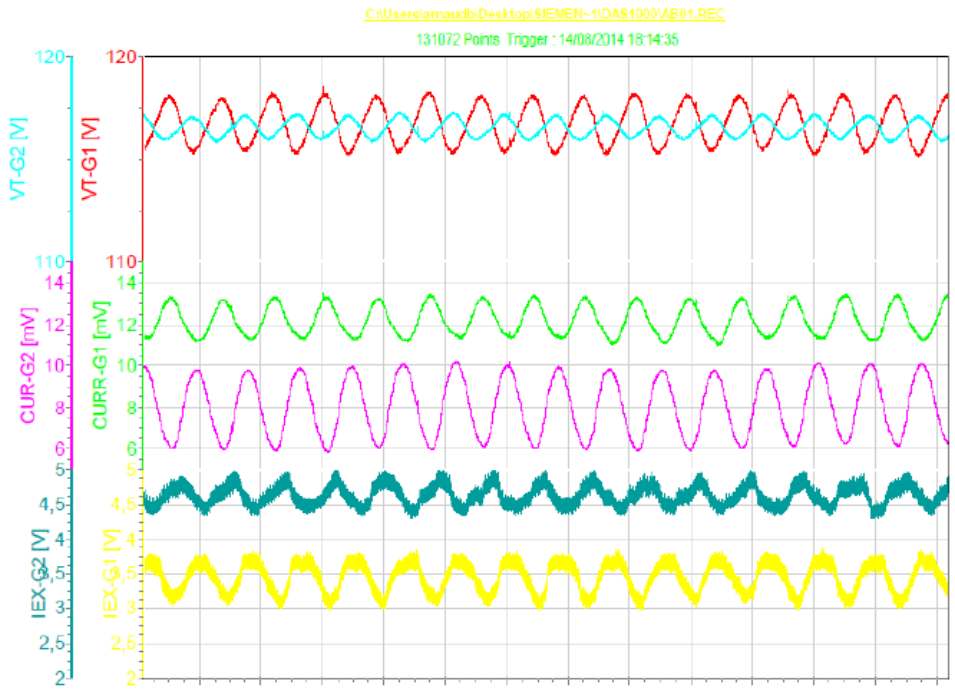

Figure 2: Measurements of the RMS voltage, current and the excitation voltage at engine speed = 750 RPM and AVR gain = 40 for the 1940 kVA synchronous generator (G1) and the 3333 kVA synchronous generator (G2) [3].

Based on the information about the measuring equipment and the measurements presented in the graph can the amplitude of the oscillations be identified. The current of G1 has an amplitude of 3.6A and oscillates around a value of 225A. The current of the G2 has an amplitude of 7.2A and oscillates around value of 144A. The exciter voltage is measured directly where G1 oscillates around a value of 3.4V with an amplitude of 0.75V and the G2 oscillates around a value of 4.6V with an amplitude of 0.6V.

The frequency of the oscillations in the different measured parameters seems to be the same, about 2.5 Hz. It can also be noticed a difference between the two generators, as the amplitude of the oscillations in the voltage is higher for G1 than for G2. The amplitude of the current is larger for G2 than for G1. The amplitude of the exciter voltage is almost the same.

The gain for the AVR is reduced to 1 and the tests are performed again. The results are presented in Figure 3.

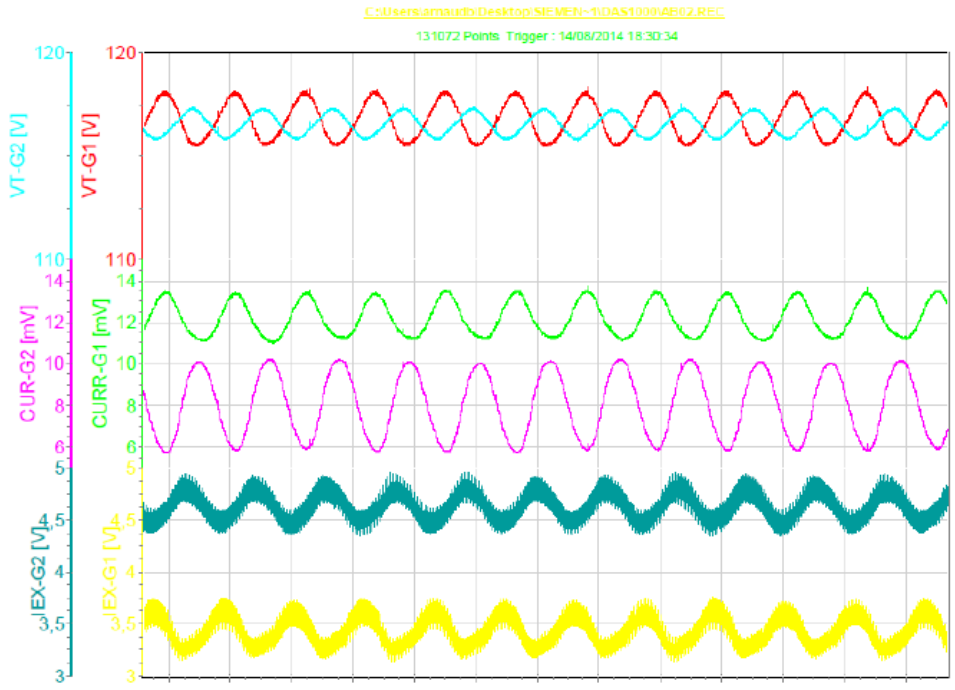

Figure 3: Measurements of the RMS voltage, current and the excitation voltage at engine speed = 750 RPM and AVR gain = 1 for the 1940 kVA synchronous generator (G1) and the 3333 kVA synchronous generator (G2) [3].

The magnitude of the oscillations seems to be somewhat the same as for the situation with the AVR gain set to 40 presented in Figure 2. The main difference is that the frequency of the oscillations is reduced to 1.756 Hz [3].

The speed of the engines is increased to 1000 RPM and the tests for the gain of the AVR's are done again.

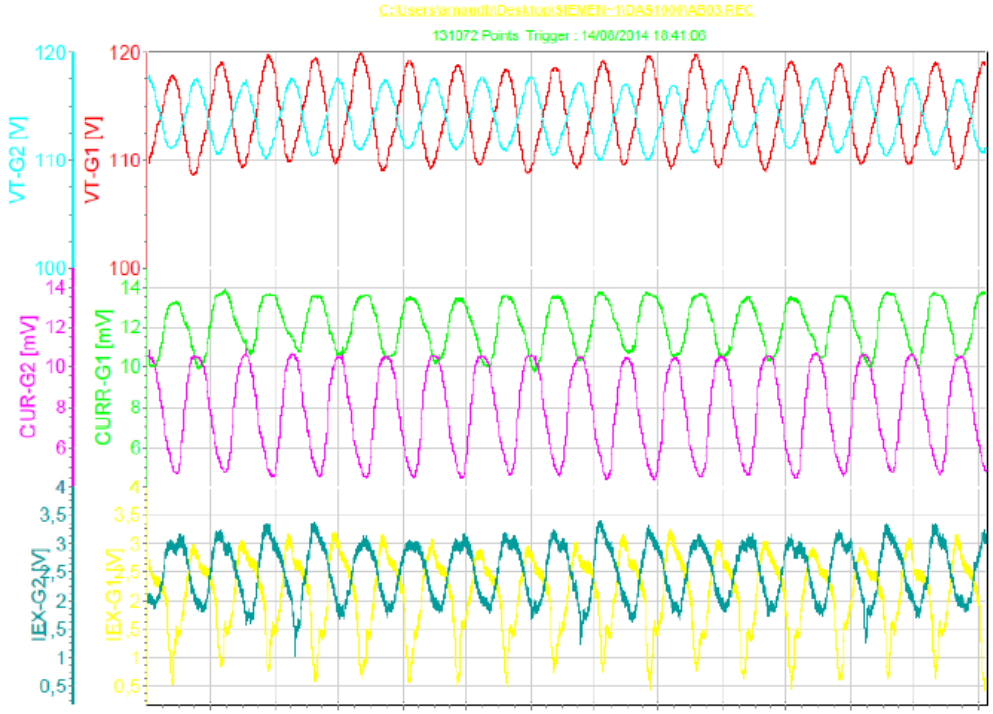

Figure 4: Measurements of the RMS voltage, current and the excitation voltage at engine speed = 1000 RPM and AVR gain = 40 for the 1940 kVA synchronous generator (G1) and the 3333 kVA synchronous generator (G2) [3].

The oscillations are now 2.68 Hz and the oscillations have therefore increased when the speed of the engines was increased. The amplitude of the current in G1 is oscillating around 216A with an amplitude of 5.4A and G2 is oscillating around 144A with an amplitude of 10.8A. The exciter voltage of G1 is oscillating around 2.5V with an amplitude of 2V and the exciter voltage of G1 is oscillating around 2.5V with an amplitude of 1V.

The frequency of the oscillations has increased when the speed of the engine is increased and the amplitude of the oscillations has also increased.

The test for the AVR gain is tested for 5 values between 1 and 40 and presented in Table 1

Table 1: AVR gain test results [3]

	Test A	Test B	Test C	Test D	Test E
AVR Kg (*)	40	30	20	10	1
Oscillation Frequencies in Hertz with Engine at 1000RPM	2.680	2.439	2.049	1.588	1.171
Oscillation Frequencies in Hertz with Engine at 750RPM	2.366	2.221	2.066	1.911	1.756

From the tests it can seem like the frequency of the oscillations can be decreased by decreasing the AVR gain but the amplitude of the oscillations seems to remain quite close to the same value. Decreasing the AVR gain to one is not desirable due to the fact that you want the AVR to react to load changes fast.

Another test is described in [3] where the AVR is disconnected and the field winding of the synchronous generator is supplied by two voltage sources (fixed field current). The tests yielded the same results with the same instability problem.

3 Summary of previous work at NTNU

The problem under study in this master's thesis has been analyzed in different projects at NTNU during the last couple of years. Short summaries from the projects is presented to give an introduction to the work that has already been done and to give the reader a broader understanding of the problem discussed in this thesis.

3.1 Specialization project (2015)

The specialization project at NTNU in 2015 [4] presented two new models in PSCAD to study the observed instability problem for the most instable 1940 kVA synchronous generator. There were some indications that the real-life system was observed to be stable when the rectifier type was changed from a standard diode rectifier with no possibility to control the output voltage, to a thyristor rectifier with a limited possibility to control the output voltage. The first model was operating with a diode rectifier and the other one with a thyristor rectifier in order to see if the system became stable with a different rectifier type. A simple model for the battery at the DC-link with a small resistance in series with a large capacitance was used during the simulations in the specialization project.

The simulations yielded a result were the instability happened at almost every load levels between 0 MW and 1.9 MW with increasing frequency of the oscillations and decreasing amplitude of the oscillations when the load was increased. However, the system was observed to be stable very close to the rated capacity of the synchronous generator of 1.94 MW.

The simulations indicated that the rectifier type had no direct influence on the stability problem. Oscillations was observed in the output power, speed and exciter voltage of the synchronous generator and in the voltages at both sides of the rectifier. The only significant change in the oscillations was found to be a little decrease in the amplitude of the oscillations.

Based on [5], a solution to instability problems in power systems where a synchronous generator is operating together with a rectifier is presented. The solution is to increase the damping of the synchronous generator by installing a short-circuited q-axis damper winding on the rotor and by increasing the resistance in the q-axis of the rotor. This was also the conclusion of the master's thesis from 2015 [2].

It is however brought into question how applicable this solution is to an already existing system since it basically would mean to change the rotor of the instable 1940 kVA synchronous generator.

3.2 Specialization project (2014)

The specialization project undertaken in 2014 by Torunn Husevåg Helland [1] analysed the stability problem with a model in DIgSILENT PowerFactory. The system was simulated both with and without a rectifier for different types of disturbances. Stability analysis during disturbances, load ramping and torque variations was tested. In addition, the stability impact of the voltage regulator (AVR) was studied.

The main findings were that the consumption of reactive power, high values of the linearization constant K5 in the AVR and high values of the internal synchronous reactances faster leads to instability. The introduction of a rectifier did not lead to instability in this study.

3.3 Master's thesis (2015)

The master's thesis from 2015 by Torunn Husevåg Helland [2] was a continuation of the work in the specialization project by the same person from 2014 [1].

A MatLab/Simulink model was the basis for the work in the thesis. It was a simplified model which just studied the interaction between the instable synchronous generators and a diode-bridge rectifier with a battery connected at the DC side of the diode rectifier. An extensive sensitivity analysis of every parameter of the components in the simulation model was undertaken to observe where and at what time the instability occurred.

The introduction of the diode-bridge rectifier is found to be crucial to the instability phenomena. It is also found that the system with the 1940 kVA regain its stability when the synchronous generator was supplying a load close to the maximum power output of 1.94 MW. The sub-transient and transient internal synchronous reactances is also found to be crucial parameters for the instability problem.

In order to make the 1940 kVA asynchronous generator stable it was found that the relationship between the sub-transient q-axis and d-axis reactances should be less than 0.46 and the relationship between the transient q-axis and d-axis reactances should be less than 5.41.

The recommendations from the thesis to fix the stability problem observed in the synchronous generators was to add an additional q-axis damper winding to the rotor of the synchronous generator.

4 Theory

This chapter consists of summaries from the different reports and articles concerning the problem discussed in this master's thesis.

The report in [6] from 1980 investigates the problem with a rectifier-loaded synchronous generator and the observed instability that occur. The report states that it is not only the synchronous reactances that is important in these types of systems, the transient and subtransient reactances is equally important.

Introducing an active load, transient oscillations can occur due to the oscillations caused by the diodes in the rectifier. The current and voltage will start to oscillates with a high frequency and a stable operation is not possible to obtain [6].

A test is shown in the report for a diode-rectified system. The test is shown in Figure 5.

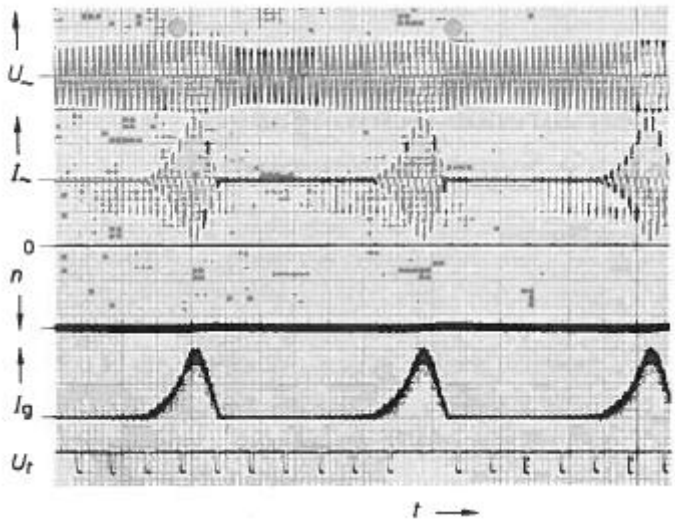

Figure 5: Voltage U, the current from the synchronous generator, I, the speed of the synchronous generator, and the current through the rectifier, Ig. Time steps of 0.1 seconds [6].

When the current trough the rectifier starts to experience an instable operation, the voltage and current from the synchronous generator starts to oscillate. It is shown in this test that the behavior of the rectifier impacts the transient current of the synchronous generator and ultimately making the system have an undesirable operation [6].

A stability criterion is given based on the simulations of the system:

$$X_q < 2 * x'_d \qquad \text{Eq. 1}$$

It is also stated that the oscillations that is observed in the output voltage can be associated with physical oscillations of the rotor angle [6].

In [5] is a synchronous generator connected to a diode-bridge rectifier under study. The aim for this report is to investigate the relationship between the synchronous generator and the rectifier. Other reports tend to look at the synchronous generator as an ideal voltage source under these kinds of investigation and only look at the behavior of the load and the rectifier. When the system is isolated and not working against a stiff grid it is important to analyze the factors that may cause that instability and then the synchronous generator is the key to understand the instability that occur [5].

The work yields a stability criterion equal to the one given in [6], but this stability criterion is believed to be too harsh to meet for conventional generator design and another stability criterion for generators with an additional short-circuited q-axis winding is given in equation 2.

$$\frac{1}{x_q} + \frac{1}{x'_q} \geq \frac{1}{x'_d} \qquad \text{Eq. 2}$$

It is stated that due to the fact that $x'_q < x_q$ for a synchronous generator, the stability criterion given for a synchronous generator with a short circuited q-axis winding is easier to fulfill. The simulations have yielded a result based on this equation that shows that the low-frequency oscillations are no longer present in the system [5].

The observed instability in these kind of systems is often considered to be instable but a good explanation to why this is experienced is not yet given. The work undertaken in [7] aims to find a physical explanation to the experienced instability problem. The basis for the simulations are a simple model for a rectifier-loaded system with just the synchronous generator, a rectifier and a load modelled as a voltage source. The system is linearized and the stability study is based on the movement of the eigenvalues obtained [7].

A parameter analysis is undertaken on a set of different parameters found in the model. A deviation of 10 % on the different parameters is used. It is observed that by increasing the direct-axis damper resistance and the field resistance yields a positive influence on the eigenvalues, i.e. they are moving to the left. Increasing the quadrature-axis damper resistance, and the quadrature inductance, the commutation inductance and the DC inductance has a negative influence on the eigenvalues, i.e. they are moving to the right [7].

An attempt to describe the physical behavior is tried; An increase in a resistive load of a diode-rectified system results in a sudden increase in the quadrature-axis current. As a result, the quadrature-axis flux increases fast due to a relatively small quadrature-axis damper time constant. However, the resulting decrease of the direct-axis flux flows very slowly due to a

relatively large time constant of the excitation winding. After a sudden loading will the total machine flux increase in the first instance and decrease to its initial value, which is lower than its original value afterwards. The conclusion is that all the parameters studied can affect the systems stability problem but the quadrature-axis damper winding resistance is of utmost importance for stable behavior of the system [7].

5 Basic theory

5.1 Synchronous generators

The synchronous generator is the heart of every power system and generates the power. The synchronous generator is built up by a rotor with excitation windings and an armature with three-phase windings. The current induced to the stator windings by the rotor is supplying the load. The rotor is driven by a prime mover which can be for example a diesel engine or a hydro power turbine. During operation, a three-phase voltage is induced into the armature windings by the magnetic field set up by the rotor. The displacement of 120 degrees for the armature windings make it possible to induce three-phase voltages into the armature. The magnitude of the voltage induced to the armature windings is controlled by the excitation current in the excitation windings of the rotor and the frequency is dictated by the rotor speed and number of poles shown by equation 3 [8], [9].

$$Number\ of\ poles = \frac{f * 120}{n} \qquad \text{Eq. 3}$$

Where f is the frequency in Hz and n is the speed of the rotor in rounds per minute.

Based on the design of the synchronous generator, two different rotors are commonly used. Figure 6 shows the basic principle for a synchronous generator with a round rotor and a salient rotor [8], [9].

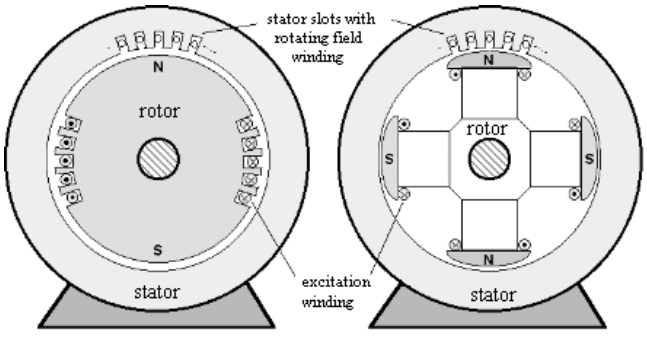

Figure 6: Synchronous generator design A) round rotor. B) Salient rotor [8]

The salient rotor which is mainly used in application where the speed is low has the excitation windings mounted on the salient rotor poles. In addition, an extra short-circuited rotor winding (often called amortisseur winding) is added to help damp mechanical oscillations in the rotor [9]. During normal operation, when the rotor is operating at a synchronous speed

the winding will not carry any current. When the load changes and the speed of the rotor begins to oscillate around the synchronous speed it induces a voltage and a current in the damper windings. The current flowing in the damper windings interacts with the magnetic field of the stator and produces a damping force to the oscillations obtained during the load change [9].

Round rotors are used for high-speed applications where the prime mover often is a gas or steam turbine. The rotor is often small in diameter and long to maintain a stable operation. It has a small number of poles which is implemented into the rotor making it cylindrical [9].

During load changes and different load levels, the ability to control and regulate the excitation current in the rotor and thereby the induced voltage to the stator windings is an important factor. The relationship between the induced voltage to the stator and the excitation current is linearly dependent during no-load situation. The change itself is not enough, the exciter also must respond quick enough during temporary faults or load changes in order to maintain the stability [9].

Different types of excitation system can be used. The first type of exciters were DC-generators which induces a DC-current trough brushes and slip rings to the rotor windings. Figure 7 shows a schematic drawing of a synchronous generator with a DC excitation system. The DC excitation generator is mounted on the same shaft as the rotor of the synchronous generator. The excitation current Ix is supplied to the rotor windings via brushes and slip rings. The excitation current Ix is controlled by the pilot exciter. In newer designs, the excitation current is controlled by an automatic voltage regulator [10], [9].

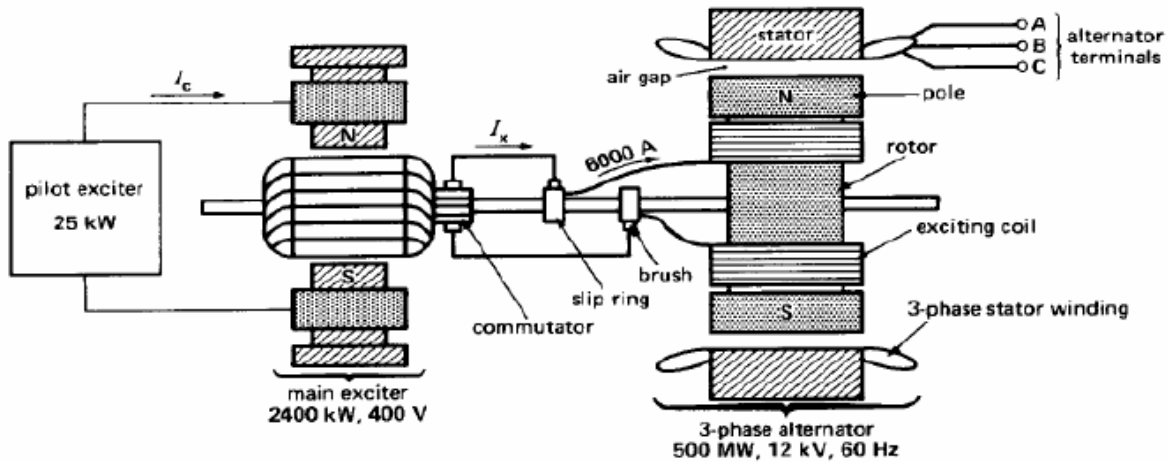

Figure 7: DC excitation of a synchronous generator [10]

At larger power ratings of the synchronous generators it was common to use several cascaded DC exciters in order to be able to provide a large enough excitation current. This increased the complexity of the system and the time constant of the system became larger and based on the wish to be able to respond quick to different load situations it is not desirable to have a "slow" excitation system [9].

The introduction of power electronics made it possible to use AC generators to provide the excitation current to the rotor windings by rectifying the current and supply it through brushes and slip rings.

To avoid the maintance caused by the wear of the brushes and slip rings a brushless excitation system is more and more common today. A brushless excitation system and a synchronous generator is shown in Figure 8.

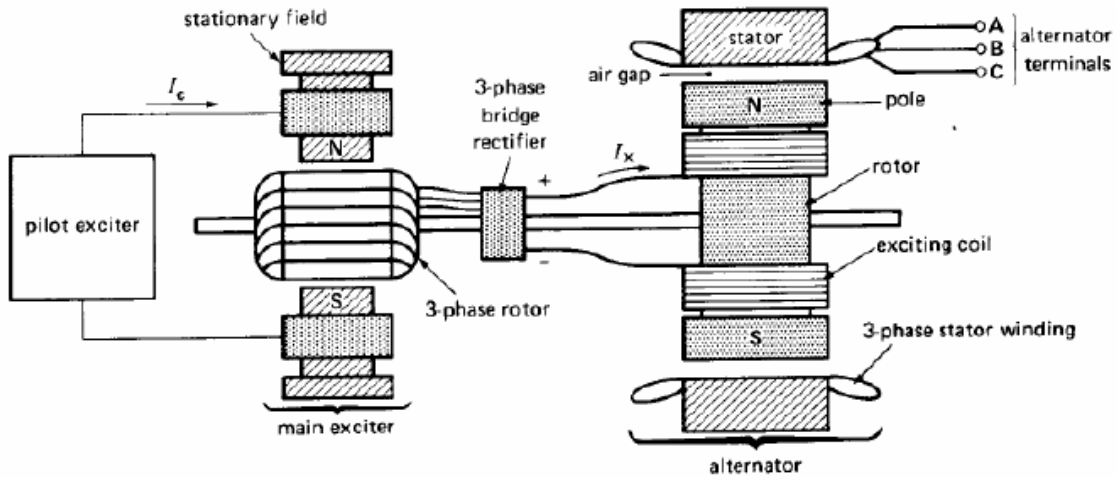

Figure 8:Brushless excitation of a synchronous generator [10]

The rotor of the AC exciter is mounted on the same shaft as the rotor of the synchronous generator in addition to a 3-phase electronic rectifier that provides the DC excitation current to the rotor windings. The rectifier replaces the commutator, brushes and slip rings which makes the system more reliable [9].

The control of the exciter is done by an automatic voltage regulator (AVR). The AVR measures the voltage at the terminals of the synchronous generator. It calculates the voltage error ΔV between the actual voltage provided by the synchronous generator with the desired voltage defined in the AVR. The error signal is then used to regulate the DC voltage from the exciter to the rotor in order to maintain the desired voltage at the terminals of the synchronous generator [9].

5.2 Power electronics

5.2.1 Diode rectifier

The most common rectifier is the diode rectifier. The diode and the characteristics of the diode is shown in Figure 9.

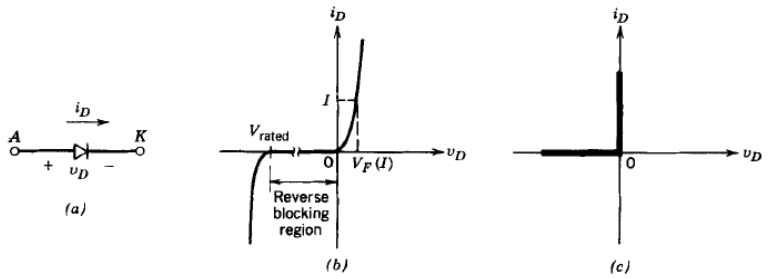

Figure 9: a) Diode, b) I-V characteristic, c) Idealized characteristic [11]

The diode is, if we are looking at it very idealized, a simple on/off switch which is triggered by the voltage across it. When the voltage across the diode is forward biased it begins to conduct. When the voltage across the diode switches and the diode becomes reverse biased it stops to conduct. If a sinusoidal voltage is applied to the diode it will conduct in the positive half-period and block in the negative half-period [11].

By placing the diodes in a bridge as shown in Figure 10 it is possible to rectify three-phase voltages. This is a very simple and low-cost rectifier, but it has the disadvantage that it has no direct control for the amplitude of the DC-side voltage [11].

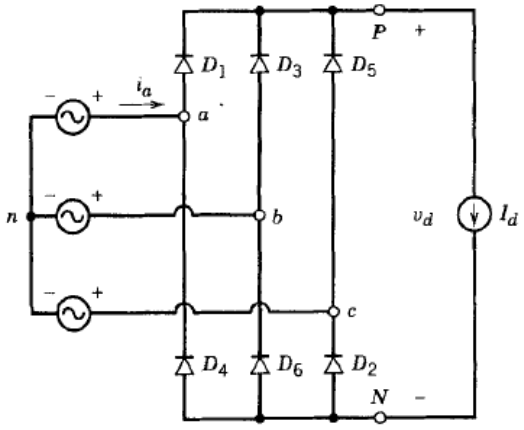

Figure 10: Three-phase, full-bridge rectifier [11]

The diodes in the rectifier will each conduct for a period of 120 degrees. The diode with the highest potential at its anode in the upper part of Figure 10 (D1, D3 or D5) will be forward biased and start to conduct. The other two diodes will then be reversed biased and block the

current flowing through the diode. The corresponding diode in the lower part of Figure 10 (D4, D6 or D2) with the lowest potential at their respective cathode will conduct [11].

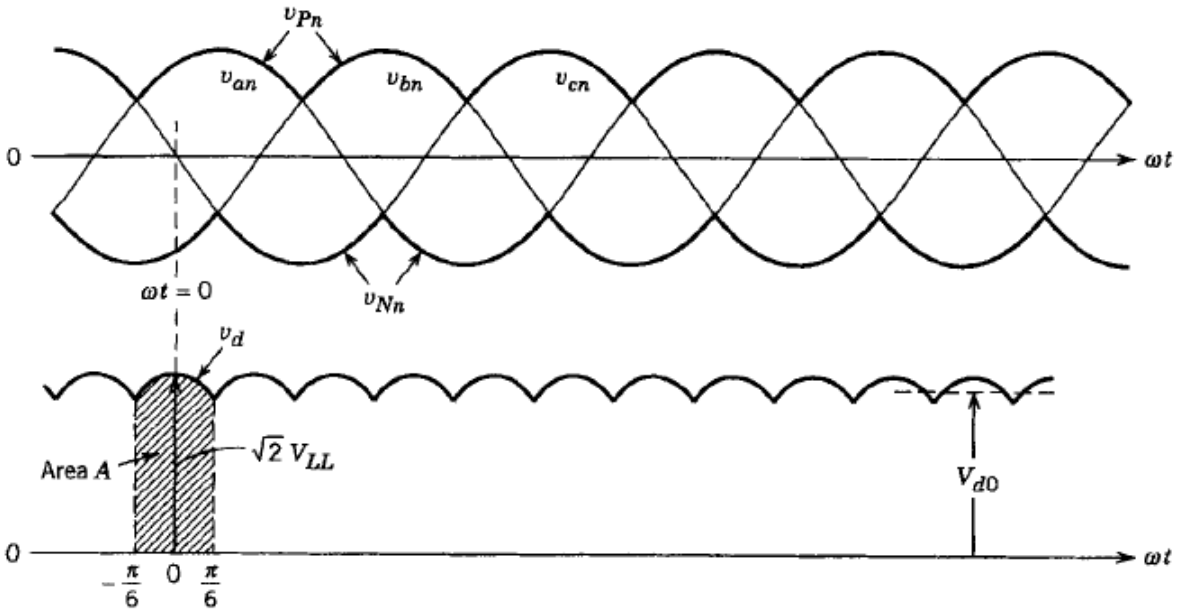

Figure 11: The Ac voltages and the DC voltage for the diode rectifier [11]

Figure 11 shows the AC voltage and the rectified DC voltage, V_d, for the diode rectifier. The instantaneous DC voltage, V_d, is defined as the difference between V_{pn} and and V_{nn} of the AC voltage. Because each diode is conducting for 120 degrees will the instantaneous waveform of V_d consists of six segments per cycle of the line frequency [11].

The average value of the output DC voltage can be obtained by considering one of the six segments which is marked in grey in Figure 11. Considering the line-to-line voltage V_{ab} to be at its maximum at this point yields an instantaneous DC voltage, V_d, given by equation 4 [11]:

$$v_d = v_{ab} = \sqrt{2} * V_{LL} * \cos \omega t \qquad for \ -\tfrac{1}{6}\pi < \omega t < \tfrac{1}{6}\pi \qquad \text{Eq. 4}$$

By integrating the instantaneous voltage, V_d over the area A and dividing by the interval between $-\frac{\pi}{6}$ and $\frac{\pi}{6}$, the average DC output voltage, V_{do}, becomes [11]:

$$V_{do} = \frac{1}{\pi/3} \int_{-\pi/6}^{\pi/6} \sqrt{2} * V_{LL} * \cos \omega t \ d(\omega t) = \frac{3}{\pi} * \sqrt{2} * V_{LL} = 1.35 * V_{LL} \qquad \text{Eq. 5}$$

Equation 5 shows that the average DC output voltage for a basic full-bridge diode rectifier is about 35 % larger than the input line-to-line voltage to the rectifier.

5.2.2 Thyristor rectifier

The thyristor can be considered as a more advanced diode. The thyristor and its I-V characteristic is shown in Figure 12.

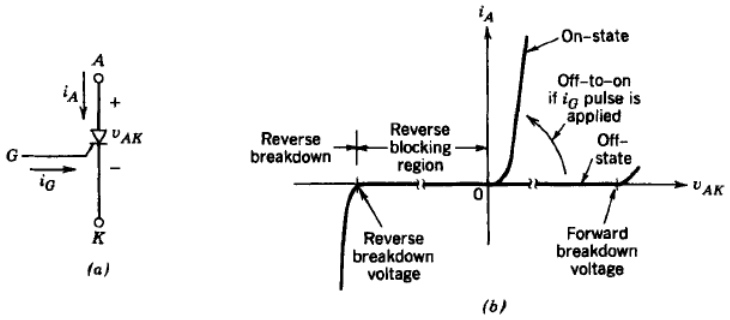

Figure 12: a) Thyristor diagram, b) I-V characteristic for the thyristor [11]

The thyristor is in principle the equal to a diode and the I-V characteristic is almost equal. The difference between the diode and thyristor is that the thyristor will be blocked when forward biased until a trigger signal is enabled at the thyristor gate. When the gate is triggered by a positive signal it goes from off-state to on-state and is conducting until it is reverse-biased [11].

The advantage of the ability to trigger the thyristor at a desired time makes it possible to control the output voltage to a certain extent. It is however not possible to stop the thyristor from conducting when it is already triggered and therefore it has to conduct until it is reverse-biased [11].

For practical applications, six thyristors can be used to create a full-bridge rectifier as shown in Figure 13.

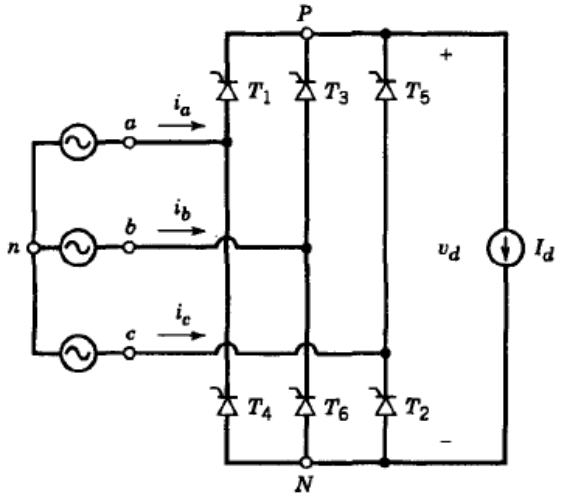

Figure 13: Full-bridge, thyristor rectifier [11]

Based on the fact that the thyristor is in principle a diode, equation 5 is still valid and it follows that the output voltage for the thyristor rectifier when triggered at t=0 is:

$$V_{do} = \frac{3}{\pi} * \sqrt{2} * V_{LL} = 1.35 * V_{LL}$$

When the thyristors is triggered at time different from zero. The effect of the firing angle α is shown in Figure 14.

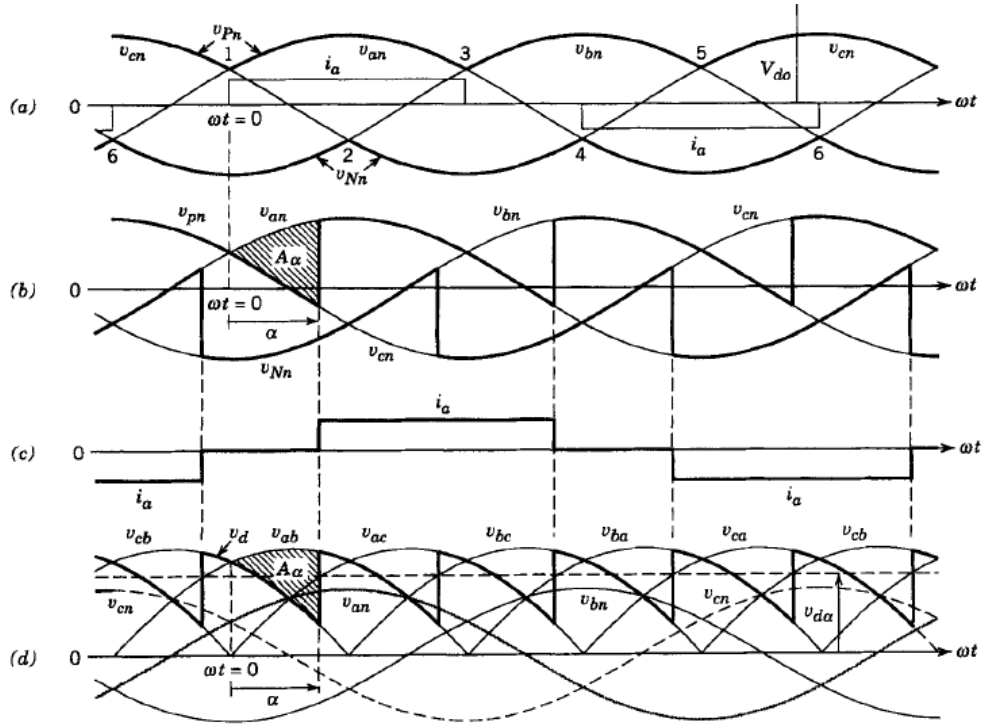

Figure 14: Waveforms for the thyristor rectifier

The average DC voltage can be calculated based on the waveforms in Figure 14 b and d. The volt-second area Aα (every 60 degrees) results in a reduction in the average DC voltage compared to the input AC voltage, this is shown by equation 6 [11].

$$V_{d\alpha} = V_{do} - \frac{A_\alpha}{\pi/3} \qquad \text{Eq. 6}$$

Based on Figure 14 d it can be seen that the area Aα is the integral of Vab-Vcb which is equal to Vac:

$$A_\alpha = \int_0^\alpha \sqrt{2} * V_{LL} \sin \omega t \, d(\omega t) = \sqrt{2} * V_{LL} * (1 - \cos \alpha) \quad \text{Eq. 7}$$

Based on equation 6 and equation 7, the average DC output voltage, $V_{d\alpha}$, for a full-bridge thyristor rectifier is given by equation 8 [11].

$$V_{d\alpha} = \frac{3 * \sqrt{2}}{\pi} * V_{LL} * \cos \alpha = 1.35 * V_{LL} * \cos \alpha \quad \text{Eq. 8}$$

Based on equation 8, it is possible to regulate the voltage at DC side of the thyristor rectifier from 0 to 135 % of VLL by controlling the firing angle α.

5.3 PSS

Back in the 1950s, economic design of the synchronous generators resulted in synchronous generators with large values of the steady-state synchronous reactances, and this again resulted in poor load-voltage characteristics. The result was a transient stability problem addressed to the reduction of the field flux which resulted in a drop in the overall synchronizing torque. The solution to this problem was to use a high gain, fast acting excitation control system. However, voltage regulator action was found to introduce negative damping torque at high power output in weak grids. The negative damping gave rise to oscillatory instability problem. These problems resulted in an attempt to modify the voltage regulator reference input trough an additional signal, which was meant to produce positive damping torque. The control circuit that modified the voltage regulator reference signal was called a power system stabilizer (PSS) [12].

The primary goal of the PSS is to introduce a component of electrical torque in the synchronous machine rotor that is proportional to the deviation between the actual speed and the observed speed. When the rotor oscillates, this torque acts as a damping torque to counter the oscillations [12].

One common used structure of the PSS is shown in Figure 15. The blocks consist of factors that controls the gain, phase compensation, a washout filter, torsional filters when there are speed and frequency inputs and output limiters.

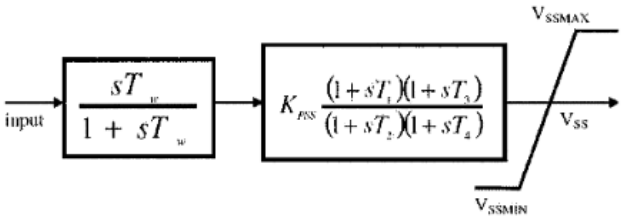

Figure 15: Common used structure in a PSS [12]

The washout circuit is a high-pass filter that prevents any steady change in the speed, frequency and power affecting the field voltage because of the PSS action. The PSS should be design to act just in the transient period of the stabilization signal. For local modes, Tw = 1-2 s is satisfactory. For interarea modes a longer Tw of about 10-20 s is proposed [12], [13].

Phase compensation block is used to counter the phase lag introduced in the transfer functions of the exciter system. In order to achieve pure damping torque from the PSS, the phase compensator blocks must cancel the phase-lag [12].

The phase lag, φ, can be obtained from the eigenvalue which is in interest to stabilize. This is done by finding the angle of the eigenvalue based on the x-axis and the imaginary axis.

When phase shift is found, the filter need to be tuned in order to make the power system stabilizer only compensate at the desired frequency. This is shown in equation 9 and equation 10 [13], [14].

$$T1 = \frac{1}{\omega 1} * tan\left(45° + \frac{\varphi}{2n}\right) \quad \text{Eq. 9}$$

$$T2 = \frac{1}{\omega 1} * tan\frac{1}{\left(45° + \frac{\varphi}{2n}\right)} \quad \text{Eq. 10}$$

The washout time constant, Tw, is further chosen according to [13], [12]:

1: “It should be long enough so that its phase shift does not interfere significantly with the signal conditioning at the desired frequencies of stabilization.”

2: “It should be short enough, that the terminal voltage will not be affected by regular system speed variations, considering system-islanding conditions, where applicable”.

5.4 Modal analysis

By linearizing the equations describing the system it is possible to find the eigenvalues of the system. Modal analysis or eigenvalue analysis describes the small signal behavior of the system. In other words, the behavior linearized around one operating point. This means that the analysis will not take into account the nonlinear behavior in the system during large changes.

The eigenvalue analysis analyses the dynamic behavior under different characteristic frequencies, commonly named “modes”. The linearized system gives the eigenvalues of the system. The definition of an eigenvalue, λ, is conjugate complex number given as:

$$\lambda = \alpha +/- j\Omega \qquad \text{Eq. 11}$$

α is the real part of the eigenvalue and Ω is the imaginary part of the eigenvalue which describes the frequency of the oscillations in rad/s of the oscillatory mode.

If the eigenvalue is characterized by only the real part, α, it is considered as non-oscillatory. If α<0, the eigenvalue is considered to be stable, but if α>0 it is characterized as unstable and exponentially increasing.

If the eigenvalue is complex, the eigenvalue, λ, is characterized as oscillatory. The stability related to the oscillatory eigenvalue depends on whether the real part of the eigenvalue, α, is positive or negative. If it is negative, the corresponding oscillatory eigenvalue is considered as stable. If it is positive, the corresponding eigenvalue is considered unstable.

It is desired that all the oscillations experienced in an electrical system is damped out as quick as possible to enhance the system stability, therefore is the damping ratio of the eigenvalues also a critical parameter. The damping ratio, ζ. is defined as:

$$\zeta = \frac{-\alpha}{\sqrt{\alpha^2 + \Omega^2}} \qquad \text{Eq. 12}$$

The effect of the damping ratio on different oscillatory eigenvalue is shown in Figure 16.

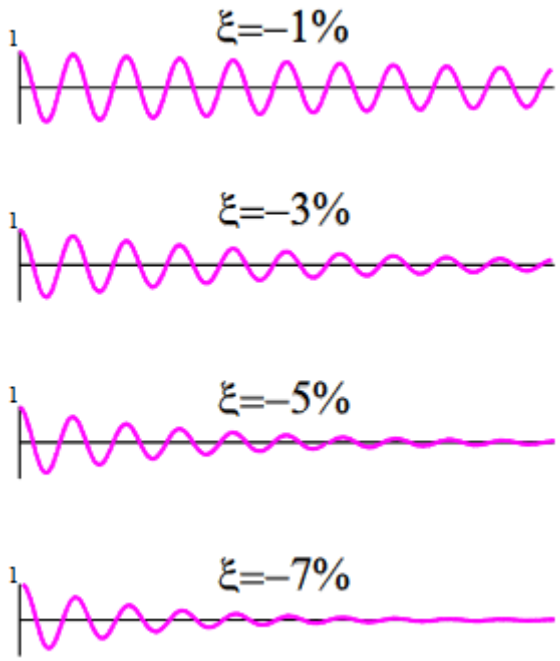

Figure 16: Effect of damping ratio on oscillatory modes [15]

The minimum acceptable level of damping is not defined in theory but in practice is a damping ratio equal to or above 5 % considered adequate. A damping ratio of 5 % means that in 3 oscillation periods, the amplitude is damped out to about 32 % of its initial value. A damping ratio smaller than 5 % is considered weakly damped and is not desired [9], [15].

6 Simulations in PSCAD

6.1 Description of the model

The model used in PSCAD was built during the specialization project in the autumn of 2015 [4]. It is a simplified model of the real-life system where the focus has been on the interaction between the synchronous generator and the rectifier. The model is shown in Figure 17.

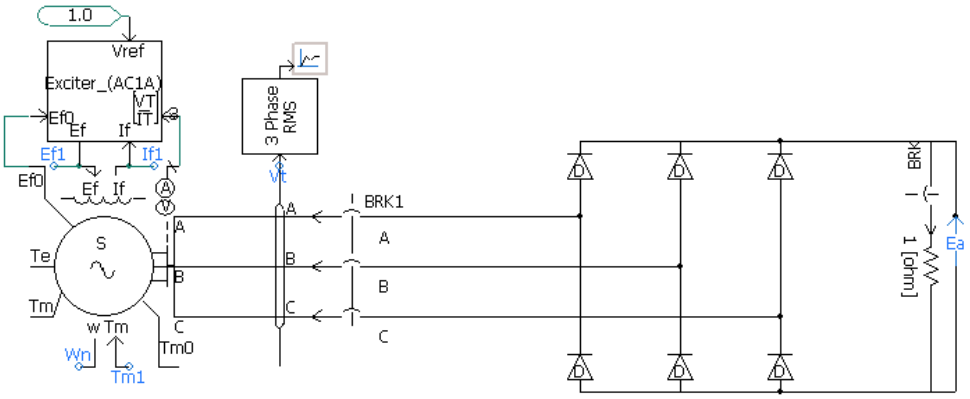

Figure 17: Simulation model in PSCAD

The model has a 1940 kVA synchronous generator with parameters according to the actual synchronous generator found onboard the tug-boat. The block diagram of the AVR and the data for the AVR is given in appendix A. The rectifier is built up as a basic diode rectifier based on the information of the system onboard the tugboat and theory presented in section 5.2. The load is attached at the end of the model (1 ohm in the figure). Since the model is modelled as ideal with no losses only active power flow in the system.

The simulations are done over a period of 20 seconds. The breaker named “BRK1” engages the rectifier at t = 2.5 seconds and the breaker named “BRK” engages the load at t = 5 seconds. At t = 15 seconds the load and rectifier is disengaged.

Figure 18 presents the governor and prime mover for the simulation model in PSCAD. The diesel engine model named “IC engine” in the figure regulates the output torque “T_{m1}” according to the fuel valve opening that is controlled by the governor. The governor is a PI controller with the difference between the reference speed “W_{ref}” and the actual speed of the synchronous generator named “W_n” as input. In addition, the governor has upper and lower restrictions and a time constant to simulate the mechanical and electric time constant of the prime mower and the governor.

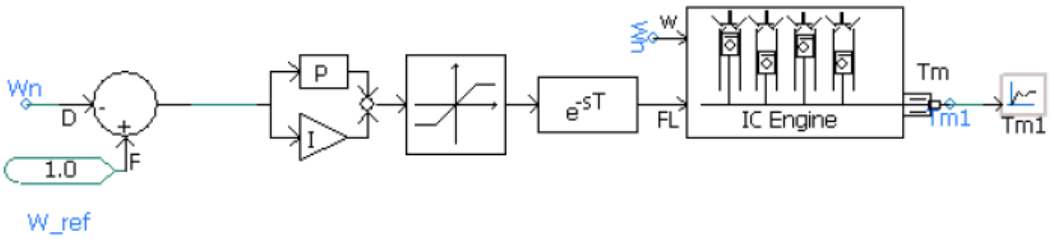

Figure 18: Prime mower and governor

The actual parameters of the prime mower and governor are presented in appendix B

The loads during different simulations is connected directly to the DC bus of the model as mentioned. Based on the equations of the rectifier in section 5.2, the value of the purely resistive load is calculated as follows:

$$R_{load} = \frac{U^2}{P} = \frac{(1.35 * V_{LL})^2}{P} \qquad \text{Eq. 13}$$

- Where R_{load} is the resistance of the load in Ω, U is the voltage in volts, P is the load in MW and V_{LL} is the line-to-line voltage of the synchronous generator.

The values of the resistances presented in Table 2 is used as the load values throughout this section about the PSCAD model.

Table 2:DC loads for the PSCAD model

Load [MW]	R_{load} [Ω]
0.5	1.73
1	0.87
1.5	0.58
1.9	0.46

For the different simulations where oscillations are observed, plots which shows the oscillations better is provided in the appendices.

6.1.1 Initial condition

The initial condition for the 1940 kVA synchronous generator supplying a load of 1 MW through the diode rectifier is shown in Figure 19.

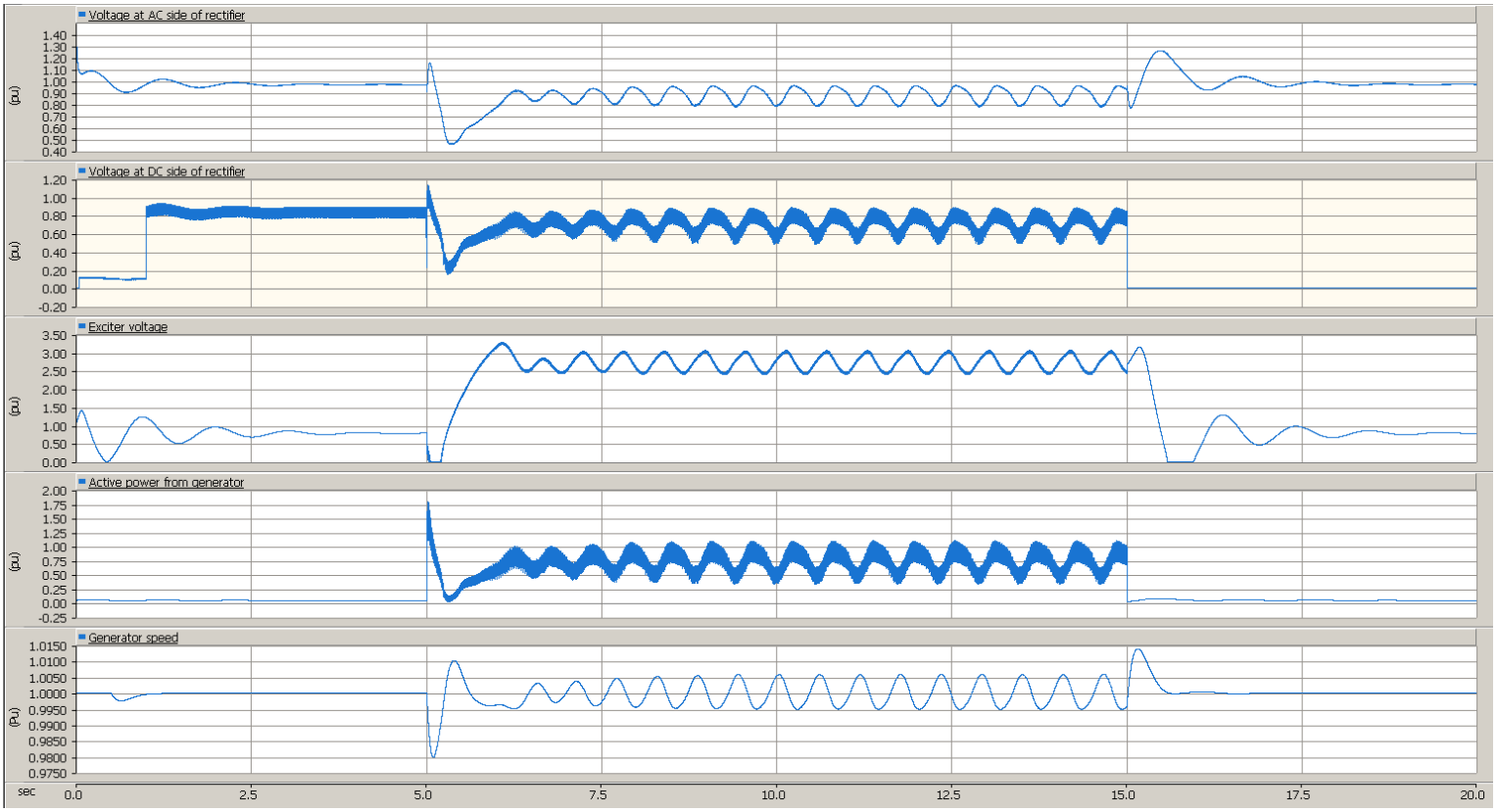

Figure 19: Initial condition of the system supplying a load of ca. 1 MW. Voltage at AC side of rectifier, voltage at DC side of rectifier, exciter voltage, active power from the synchronous generator and the speed of the synchronous generator.

Every measured parameter is oscillating. The observed oscillations are neither increasing or decreasing in amplitude and can be regarded as standing oscillations. Figure 20 show the oscillation found in the active power supplied by the synchronous generator. The oscillation has a frequency of about 1.7 Hz.

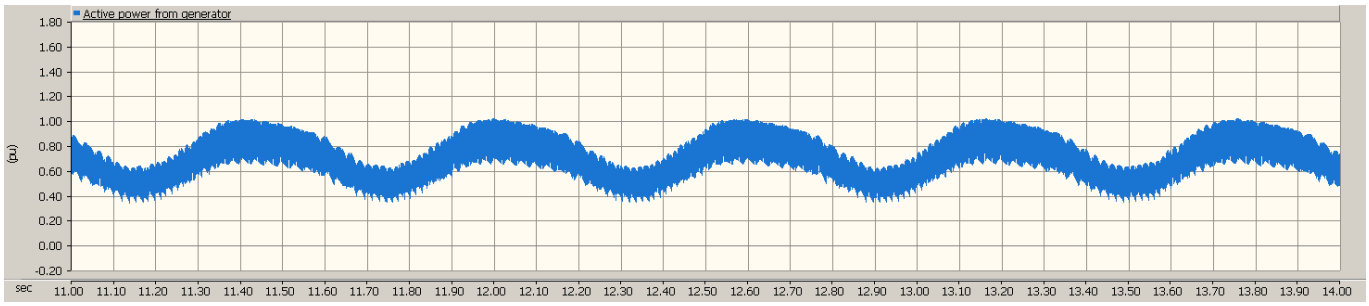

Figure 20:Detailed plot of the oscillation in the active power from the generator

It can also be noticed that the curve for the active power and DC voltage is quite “thick” in the simulations plots compared to the other measured parameters. This is due to the switching frequency of the diodes in the rectifier. The oscillations caused by the switching of the rectifier is 400-500 Hz and often referred to as “ripple”. The ripple of the DC voltage is shown in Figure 21 .

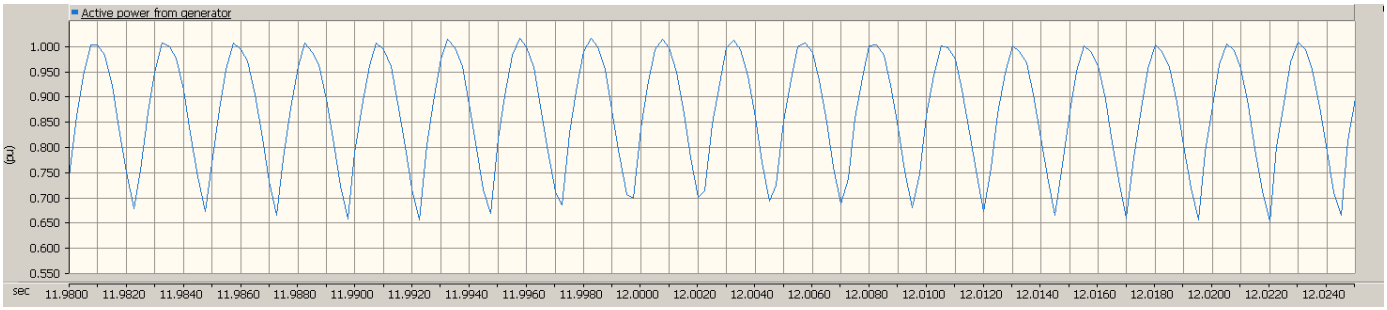

Figure 21: Switching frequency of the full-bridge diode rectifier

This “instability” can easily be reduced with a capacitor connected to the DC terminal of the rectifier.

6.2 Increasing the load

Two loads of 1 MW and 1.9 MW is tested to see how the loading of the synchronous generator affects the observed instability.

6.2.1 Load = 1 MW

The load of 1 MW is added to the system at t = 5 s and the result is shown in Figure 22. More detailed plots of the oscillations can be found in appendix C.

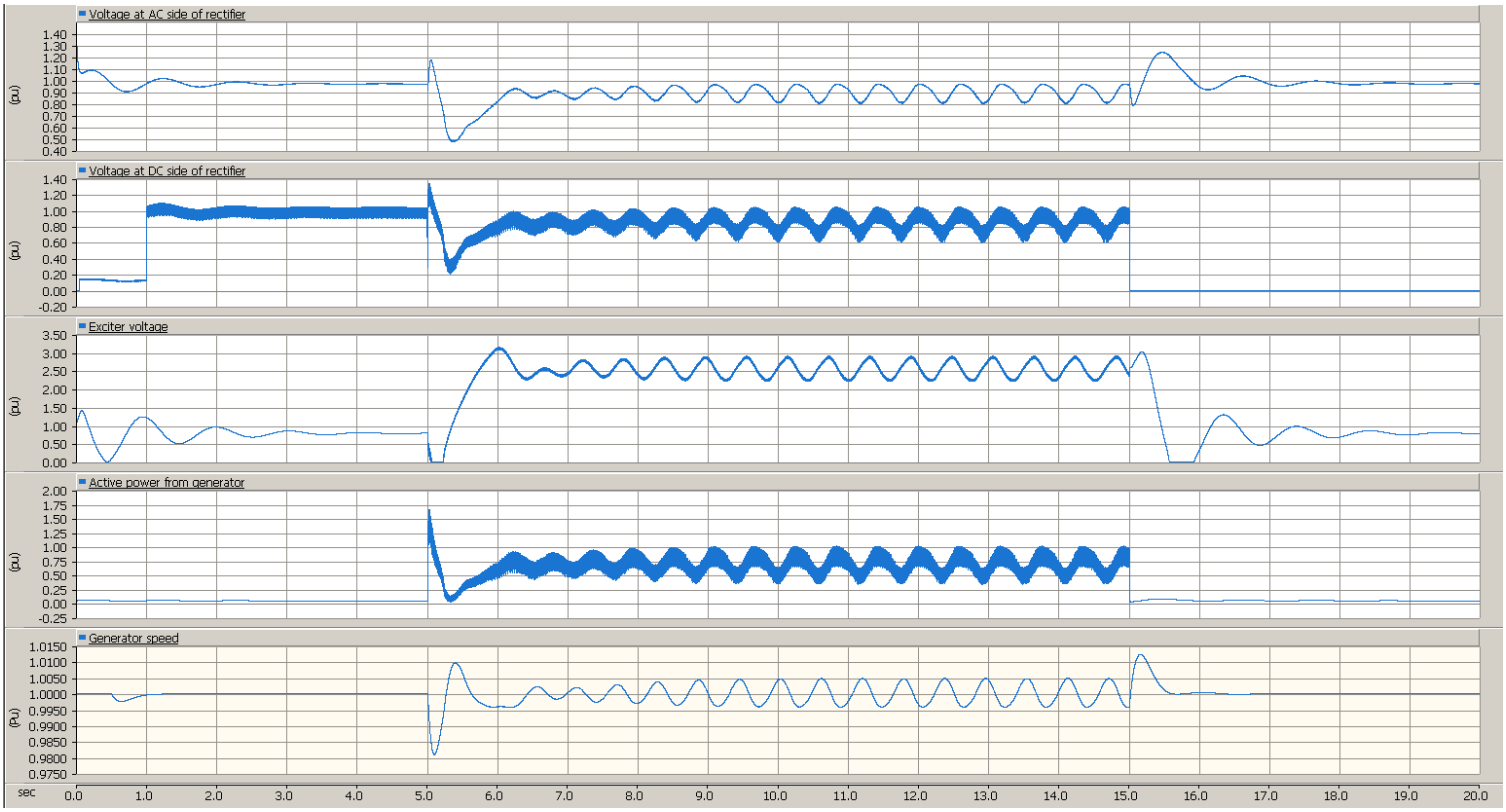

Figure 22: Synchronous generator supplying a load of 1 MW through a rectifier and no battery connected. Voltage at AC side of rectifier, voltage at DC side of rectifier, exciter voltage, active power from the synchronous generator and the speed of the synchronous generator.

The system is clearly not stable and all the observed parameters is oscillating with frequency of about 1.7 Hz and can be considered as standing due to constant oscillating amplitude in the parameters.

The voltage at the AC side oscillate with an amplitude of about 0.2 p.u. around the value of 0.9 p.u. It can also be noticed a quite deep voltage dip in the AC voltage during the introduction of the load to the system. The DC voltage oscillates with a larger amplitude than the AC voltage of about 0.4 p.u.

The exciter voltage is increasing to about 2.5 p.u. when the load is added to the system and is oscillating around this value with an amplitude of around 0.5 p.u. throughout the simulation.

The output power from the synchronous generator has a quite severe oscillating amplitude of 0.5 p.u. In other words, it is switching between 1 MW and 1.9 MW almost twice per second. This is clearly not a desirable operation of the system.

The speed of the synchronous generator is oscillating with a low amplitude between 0.9950 p.u. and 1.0050 p.u., but is noticeable and not desired.

6.2.2 Load = 1.9 MW

A load of 1.9 MW is added to the system. This is quite close to the upper operating limit for the 1940 kVA synchronous generator. The simulations are presented in Figure 23. More detailed plots of the oscillations can be found in appendix C.

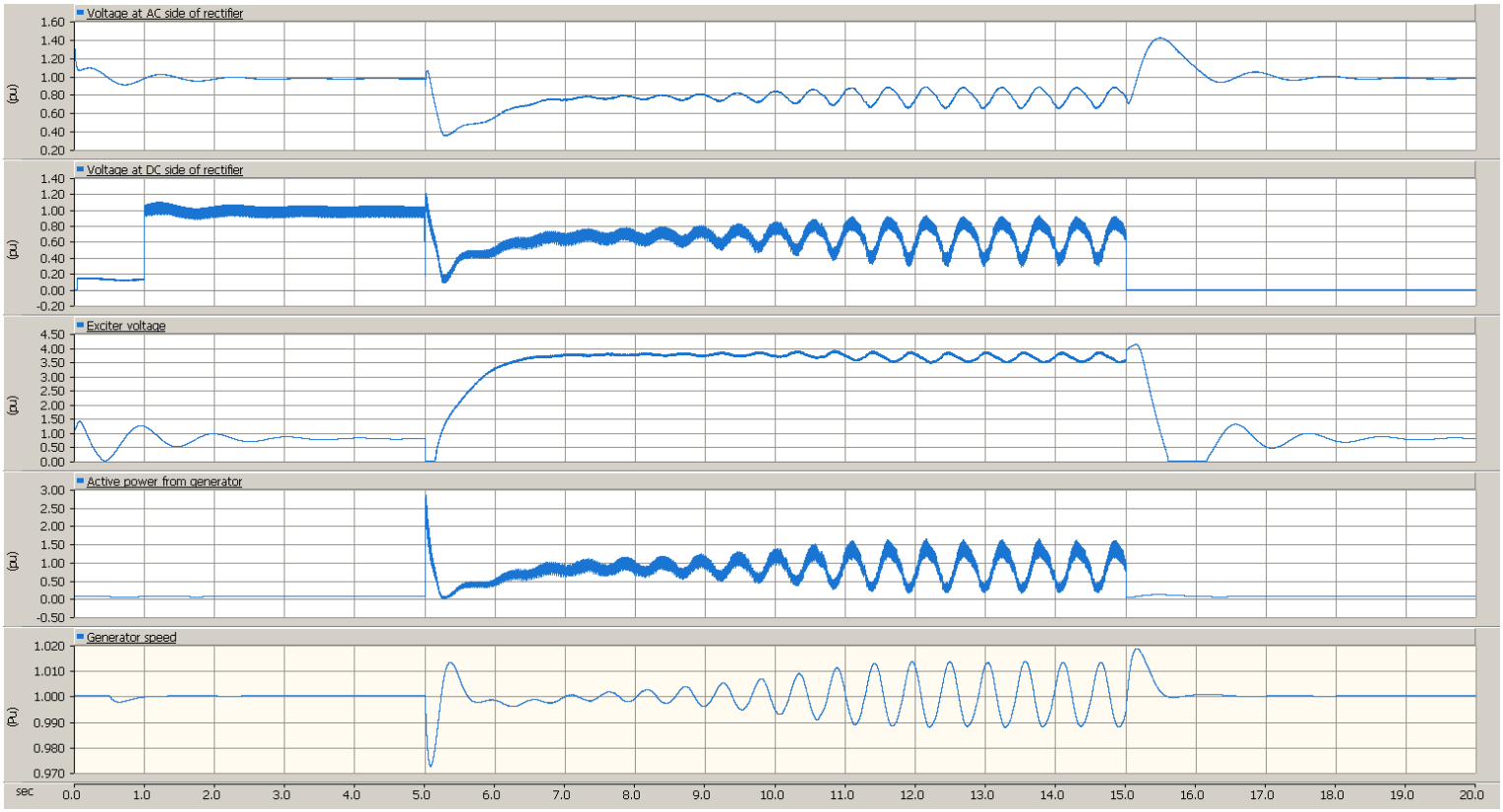

Figure 23: Synchronous generator supplying a load of 1.9 MW through a rectifier and no battery connected. Voltage at AC side of rectifier, voltage at DC side of rectifier, exciter voltage, active power from the synchronous generator and the speed of the synchronous generator.

All the parameters have an oscillating frequency around 1.87 Hz which is a little increase compared to the situation with a load of 1 MW. The instability is however not very noticeable

right after the connection of the load at t=5s. The oscillations are increasing in amplitude until t=12 s and maintain this amplitude throughout the rest of the simulation.

The AC voltage has a larger voltage dip at t=5s compared to the situation with the 1 MW load due to the increased load. At t=7s a new operating point of 0.8 p.u. is reached and the AC voltage starts to oscillate around this value with an increasing amplitude. The amplitude reaches its maximum of 0.2 p.u. as mentioned around t=12s.

It follows that the oscillating DC voltage is also increasing in amplitude like the AC voltage. The DC voltage is oscillating with an amplitude of 0.4 p.u.

The exciter voltage reaches a value of about 3.7 p.u. after the load is added to the system and seems to be quite stable until it starts to have noticeable oscillations at t=8s and around t=12s the oscillations has an amplitude of 0.3 p.u. and can be considered as standing oscillations until the load is disconnected.

The active power from the generator has a quite severe amplitude of 1.25 p.u. after t=12s.

The amplitude of the synchronous generator speed is increasing and oscillating with an amplitude of 0.02 p.u. at its maximum.

6.3 Increasing the load with a battery connected

The real-life system has as mentioned in chapter 2 a battery connected to the DC-side of the rectifier. The simulations in this section is taken to see if the battery can cause an increased or decreased stability compared to the observed instability without the battery connected.

The PSCAD model used in this section of the thesis is shown in Figure 24.

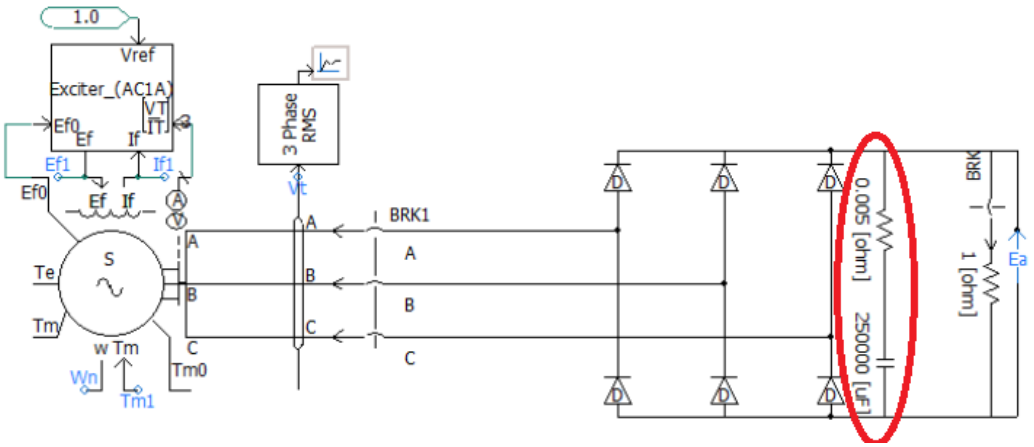

Figure 24: PSCAD model with a battery connected to the DC side of the rectifier.

The PSCAD model is almost identical to the previous one used, but a simple model of a battery marked by a red circle in the figure is connected. The battery is modelled as a small resistance to simulate the internal resistance of a battery in series with a (infinitely) large capacitor.

6.3.1 Load = 1 MW

For comparison, the same load steps as with the model without a battery connected, is used, starting with a load of 1 MW. The simulations are shown in Figure 25. More detailed plots of the oscillations can be found in appendix D.

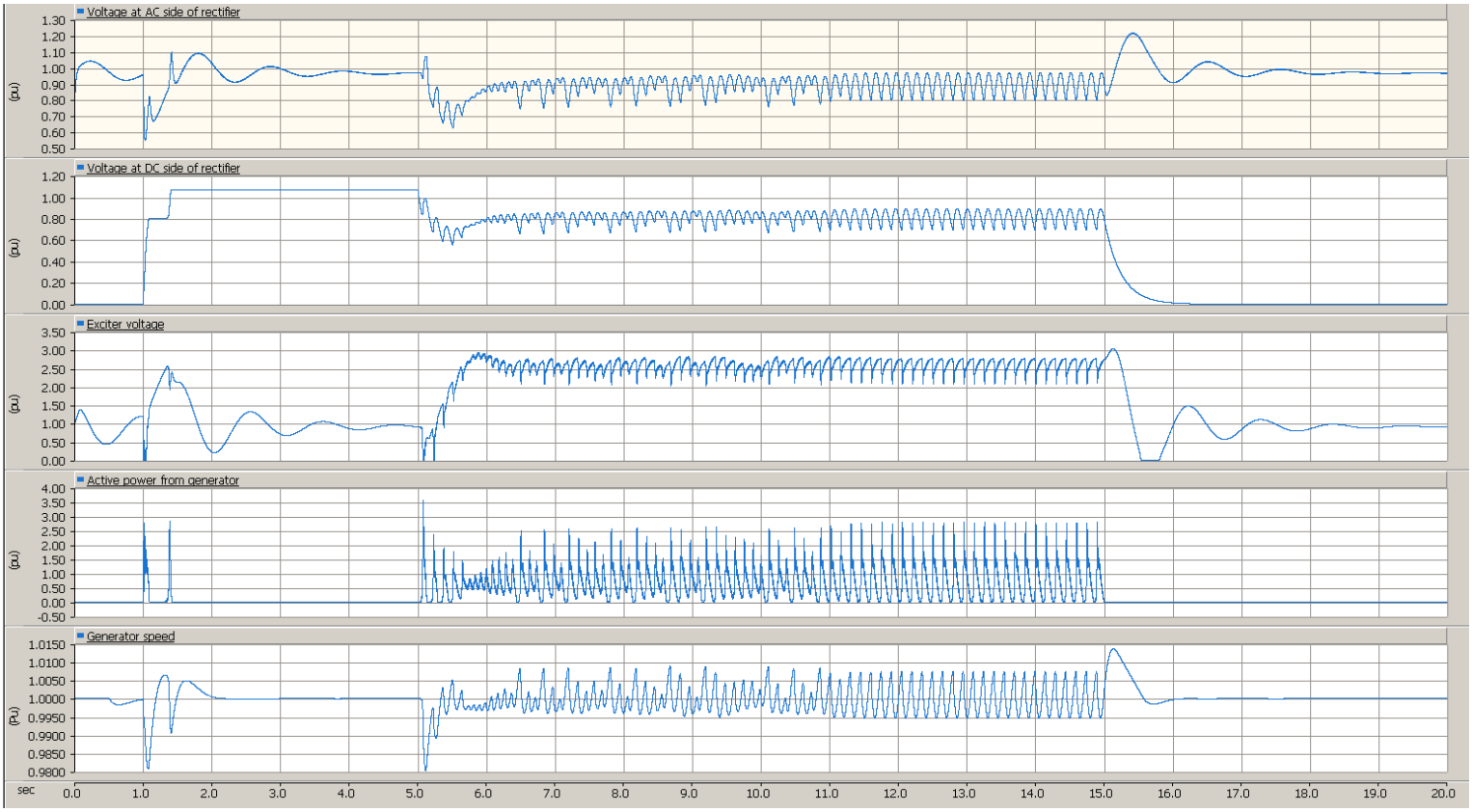

Figure 25: Synchronous generator supplying a load of 1 MW through a rectifier and a battery connected. Voltage at AC side of rectifier, voltage at DC side of rectifier, exciter voltage, active power from the synchronous generator and the speed of the synchronous generator.

Adding the battery to the system clearly do not make the system more stable. All the parameters are now oscillating with a greater frequency than before of around 6.67 Hz. From the load is connected at t=5s to around t=12s, the oscillation in the parameters has not got a constant amplitude. From t=12s, the oscillations are more or less at a stable amplitude for all the parameters.

The AC voltage has an amplitude of 0.15 p.u. and oscillating around the value of 0.9 p.u. This is quite the same as without the battery, only with a slightly smaller amplitude.

The DC voltage is oscillating around 0.8 p.u. with an amplitude of 0.2 p.u. The observed amplitude is half of the situation without the battery connected. It can also be noticed that the ripple in the DC voltage caused by the rectifier is gone due to the battery.

The exciter voltage rises to 2.5 p.u. after the load is added and is oscillating with an amplitude of 0.5 p.u., the same as without the battery connected.

The active power from the synchronous generator oscillates between 0 and 2.5 p.u. and the speed of the synchronous generator also starts to actively oscillate with a higher amplitude.

6.3.2 Load = 1.9 MW

The load is increased to 1.9 MW to see how the system will behave close to the limit of the generator with a battery connected to the DC-side of the rectifier. The simulations are presented in Figure 26.

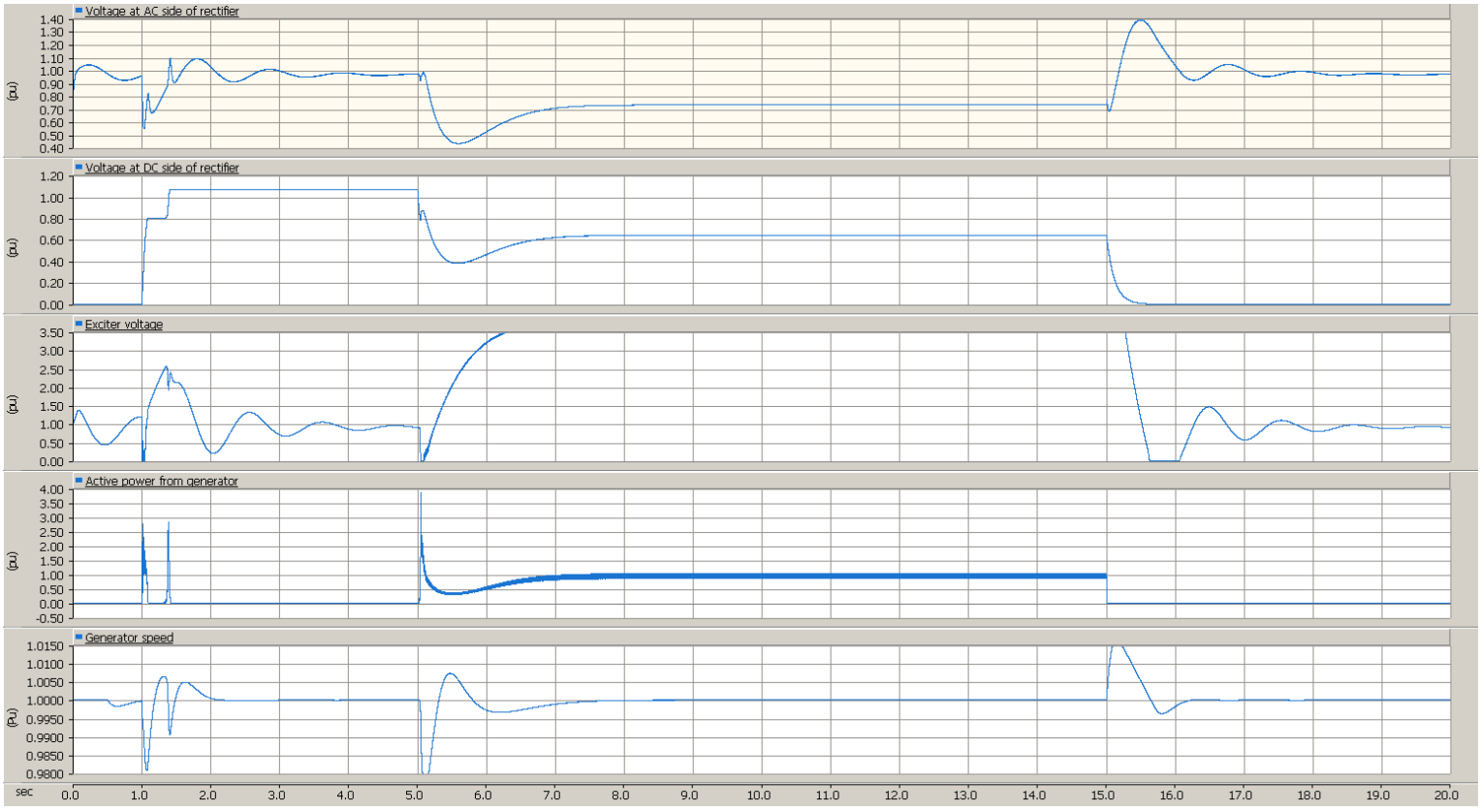

Figure 26: Synchronous generator supplying a load of 1.9 MW through a rectifier and a battery connected. Voltage at AC side of rectifier, voltage at DC side of rectifier, exciter voltage, active power from the synchronous generator and the speed of the synchronous

All the measured parameters are stable in contrast to the situation without the battery connected. Without the battery connected to the system, it seemed quite stable in the start and the instability increased through the simulation.

It is however observed quite low voltages at both sides of the rectifier. The AC voltage drop to 0.4 p.u. during the connection of the load at t=5s and is increasing to a stable operating point at around 0.7 p.u. The DC voltage is also having a dip at 0.4 p.u. and stabilizes at 0.6 p.u.

The exciter voltage is increasing to raise the voltage at the terminals of the generator but it has little effect.

The active power from the synchronous generator and the speed is operating at the desired point and is stable.

6.4 Inertia constant

The inertia constant of a synchronous generator is defined by equation 14.

$$H = \frac{J * (2\pi * f_n)^2}{2 * S_n} \quad \text{Eq. 14}$$

It can be seen from the equation for the inertia constant that it expresses the angular momentum of the rotor with reference to the power rating of the synchronous generator. This make it easy to compare the angular momentum of the rotors on different synchronous generators with different ratings. The inertia constant is given the symbol H and is therefore also referred to as the H-constant. The unit of the inertia constant is seconds. The inertia constant quantifies the kinetic energy of the rotor at synchronous speed in terms of number of seconds it would take the generator to provide an equivalent amount of electrical energy when operating at a power output equal to its MVA rating [9].

Due to the fact that the inertia constant H describe the angular momentum of the rotor it has a significant impact on the stability of electrical systems. In [2] it was stated that the inertia constant had little or no impact on the stability of the instable system in question. This result seems quite strange when the results of [1], [4] and [2] implies that the synchronous generator could be poorly damped. In this chapter the inertia constant, H, is increased on the instable 1940 kVA synchronous generator to see which effect it will have on the instable operation.

The inertia constant is simulated for a range of values from a very small inertia constant of 0.1 s to a quite large inertia constant of 5 s. more plots from the simulations are found in appendix E.

The instability in the system seems to be affected in a negative way for loads unequal to the rated capacity of the synchronous generator based on the findings in chapter 6.3. The observed instability during the measurements mentioned in section 2.3 was also without the battery. The simulations in this chapter is therefore done without the battery connected and the PSCAD model in Figure 17 is the basis for the simulations.

6.4.1 H = 0.1 s

Starting with a low value for the inertia constant of H=0.01 s and a load equal to 1 MW. The simulations are presented in Figure 27. More detailed plots of the observed oscillations are found in appendix E.

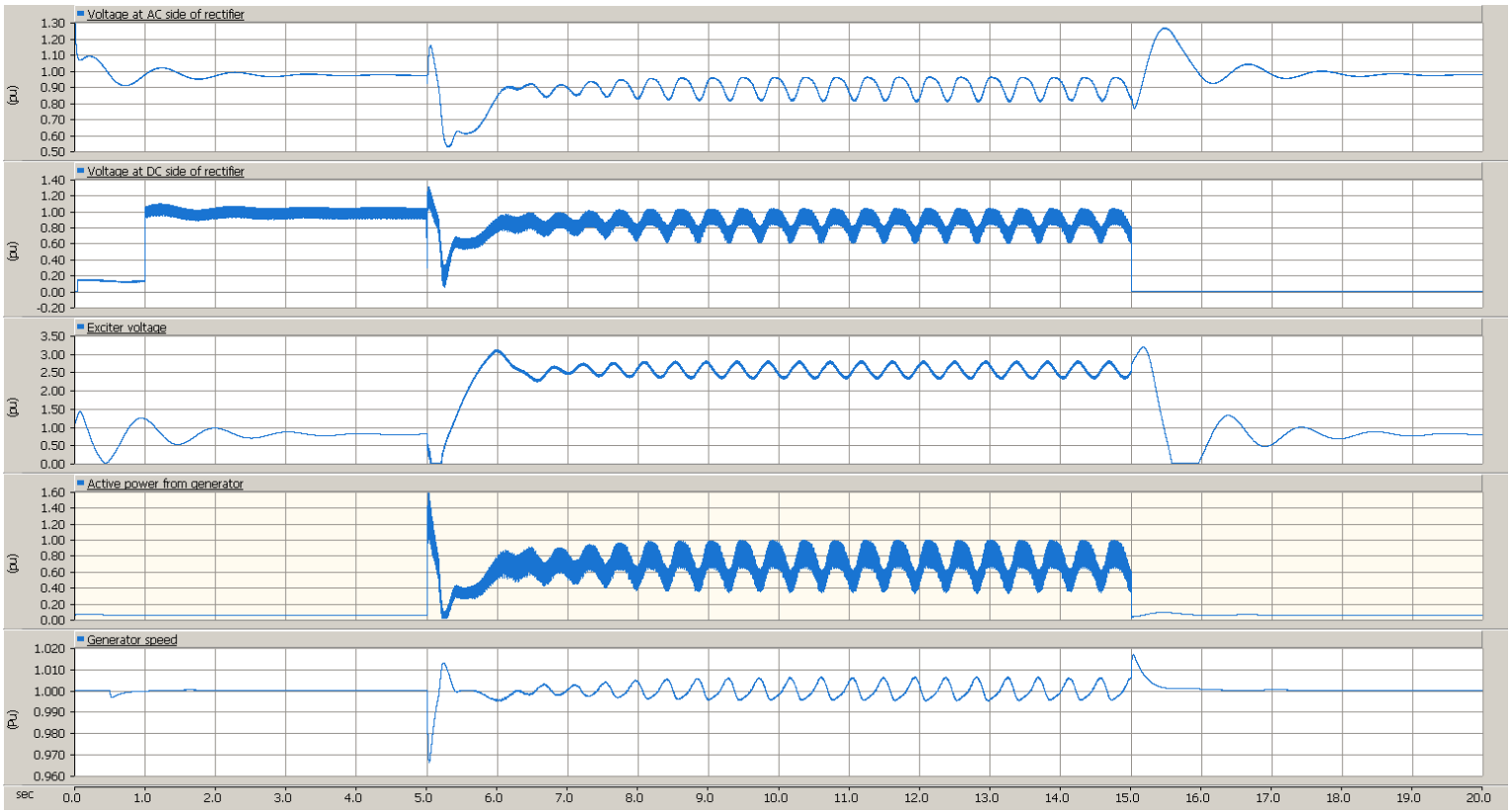

Figure 27:Synchronous generator supplying a load of 1 MW through with H = 0.1 s. Voltage at AC side of rectifier, voltage at DC side of rectifier, exciter voltage, active power from the synchronous generator and the speed of the synchronous generator.

The observed oscillations are starting with a quite low amplitude and increasing towards standing oscillations for all the parameters. The frequency of the observed oscillations is about 2.2 Hz.

After around t=10s, the AC voltage is oscillating with an amplitude of 0.15 p.u. around the value of 0.9 p.u. The DC voltage is oscillating with an amplitude of 0.4 p.u. around the value of 0.8 p.u.

The exciter voltage is increasing towards 2.5 p.u. and is oscillating around this value with an amplitude of 0.5 p.u.

The active power is oscillating between 0.5 p.u. and 1 p.u.

The speed of the synchronous generator has some small oscillations around the nominal speed of 1 p.u.

6.4.2 H = 1 s

The inertia constant is increased by a factor of ten to H=1 s for the synchronous generator. This is close to the actual value of the inertia constant for the instable synchronous generator. The load is still 1 MW.

The simulations are shown in Figure 28. More detailed plots are provided in appendix E.

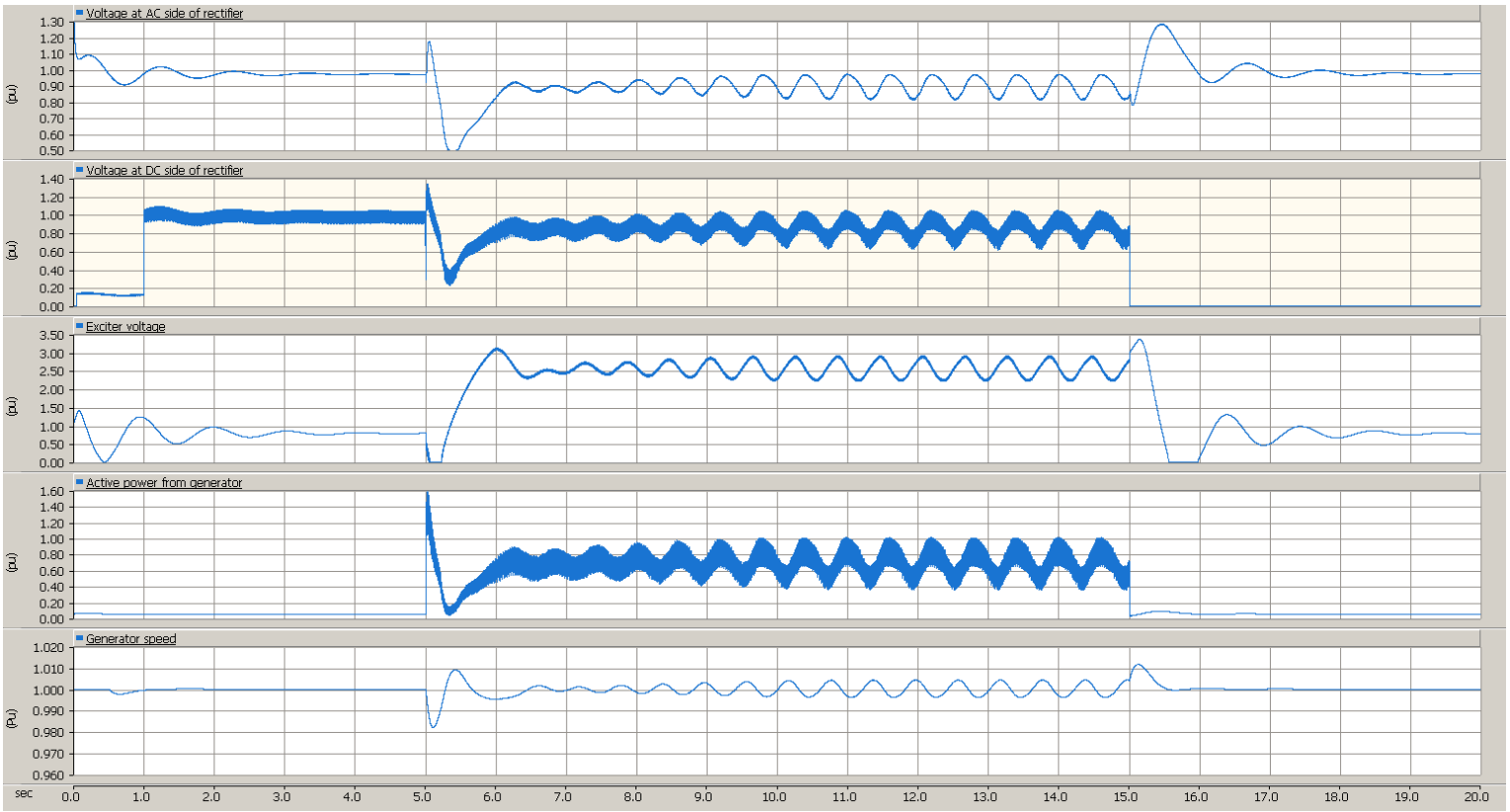

Figure 28:Synchronous generator supplying a load of 1 MW through with H = 1 s. Voltage at AC side of rectifier, voltage at DC side of rectifier, exciter voltage, active power from the synchronous generator and the speed of the synchronous generator.

The oscillations are also here starting with a lower amplitude and increasing to standing oscillations for all the parameters. The frequency of the observed oscillations is about 1.67 Hz, decreasing by 0.53 Hz from the situation with H=0.1 s.

After around 9 s, the AC voltage is oscillating with an amplitude of 0.15 p.u. around the value of 0.9 p.u., the same as for the situation with H=0.1 s. The DC voltage is oscillating with an amplitude of 0.3 p.u. around the value of 0.8 p.u.

The exciter voltage has an oscillating with an amplitude of 0.65 p.u. around the value of 2.5 p.u.

The active power is also here oscillating between 0.5 p.u. and 1 p.u.

The speed of the synchronous generator has some small oscillations around the nominal speed of 1 p.u.

6.4.3 H = 2 s

Increasing the H-constant to H = 2 s yields an interesting result presented in Figure 29. More detailed plots are found in appendix E.

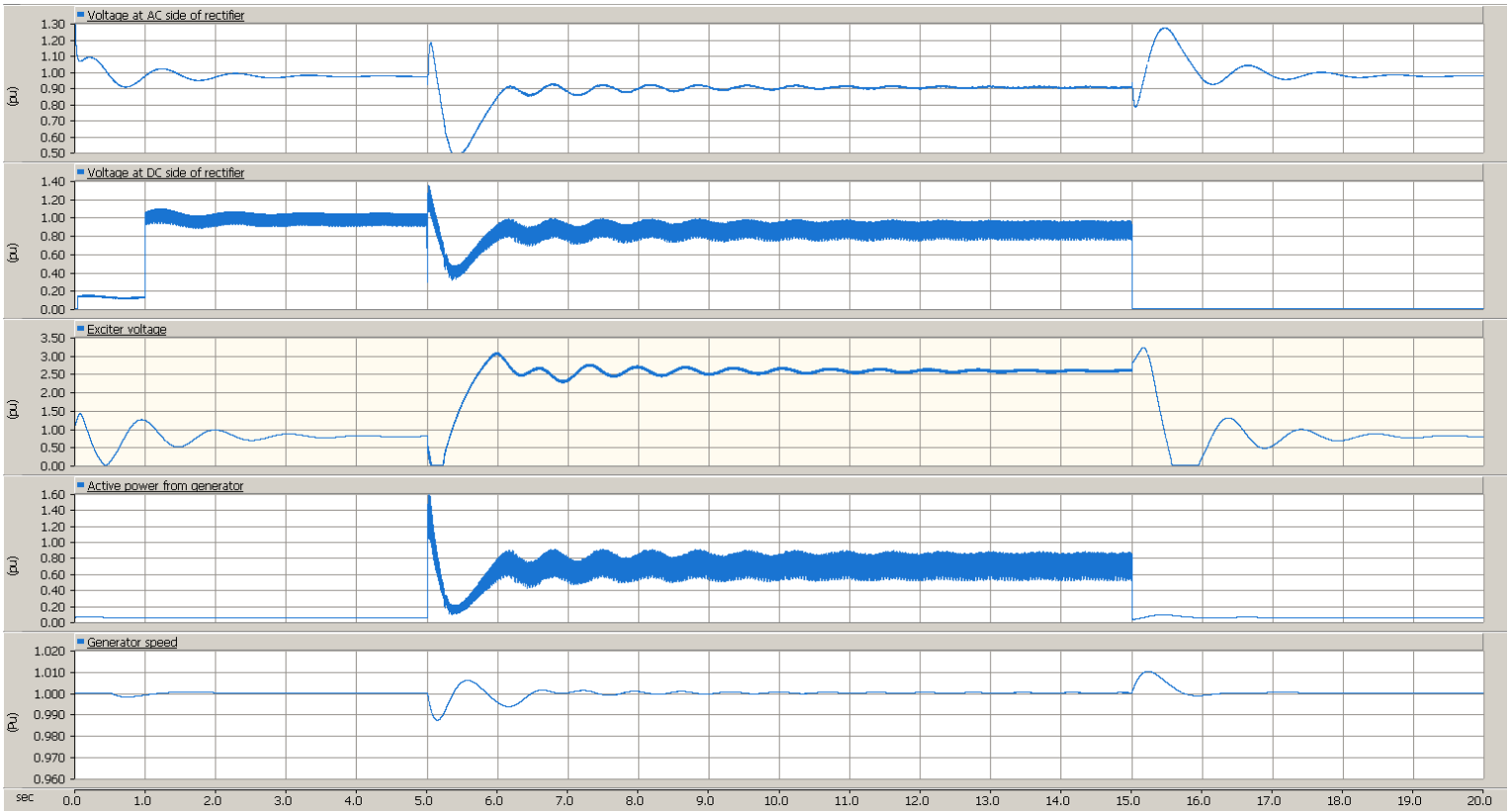

Figure 29: Synchronous generator supplying a load of 1 MW through with H = 2 s. Voltage at AC side of rectifier, voltage at DC side of rectifier, exciter voltage, active power from the synchronous generator and the speed of the synchronous generator.

Doubling the inertia constant from the last simulations seems to make the system nearly stable. Some oscillations are observed right after the rectifier and load is connected at t=5 s which is the same as can be observed at the same instance in the other simulations for the inertia constant. It is however noticed that the oscillations that grew to standing oscillations in the previous simulations, is here nearly damped out. By investigating the more detailed plots it is noticed an oscillation frequency of 0.35 hz which is present in the simulation.

The amplitude of the oscillations is very small and it is obvious that increasing the inertia constant is enhancing the stability of the system.

6.4.4 H = 5 s

The simulation with H = 2 s was nearly stable and to clarify that the system is able to become stable by increasing the damping of the synchronous generator, the inertia constant is increased to H=5 seconds. The simulations are shown in

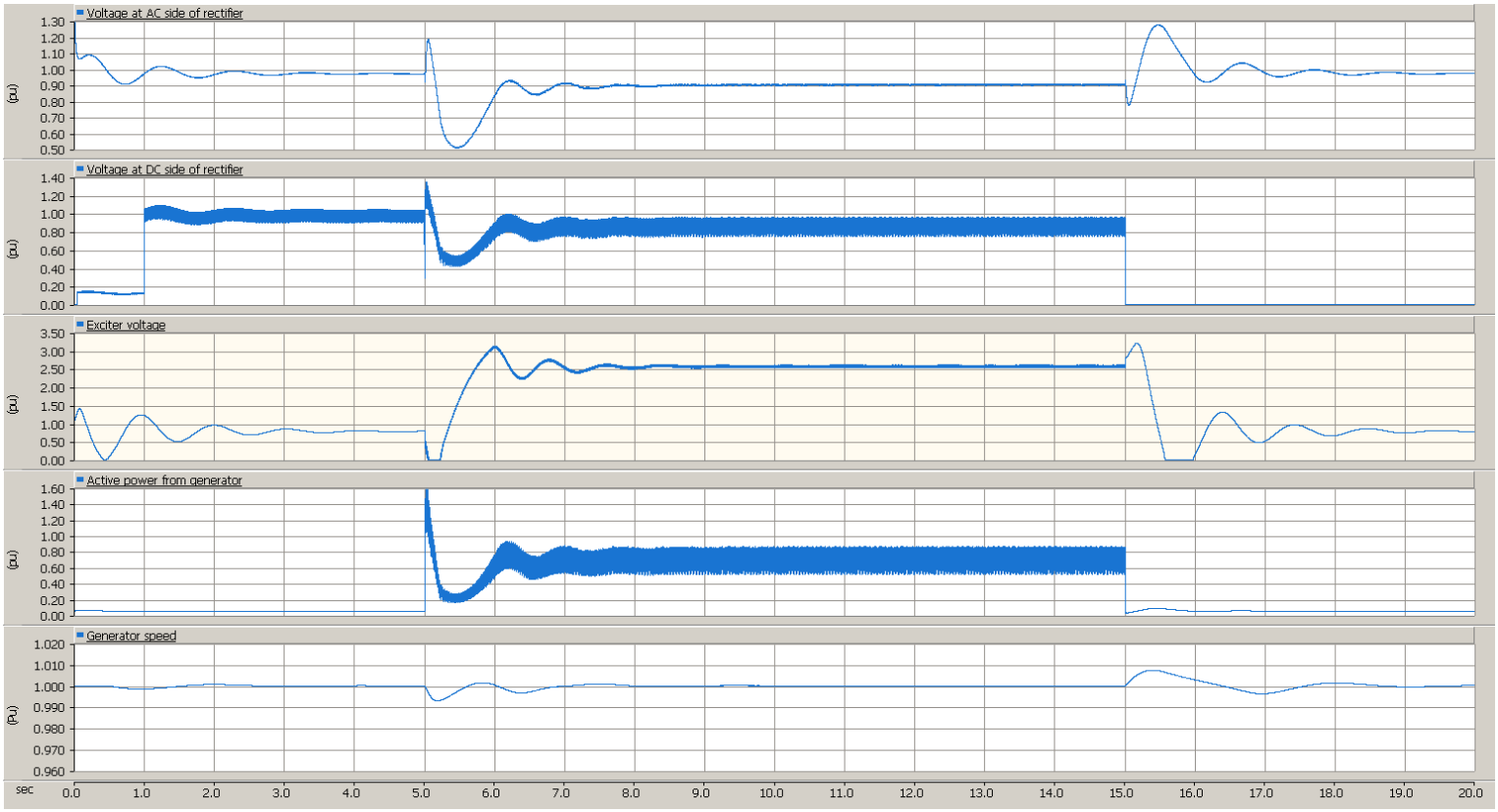

Figure 30.

Figure 30: Synchronous generator supplying a load of 1 MW through with H = 5 s. Voltage at AC side of rectifier, voltage at DC side of rectifier, exciter voltage, active power from the synchronous generator and the speed of the synchronous generator.

The system is stable and the disturbance caused by connecting the load at t=5 s is now damped out after 3.5 s and remains stable. The only noticeable disturbance in the system at this point is the ripple in the DC voltage caused by the rectifier which is also noticeable in the active power supplied by the synchronous generator.

6.5 Q-axis damper winding

Based on the theory presented in section 4, a q-axis damper winding is added to the synchronous generator to see the affect it will have. A damper winding has a high resistance/reactance ratio. In the subtransient state these windings act as a perfect screen and the changes in the in the armature flux cannot penetrate them. In the transient state the air-gap flux, which rotates at the synchronous speed, penetrates the damper windings and induces an emf and current in them whenever the rotor speed deviates from the synchronous speed. This induced current produces a dampening torque which, according to Lenz's law tries to restore the synchronous speed of the rotor [9].

Based on equation 2, the damper winding should have a value of 0.546 p.u. which is added to the system and the simulations are shown in Figure 31.

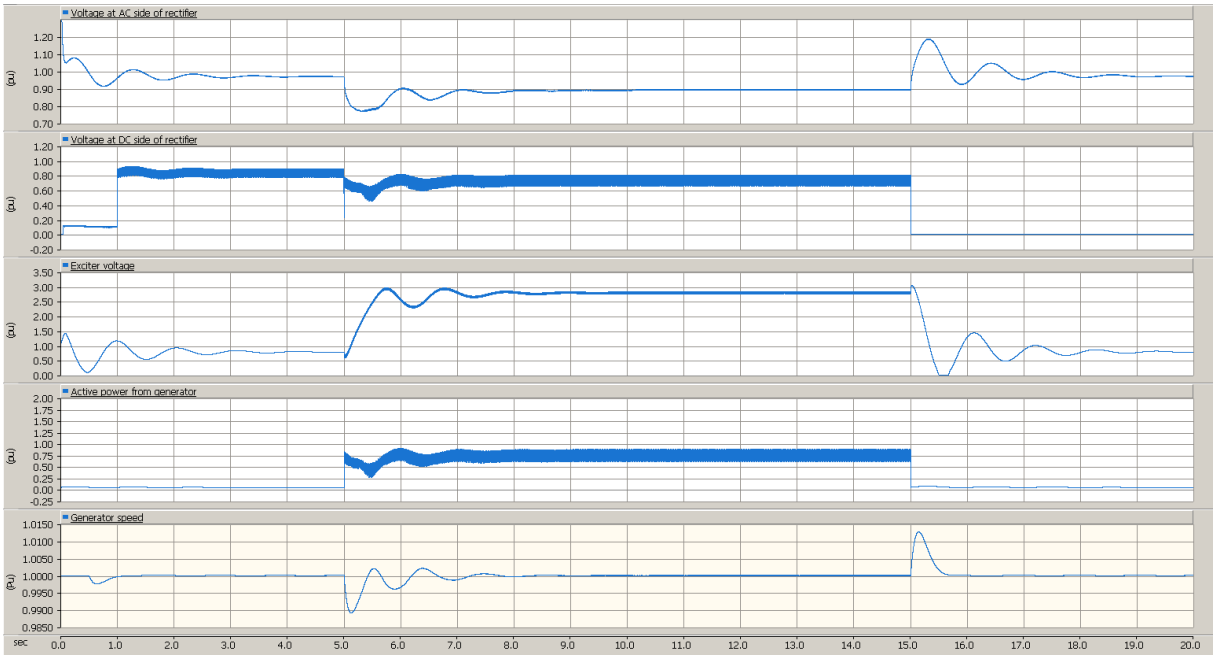

Figure 31.Simulation of an extra q-axis damper winding. Voltage at AC side of rectifier, voltage at DC side of rectifier and the exciter voltage, active power from the synchronous generator and the speed of the synchronous generator.

The system is observed to be stable. None of the parameters is observed to be oscillating or have any kind of instability problem. The only oscillations seen is the ripple in the DC voltage and active power due to the rectifier. This was also the solution in [4].

6.6 Changing the synchronous generator parameters

The tests so far have yielded results that can verify that the whole system under study is unstable and some parameters and components in the system is able to enhance the stability of the system, while others are making the system more unstable. The synchronous generator and its internal parameters has been believed to be the component in the system that has caused the instability. This is the angle of incidence for the work done in [1] and [2].

It would be interesting to change the parameters for the synchronous generator while keeping the rest of the system with its initial values. A synchronous generator with a similar voltage and MVA rating is used. The parameters for the synchronous generator used in these simulations is provided in appendix F. The inertia constant for the synchronous generator is set to H = 1 s, keeping in mind that the original synchronous generator under study in this thesis was observed to be instable with this value of the inertia constant.

The simulations are shown in Figure 32.

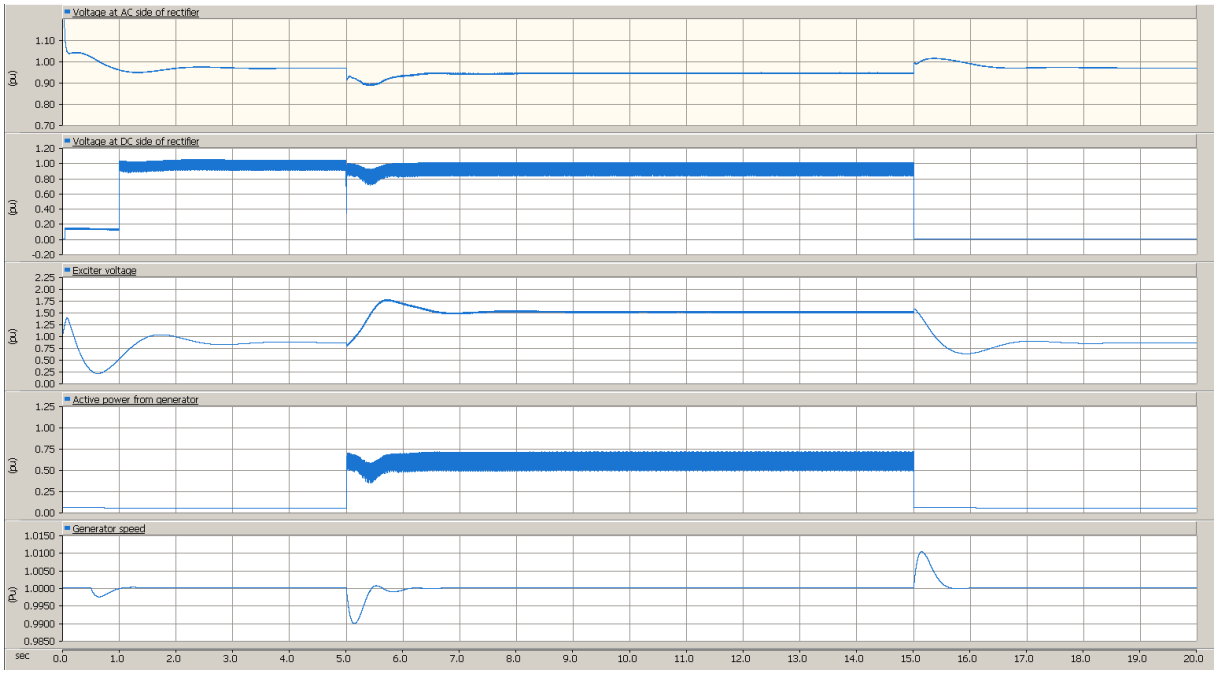

Figure 32: Synchronous generator with other internal parameters supplying a load of 1 MW. Voltage at AC side of rectifier, voltage at DC side of rectifier, exciter voltage, active power from the synchronous generator and the speed of the synchronous generator.

The system is observed to be stable for all the measured parameters. Even the voltage drop in the AC voltage during the connection of the load at t = 5s is smaller, only 10 %. By comparing these results to the results in section # it is obvious that the parameters of the synchronous generator might be a possible cause of the observed instability problems.

6.7 Transient disturbances

By observing the ripple in the DC voltage of the rectifier it is interesting to observe the currents from the synchronous generator during normal operation with/without the rectifier supplying a load of 1 MW.

Due to the fact that the synchronous generator is operating against a rectifier make the problem more complex. The currents from the synchronous generator will not be purely sinusoidal due to the constant switching caused by the rectifier. This is shown in Figure 33.

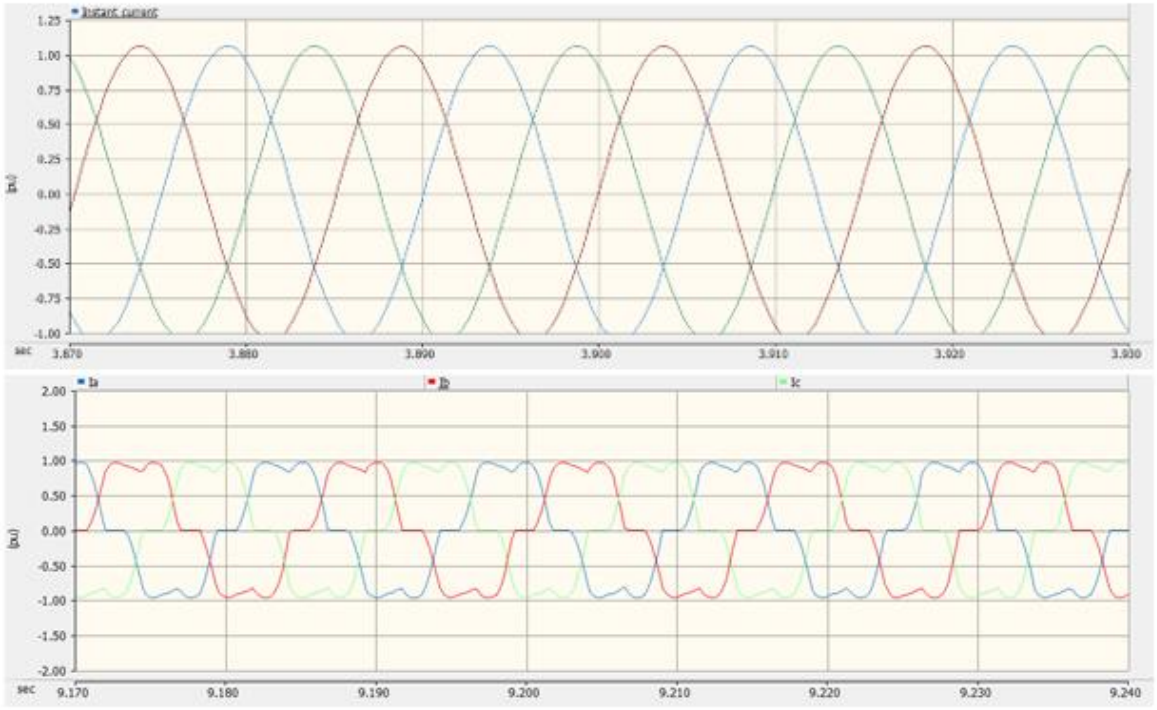

Figure 33: a) Currents without a rectifier, b) Currents with a rectifier

Figure 33 a, shows the currents from the synchronous generator when operating against just a load with no rectifier where the system is observed to be stable. The currents are purely sinusoidal and no disturbances is observed. Figure 33 b, presents the same synchronous generator when it is supplying a load through a full-bridge diode rectifier. The pure sinusoidal current is now observed to be shaped by the switching action in the rectifier. The operation with the rectifier causes the synchronous generator to constantly experiencing small disturbances caused by the switching of the diodes. This might be a problem if the system is initially marginally stable and the constant small disturbances caused by the rectifier is making the system instable during operation.

7 Simulations in DigSILENT PowerFactory

The motivation for designing a new model in DigSILENT PowerFactory in addition to the model in PSCAD is to be able to analyze the stability aspect of the system better. DigSILENT PowerFactory offers more tools to analyze stability in addition to time-domain analysis. In PowerFactory it would have been easier to model the whole system on the tugboat but based on the simulations already undertaken in previous sections of this master's thesis it seems plausible that the instability is related to the synchronous generator and the system modelled is therefore still kept simple.

A model in PowerFactory was used in [1] and [2], but the model used a bi-directional PWM (Pulse Width Modulation) rectifier which uses semiconductor switches (IGBT's) to rectify the voltage. This is a more advanced rectifier than the normal full-bridge diode rectifier used in the system onboard the tug-boat and the simulation model in [1] and [2] may not have been accurate enough. The aim for the model in this master's thesis is to be as close to the system found onboard the tug-boat as possible to recreate the instability problem.

7.1 Description of the model

The model for further studies is presented in Figure 34.

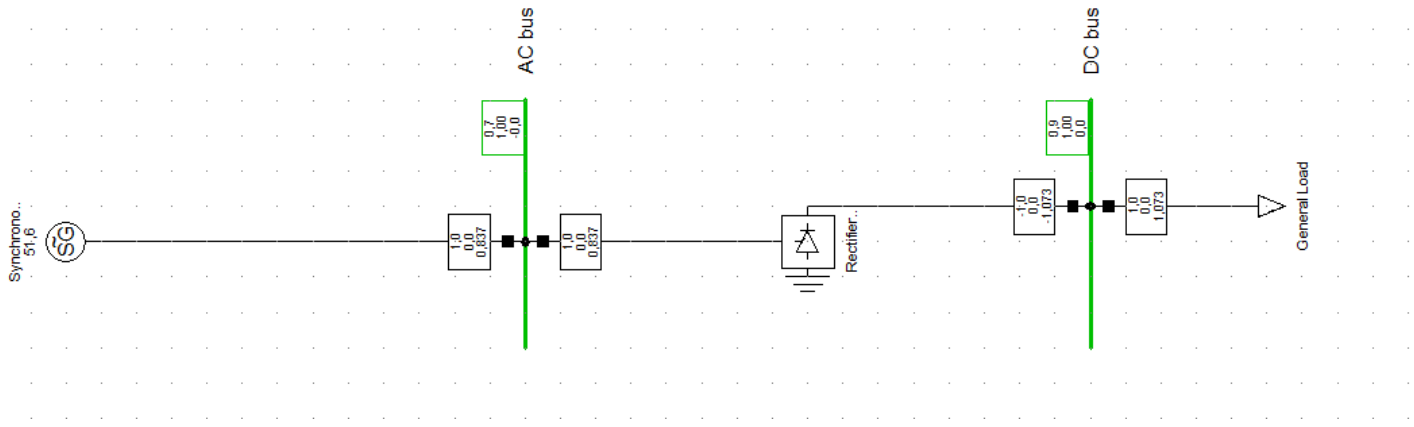

Figure 34: Simulation model in DigSILENT PowerFactory

The synchronous generator is again modelled as the most instable 1940 kVA synchronous generator.

An excitation system and voltage regulator is added to the generator to provide voltage control during the simulations. Based on the limited information of the test in [3] the AVR is a PID Basler digital excitation control. The AVR called "ESAC8B" is found in the library of

PowerFactory. The model and parameters are shown in appendix G. This is a rectified AC-supplied brushless exciter with a PID controller which is intentionally modelled as the Basler digital excitation control system voltage regulator [16].

A governor is also needed to regulate the speed and power output of the synchronous generator. A governor model should be a model of a diesel engine and the model "Degov1" is chosen. The model and parameters can be found in appendix F. This is a model of a diesel governor with a throttle feedback (or electric power feedback). The model is based on the commonly used Woodward governor which consists of an electric speed sensor, a hydro-mechanical actuator and the diesel engine. The output from the actuator is a valve position for the fuel supply to the diesel engine which is again controlling the torque provided from the diesel engine to the synchronous generator [16].

The rectifier is a basic full-bridge diode rectifier for which the theory is presented in chapter 5.2. The full-bridge diode rectifier is modelled as ideal, hence, no losses is included.

Furthermore, is the load connected to the DC-side of the full-bridge diode rectifier and the battery is excluded from the simulation since the instability problem observed in chapter 6 was present even without the battery. The observed instability in [3] was also without the battery connected.

7.1.1 Initial condition of the synchronous generator

It is interesting to see if the model is able to recreate the instable operation from the tug-boat.

The simulation is done by keeping the initial values of the parameters and letting the synchronous generator supply a load of 1 MW. It can be observed that the measured parameters in the system it is clearly not stable as shown in the plots in appendix H. All the measured parameters are oscillating with the same frequency. The active power from the synchronous generator is presented in Figure 35.

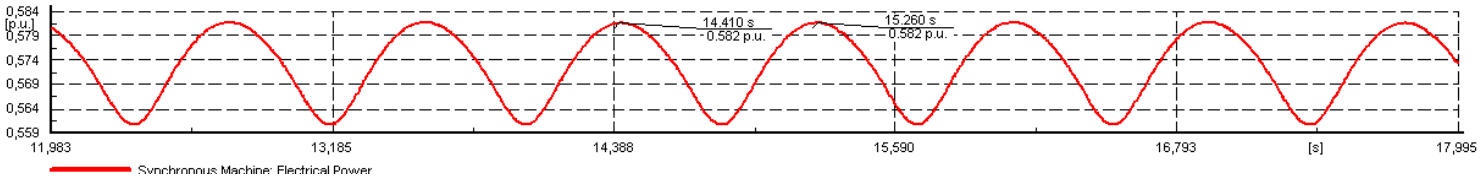

Figure 35: Observed oscillation in the active power from the synchronous generator

The instable operation is clearly present in the model and the active power is oscillating between 0.562 p.u. and 0.582 p.u. It is however observed that the period of the oscillations is larger than in the PSCAD model. The period of the observed oscillations is about 0.85 seconds, yielding an oscillations frequency in the active power of 1.18 Hz.

Analyzing the eigenvalues of the system can give better view of the instability observed in the system. The plot for the different eigenvalues is shown in Figure 36. The actual values for the different eigenvalues is given in appendix H.

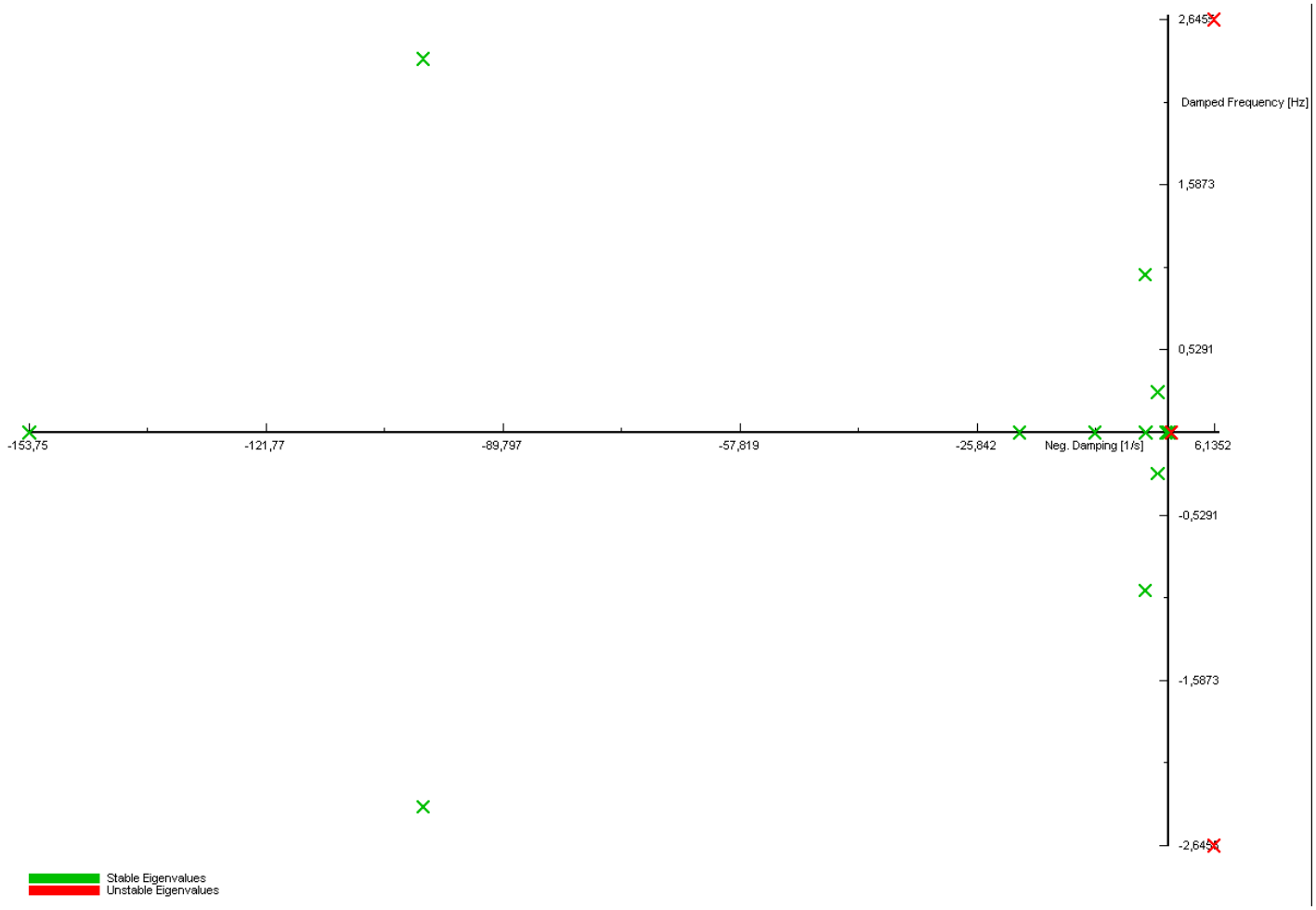

Figure 36: Eigenvalues for the initial state of the synchronous generator

It is observed four oscillatory eigenvalues with an oscillatory frequency of 0.26 Hz, 1.01 Hz, 2.4 Hz, and 2.65 Hz.

The modes of interest are presented in Table 3.

Table 3: Initial eigenvalues of the system

Name	Real part	Imaginary part	Magnitude	Angle	Damped Frequ	Period	Damping
Unit	1/s	rad/s	1/s	deg	Hz	s	1/s
Mode 00003	-100,6782354	15,05739499	101,7979972	171,4939147	2,396458842	0,417282359	100,6782
Mode 00004	-100,6782354	-15,05739499	101,7979972	-171,4939147	2,396458842	0,417282359	100,6782
Mode 00005	6,13521469	16,6221711	17,71827958	69,74098337	2,645500695	0,378000279	-6,13521
Mode 00006	6,13521469	-16,6221711	17,71827958	-69,74098337	2,645500695	0,378000279	-6,13521
Mode 00009	-3,237979285	6,361390921	7,138053257	116,9763179	1,01244681	0,987706208	3,237979
Mode 00010	-3,237979285	-6,361390921	7,138053257	-116,9763179	1,01244681	0,987706208	3,237979
Mode 00012	-1,484084741	1,633113042	2,206709252	132,2628634	0,259918013	3,847367052	1,484085
Mode 00013	-1,484084741	-1,633113042	2,206709252	-132,2628634	0,259918013	3,847367052	1,484085
Mode 00015	0,306928745	0	0,306928745	0	0	0	-0,30693

All of the oscillatory modes except one is observed to have a negative real part and is therefore considered to be stable. The oscillatory mode with a frequency of 2.65 Hz is characterized as instable due to the fact that the real part of the eigenvalue is positive. It is also observed a marginally instable non-oscillatory mode (mode00015). Some of the oscillatory eigenvalues has got a relatively low damping ratio less than 5 %, which is not desirable.

7.2 Loading of the synchronous generator

The loading of the synchronous generator is analyzed by the use of eigenvalues. The loading is increased from 0.5 MW to 1.9 MW and the effect on the eigenvalues on the system during three different load levels is presented in Figure 37.

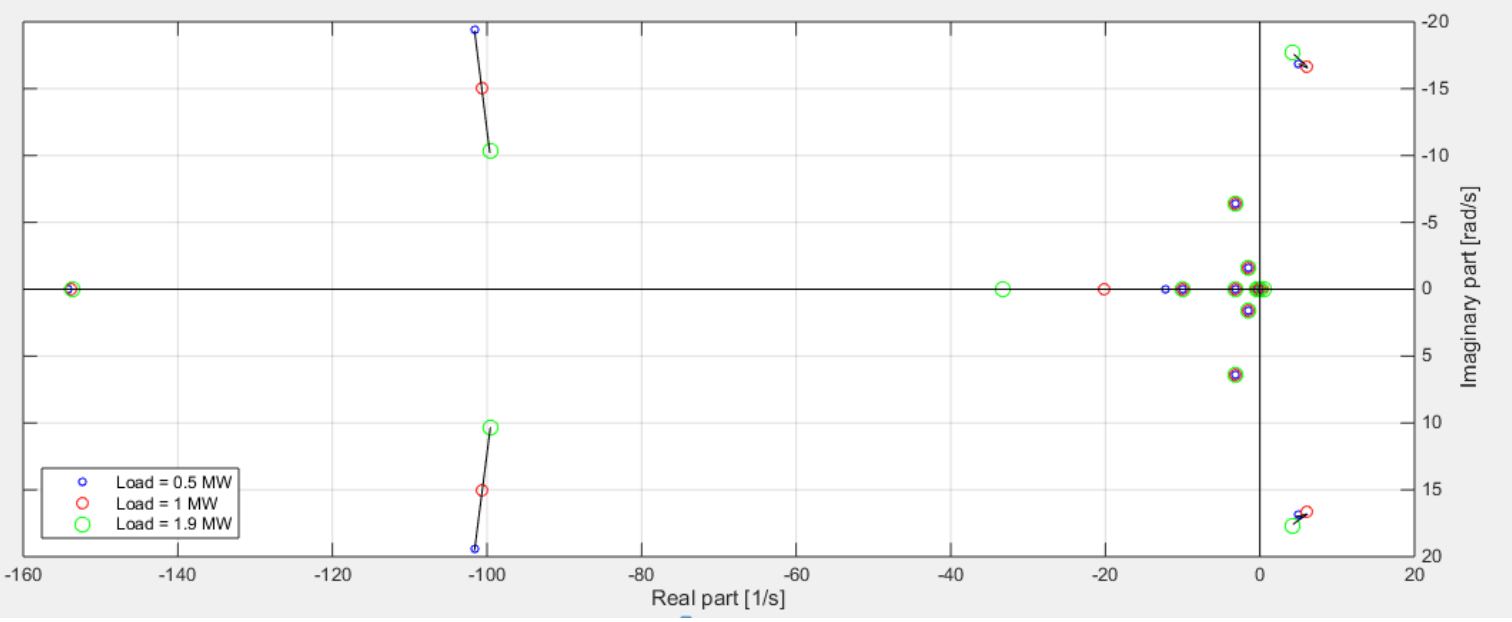

Figure 37: Eigenvalues of the system under different loads

It is observed that the damping of the instable oscillatory eigenvalue during increased loading has a slightly negative movement in the x-axis direction (becoming more stable) but also has a little increase in the y-axis, implying a greater oscillatory frequency.

The other eigenvalue that is reacting to the increased load is a stable oscillatory eigenvalue which has a positive movement in the x-axis direction and the oscillatory frequency is decreasing with increasing load.

The other observed eigenvalues in the system has little or no movement during increased loading of the system.

By comparing this to the load test for the model in PSCAD, it was also there observed an small increase in the oscillatory frequency during increased loading.

7.3 Impact of AVR

The impact of the gain on the AVR to the system is tested to see how the AVR contribute or not to the damping of the eigenvalues. The test done by the manufacturer of the AVR discussed in section 2 is used as a basis for this analysis. The AVR gain, Ka, is decreased from its initial value of 40 towards 1. The impact on the eigenvalues is shown in Figure 38 and tables with all the eigenvalues is given in appendix I.

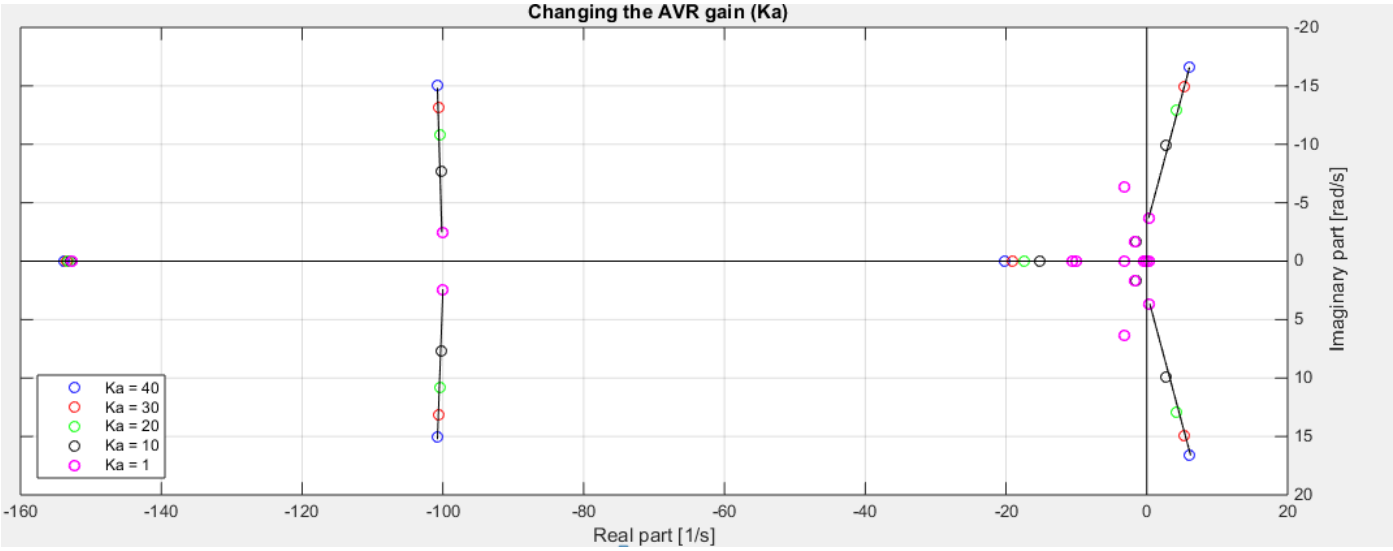

Figure 38: Eigenvalues when changing the AVR gain Ka.

Two of the eigenvalues is observed to have a significant movement by decreasing the gain in the AVR. It is also observed that a non-oscillatory eigenvalue is moving in a positive direction along the x-axis, meaning that this eigenvalue is becoming less stable, but still way of from becoming instable. The other eigenvalues in the system have little or no effect of the change in the AVR gain. The two oscillatory eigenvalues that was observed to be most affected by the change in the gain is presented in Table 4.

Table 4: The changes of the oscillatory eigenvalues when decreasing the gain of the AVR

Ka	Osc. mode 1		Osc. mode 2	
	Real part [1/s]	Damped frequency [Hz]	Real part [1/S]	Damped frequency [Hz]
40	-100,68	2,39	6,13	2,65
30	-100,51	2,09	5,26	2,38
20	-100,34	1,71	4,20	2,05
10	-100,17	1,22	2,76	1,58
1	-100,02	0,39	0,34	0,59

It can be noticed that these two eigenvalues are the same that was experiencing movement during the test with increased load in section 6.2. The eigenvalues in question is both decreasing their oscillatory frequency when the gain is moving towards 1. While the stable oscillatory eigenvalue named “osc. mode 1” is not experiencing any large movement in the real part, is the real part of the instable oscillatory eigenvalue named “osc mode 2” becoming less positive. This implies that both the oscillatory eigenvalues are getting better damped when decreasing the gain of the AVR. The instable oscillatory eigenvalue is also becoming more stable and is only marginally unstable when the gain of the AVR is equal to 1.

It is interesting to observe how the AVR gain set to 1 is affecting the system in the time-domain analysis as well. The active power from the synchronous generator with the AVR gain set equal to 1 is shown in Figure 39.

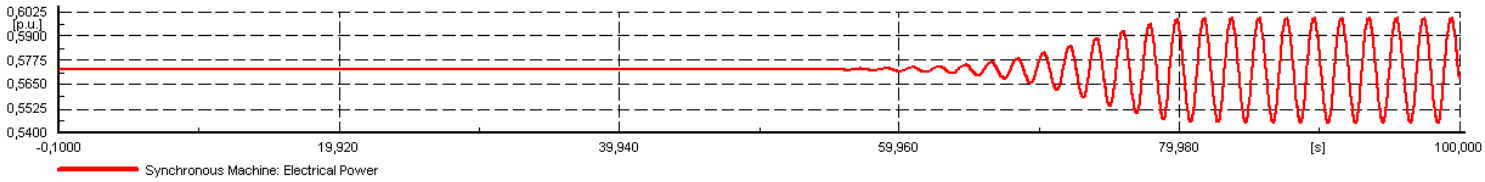

Figure 39: Active power from the synchronous generator with the AVR gain set to 1

The system remains stable for quite a while, but after about 60 seconds, oscillations is observed and they are increasing in amplitude. By t=80 s, standing oscillations is yet again observed in the active power of the synchronous generator.

This is however the same type of increase in the amplitude that was observed in the simulations with the PSCAD model. This might indicate that the model used in PSCAD is marginally unstable.

It should also be noted that even though a smaller gain of the AVR is making the system more stable based on the eigenvalues, it will make the system instable in other terms. The AVR is supposed to be able to act fast during changes in the terminal voltage of the synchronous generator as discussed in section 5.1. The AVR gain has to be tested for each system but in [9] is it mentioned that the AVR gain should be at least 20 in order to be able to act fast enough to prevent instability caused by a change in the terminal voltage.

7.4 Impact of rectifier

7.4.1 Changing the rectifier

In [2] is it mentioned that the system onboard the tug-boat is observed to become stable when the full-bridge diode rectifier was changed with a full-bridge thyristor rectifier. A simulation in [4] yielded a result that implied that the type of rectifier had no impact on the instability problem. It is however interesting to analyze the eigenvalues of the system with the two different types of rectifiers to see if there is any marginal change in the eigenvalues.

The plot for the eigenvalues of the system with the two different rectifier types is shown in Figure 40.

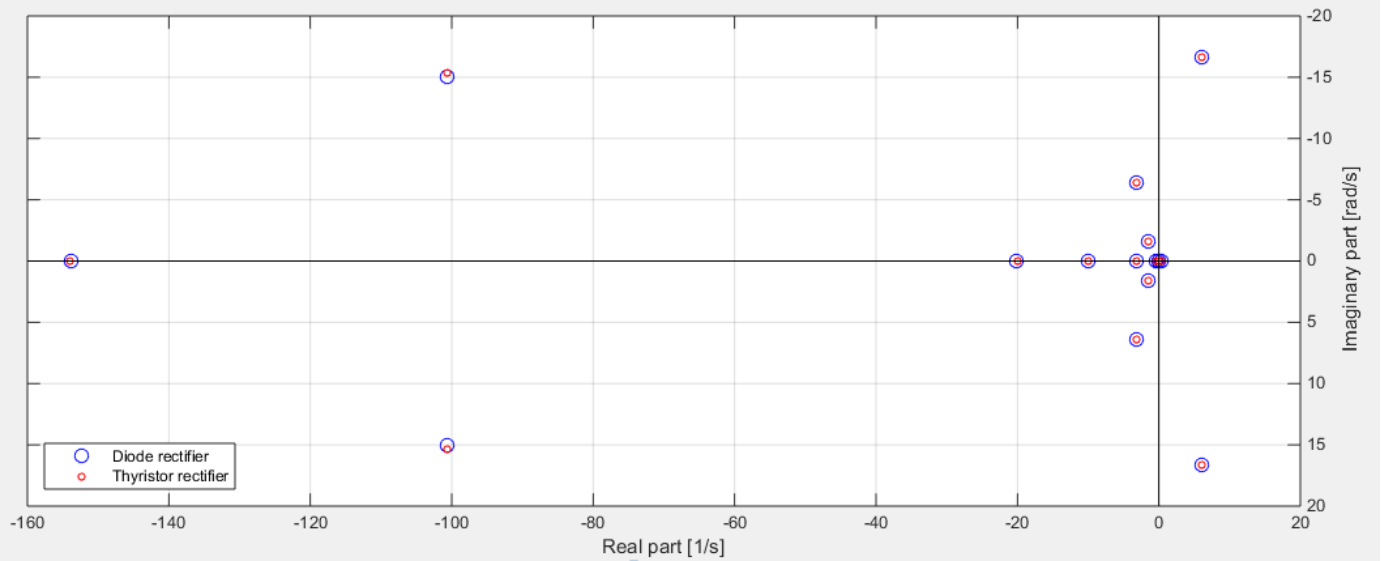

Figure 40: Eigenvalues for the system with diode-bridge rectifier and for a system with a thyristor-bridge rectifier

The eigenvalues are laying on top of each other for the two different rectifiers in the plot and only a small movement is observed in the eigenvalues. This is again shown in Table 5 where the eigenvalues for the two oscillatory modes with an observed movement is listed.

Table 5: Eigenvalues for the system with the diode-bridge rectifier and for the thyristor-bridge rectifier

	Osc. mode 1		Osc. mode 2	
Rectifier type	**Real part**	**Damped frequency**	**Real part**	**Damped frequency**
Diode	-100,68	2,39	6,13	2,65
Thyristor	-100,73	2,44	6,03	2,65

The movement in the negative direction for real part of the instable oscillatory eigenvalue is small and almost negligible when changing the rectifier type.

7.4.2 Decreasing the DC voltage

Controlling the firing angle of the thyristors in the rectifier is possible to implement in the model. The voltage at the DC terminal is then set to a predefined value and the firing angle for the thyristors is found based on equation 8 in section 5.2. The voltage at the DC side of the rectifier is set to 0.5 p.u. which would give a voltage of about 67 % of the AC voltage at the terminal of the synchronous generator.

The eigenvalues for the system with the thyristor rectifier controlled to Vdc = 0.5 p.u. and the initial reference of Vdc = 1 p.u. is presented in Figure 41. Tables for all the eigenvalues and time domain simulations is given in appendix J.

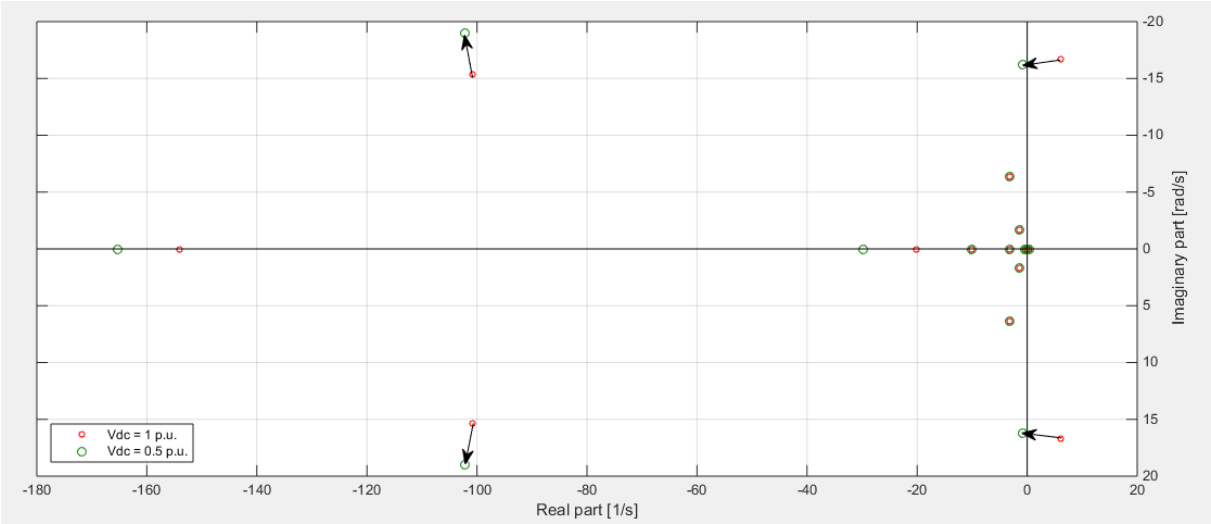

Figure 41: Eigenvalues for the system with the DC voltage of the rectifier set to 1 p.u. and 0.5 p.u.

Four eigenvalues are experiencing an effect to the decrease in the DC voltage at the rectifier. Two of them are non-oscillatory eigenvalues that is noticed to be become more negative. The two oscillatory eigenvalues that is observed to have an effect of the decreased DC voltage are the same as have been experienced to move in the other simulations as well. The new eigenvalues with Vdc = 0.5 p.u. is presented in Table 6.

Table 6: Eigenvalue for the system with the DC voltage at the thyristor-bridge rectifier set to 0.5 p.u.

	Osc. mode 1		Osc. mode 2	
Rectifier type	**Real part**	**Damped frequency**	**Real part**	**Damped frequency**
Thyristor	-102,28	3,02	-0,85	2,58

It is interesting to observe that the instable oscillatory eigenvalue is moving straight to the left and becoming marginally stable.

Taking a look at the active power from the synchronous generator in Figure 42.

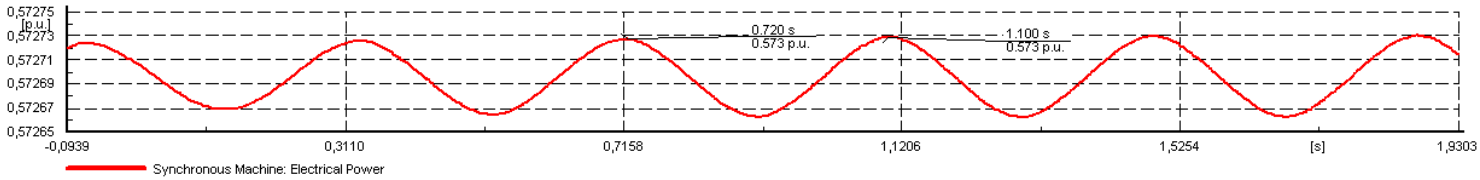

Figure 42: Active power from the synchronous generator with the DC voltage of the thyristor rectifier set to 0.5 p.u.

Oscillations is still observed and the system has not become stable, but it is noticed that the oscillations frequency has increased to 2.63 Hz compared to the initial situation with an oscillation frequency of 1.18 Hz.

7.4.3 Decreasing the DC voltage and the AVR gain Ka

So far has the simulations with the thyristor rectifier not yielded a result which is consistent with the observations onboard the tug-boat when the rectifier was changed from a diode rectifier to a thyristor rectifier. It can however be believed that some additional tuning was done to the system when the rectifier was changed. Based on the simulation done so far in this thesis have a decrease in the AVR gain been able to stabilize the eigenvalues in addition to decreasing the DC voltage at the DC terminal of the thyristor rectifier to 0.5 p.u.

A test to see if the combined effect of these two tests can enhance the stability is taken. The eigenvalues for the thyristor rectifier with Vdc = 0.5 p.u., 1 p.u. and a situation with Vdc = 0.5 p.u. and the AVR gain set to Ka = 20 is presented in Figure 43. Time domain simulations and the tables with all the eigenvalues is presented in appendix J.

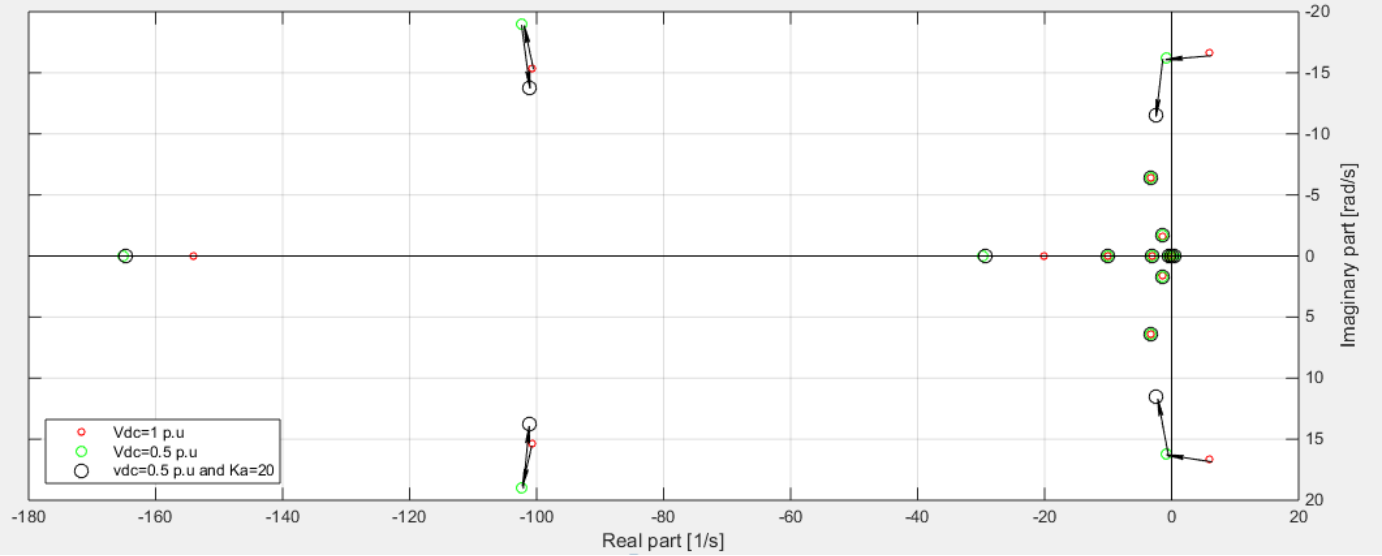

Figure 43: Eigenvalues for the thyristor rectifier with Vdc = 0.5 p.u., Vdc= 1 p.u. and Vdc = 0.5 p.u. and Ka = 20

The previous oscillatory modes are acting on the change in the two parameters. The new eigenvalues for this situation with the DC voltage of the rectifier set to 0.5 p.u. and the AVR gain, Ka, set to 20 is shown in Table 7.

Table 7:Eigenvalues for the thyristor rectifier with Vdc = 0.5 p.u. and Ka = 20

	Osc. mode 1		Osc. mode 2	
Rectifier type	**Real part**	**Damped frequency**	**Real part**	**Damped frequency**
Thyristor	-101,22	2,19	-2,40	1,83

The previous instable oscillatory eigenvalue which became marginally stable with the DC rectifier voltage set to 0.5 p.u. is now increasing its stability with both more movement towards the left on the x-axis and a lower damped frequency.

For the time-domain analysis of the active power from the synchronous generator presented in Figure 44 is it now observed that the previous standing oscillations is damped out and the system is considered to be stable.

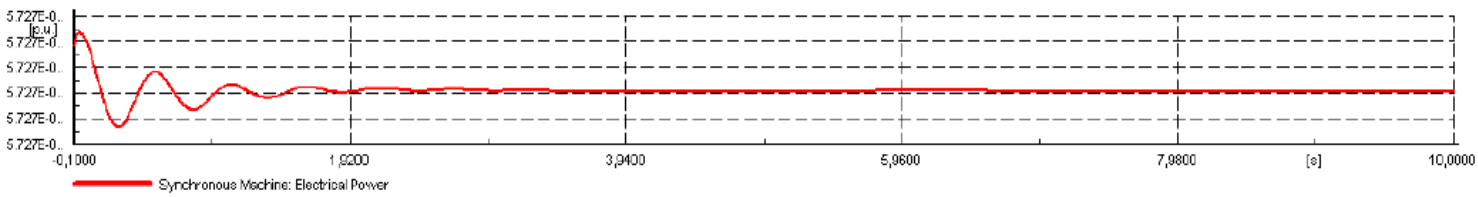

*Figure 44: Active power from the synchronous generator with reduced DC voltage of the rectifier. The scale is 5.72*10^(-01), or 0.572 p.u.*

Currents

The currents in the system is analyzed in an attempt to see why the decreased voltage at the DC terminal of the rectifier may contribute to enhanced stability. The currents in the system with the diode rectifier is shown in Figure 45.

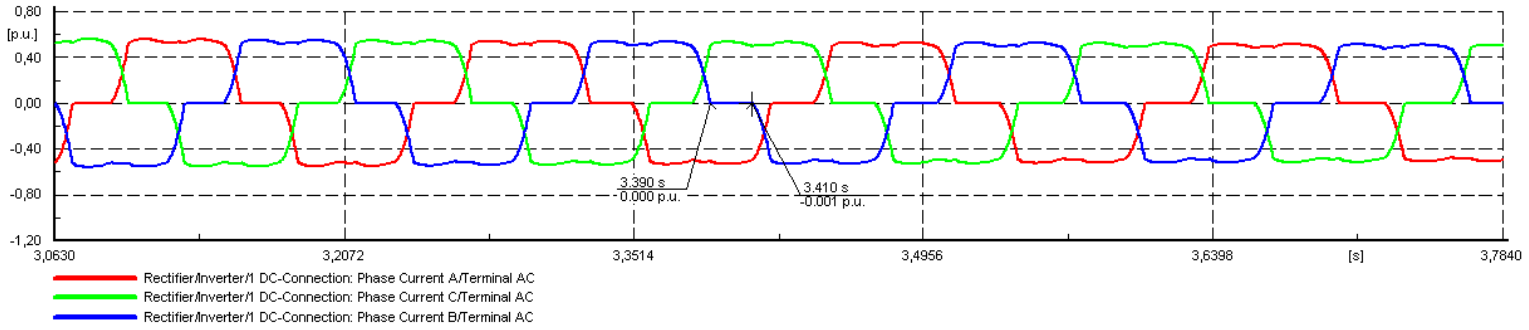

Figure 45: Currents in the system with the diode rectifier

The observed time delay in the current cause by the rectifier is about 3.410-3.390 = 0.02 s.

The currents in the system for the situation with the thyristor rectifier and the DC voltage set to 0.5 p.u. is shown in Figure 46.

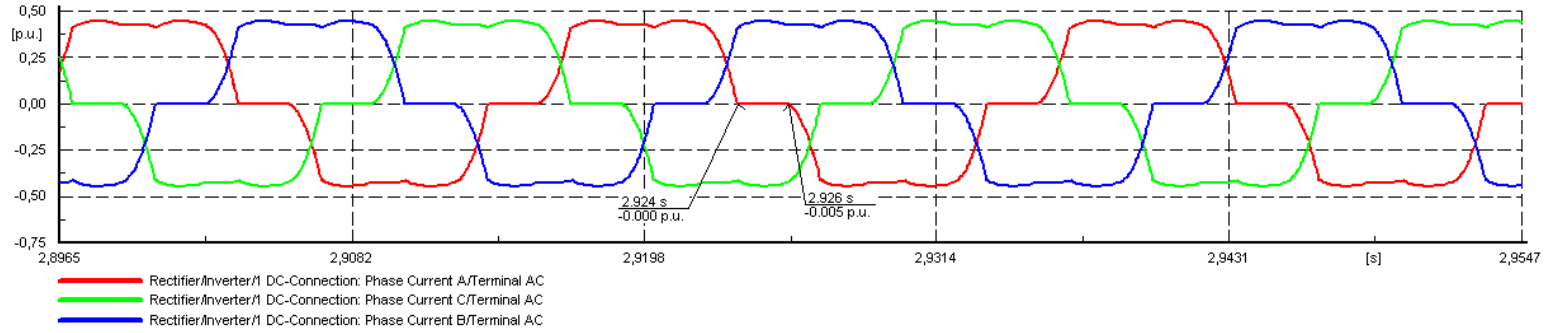

Figure 46: Currents in the system with the thyristor rectifier with the voltage at the DC terminal set to 0.5 p.u.

The time delay caused by the rectifier at this situation yields a time delay of 2.926-2.924 = 0.002 s. This is a reduction in the time delay by a factor of ten compared with the diode rectifier.

The observed transient disturbance by the rectifier seem to be of a less significant degree when the DC voltage is decreased to a lower value.

7.5 Power System Stabilizer

A power system stabilizer with speed as input named “PSS1A” is chosen to test if this can enhance the damping of the system. The reason for choosing this PSS is that it has a simple design and is easy to implement in the system. The block diagram of the PSS is given in appendix G.

The instable oscillatory eigenvalue presented in Table 8 from the initial instable system is used for the design of the lead/lag filter.

Table 8: Instable oscillatory eigenvalue used for design of the PSS

Real part [1/s]	Imaginary part [rad/s]	Damped frequency [Hz]	Angle [deg]
6,14	17,72	2,64	69,74

Based on the phase lag obtained from the simulation program is it possible to calculate the first order filter for the PSS.

$$T1, T4 = \frac{1}{\omega 1} * tan\left(45° + \frac{\varphi}{2n}\right) = \frac{1}{17.72} * tan\left(45° + \frac{69{,}74}{2 * 1}\right) = \ 0.23$$

$$T2, T3 = \frac{1}{\omega 1} * tan\ \frac{1}{\left(45° + \frac{\varphi}{2n}\right)} = \frac{1}{17.72} * tan\ \frac{1}{\left(45° + \frac{69.74}{2 * 1}\right)} = 0.000706$$

This yields the lead/lag filter used for the model:

$$Filter = (\frac{0.23 * s + 1}{0.000706 * s + 1})$$

The eigenvalues for the system with the PSS added is shown in Figure 47.

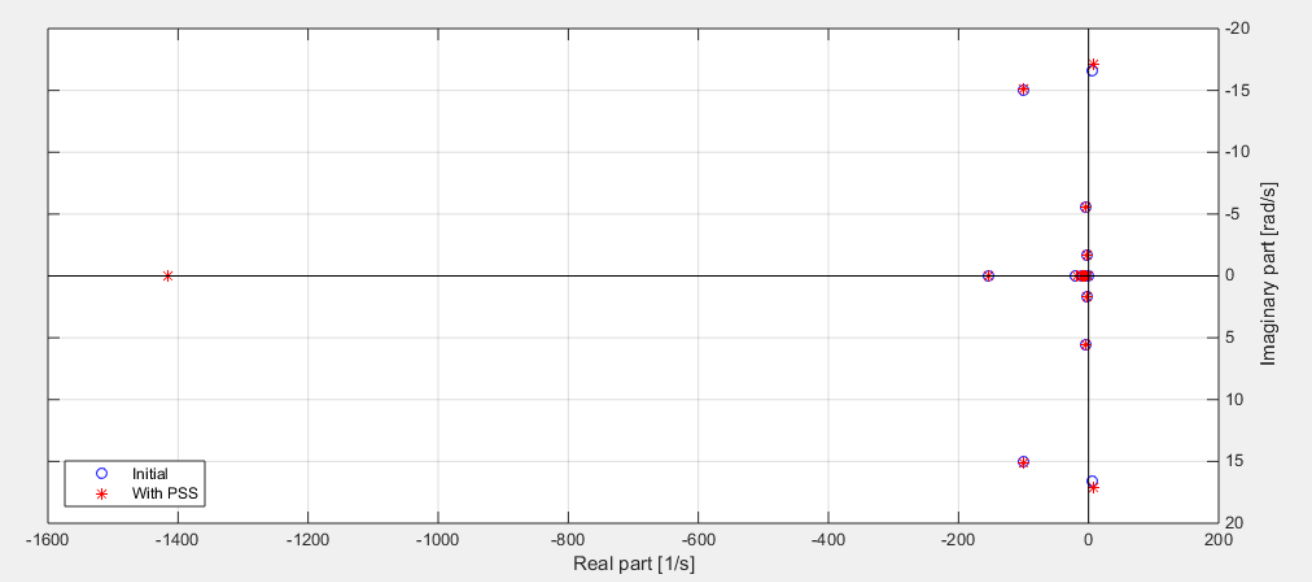

Figure 47: Eigenvalues for the instable system with a PSS added

No movement of interest is observed in the eigenvalues. It is further tried to increase the washout time constant to see the effect this will have. The eigenvalues for the increase in the washout time constant is given in Figure 48.

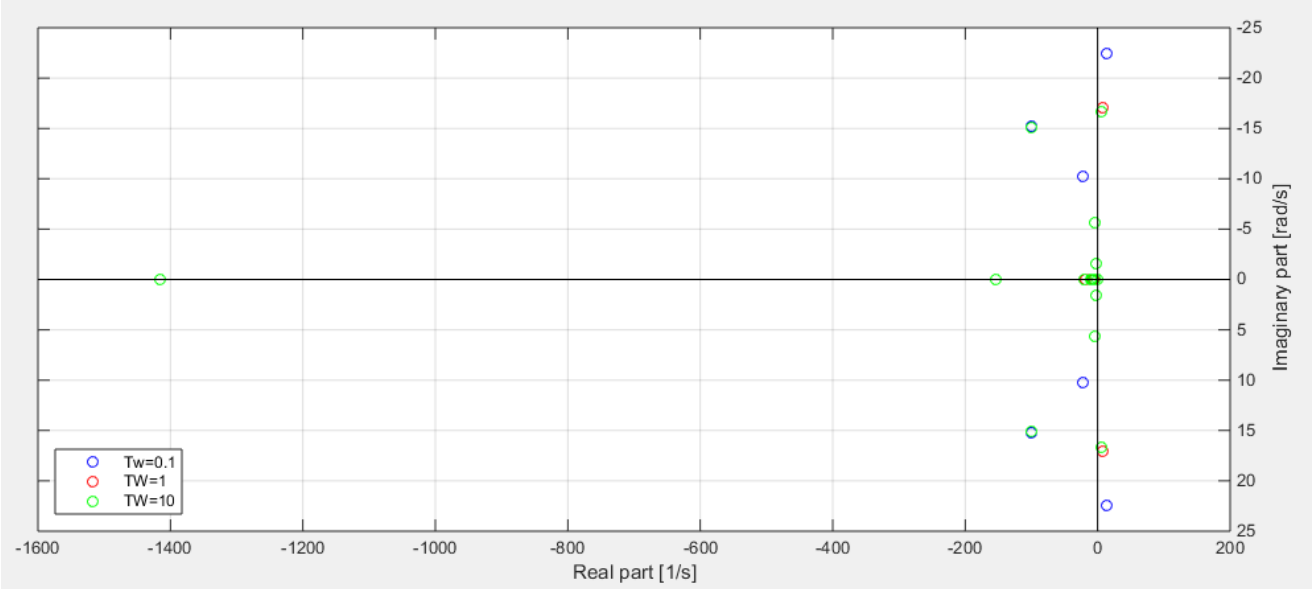

Figure 48: Eigenvalues for the instable system during increase in the washout time constant

The instable eigenvalue is increasing in both real and imaginary value when the washout time constant is decreased from Tw=1 to Tw=0.1. For the situation with Tw=10 a small decrease is observed in both real and imaginary value of the eigenvalue in question.

The effect of the gain is further tested to see if it will move the eigenvalue in any direction while keeping the same parameters for the filter and setting the washout time constant, Tw=1.

The eigenvalues for this situation is presented in Figure 49.

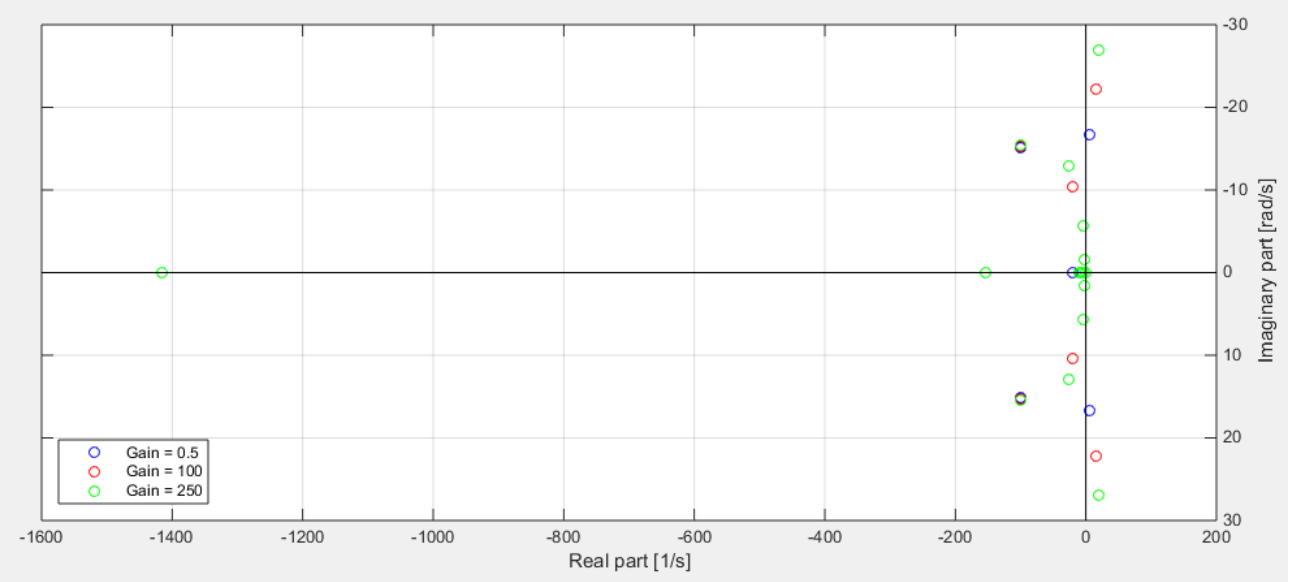

Figure 49: Effect of changing the PSS gain

The increased change in the gain of the PSS moves the eigenvalue to the right and increasing the oscillatory frequency of the eigenvalue. Decreasing the PSS gain to 0.5 gives a slight movement to the left and a decrease in the oscillatory frequency.

8 Discussion

Based on the assumption that the synchronous generator in question may have been poorly damped, a study of the inertia constant was undertaken. The inertia constant defines the rotating mass of the rotor quantified to the machine rating. Increasing the inertia constant in a synchronous machine that is experiencing oscillations in the output parameters should increase the damping of the synchronous generator and ultimately reduce the observed oscillations. The inertia constant was tested in a specter from 0.1 seconds to 5 seconds. The system became marginally stable with an inertia constant of 2 seconds. When the inertia constant was further increased to 5 seconds it became fully stable and no oscillations was observed in the output parameters.

The limited theory about this type of instability problem has got one very specific solution. The solution is to add an additional q-axis damper winding with the value of 0.546 p.u. to the rotor of the synchronous generator. This additional damper winding is designed to only work in the transient state and provide an extra dampening torque in this state. This is also discussed and concluded with in [6], [7] and [5]. This is the state were the synchronous generator is believed to operate due to the constant switching of the diodes in the rectifier. The system was stable and no instability was observed when adding the additional damper winding.

Changing the internal parameters of the synchronous generator, or in this case, change the synchronous generator with a new one with similar MVA rating and voltage level yielded a stable system. This implies that the parameters of the instable 1940 kVA synchronous generator can be the cause of the poorly damping due to the fact that the rest of the system, i.e. simulation model, was kept constant.

The simulations with the battery connected at the DC terminals made the system experience more severe instability problem with greater amplitudes of the oscillations and higher oscillation frequency. At a load close to the rated capacity of the synchronous generator the system was stable. The battery model used is however very simple and this model does not recreate the battery system that is used onboard the tug-boat. The battery should have been implemented with a control circuit that provided power when the power demand exceeded the power delivered by the synchronous generator. The battery used in the model was active all the time and this might have caused the system to be more unstable. The battery should also have risen the voltage at the DC bus during the situation with the load of 1.9 MW, which it did not.

The AVR gain was reduced from 40 to 1 in order to see how the system would react to a change in the AVR settings. It was observed that the instable oscillatory eigenvalue moved to the left, becoming more stable and the oscillatory frequency of the eigenvalue was also observed to be reduced. The reduction in oscillatory frequency was also observed in the test done by the

manufacturer of the AVR when the instability in the system was first observed. Even though the eigenvalue became barely stable when the AVR gain was reduced to 1, it was poorly damped and oscillations was observed in the system after a about 60 s. It is also worth mentioning that a AVR gain as low as 1 will not yield a satisfactory control of the exciter voltage induced into the rotor of the synchronous generator.

Based on information about an improvement of the stability by changing the rectifier on the tug-boat, it was tried to change from a full-bridge diode rectifier to a full-bridge thyristor rectifier. The result did however not yield a result that proved that a change of the rectifier was able to give a satisfactory stable system. This is however not very surprising having the theory presented in section 5 in mind. When the firing angle, α, of the thyristors in the thyristor rectifier is not controlled, the voltage will be the same at the DC terminals as for the diode-bridge rectifier. This means that the thyristor rectifier is basically working as a diode-bridge rectifier and no difference should be noticed.

Changing the firing angle, α, of the thyristor rectifier so that the DC voltage was kept at 0.5 p.u. moved the instable eigenvalues in a straight line to the left and making it more stable. The real part of the eigenvalue became negative, but only barely and the eigenvalue was poorly damped, making the system unstable. The improved stability might have been due to the fact that the time delay for the currents in the system caused by the rectifier is observed to be smaller when the DC voltage is reduced. The transient instability caused by the rectifier might then be of a smaller degree seen by the synchronous generator. By changing the AVR gain to 20 in addition to reducing the DC voltage made the instable oscillatory eigenvalue become more stable and have a smaller oscillation frequency and ultimately provide a stable system.

Adding a power system stabilizer to the model in order to enhance the damping was initially believed to be a valid solution due to the fact that other simulations related to improved damping yielded a positive result. This was however not observed. Whether it might have been poorly chosen parameters of the PSS or other factors is not answered in this thesis. A great amount of time during this thesis was used trying to implement a more advanced PSS to the model and optimize the parameters by using an optimizing method called particle swarm [17]. Due to time limitations and complications when connecting Matlab to Powerfactory in order to use Matlab for the optimization procedure of the eigenvalues in Powerfactory, it was not possible to finish this work and provide a valid solution. It is still believed that a PSS might be a solution for this kind of stability problem based on the fact that the key to solve the instability problem is related to enhancement of the damping of the synchronous generator.

9 Conclusion

It can seem plausible to connect the cause of the observed instability to the synchronous generator in the system based on the simulations that proves that an increased damping in the synchronous generator make the system stable. The enhanced damping proved by increasing the inertia constant of the synchronous generator and the additional damper winding that was added to the synchronous generator gave a satisfactory result. The aim to reduce the short-circuit currents in the system and choosing parameters of the synchronous generator based on this might have been taken at the expense of the stability related to the synchronous generator. It is however observed that other components in the system amplifies the instability when operating together with the synchronous generator.

The battery causes the instability to increase and the oscillations to become more severe. This can however not be concluded with in this thesis based on the fact that the model of the battery used is very simple and cannot recreate the actual system used onboard the tug-boat.

The rectifier makes the synchronous generator experience a constant small transient disturbance during operation due to the switching of the diodes in the rectifier. This is an additional factor that increase the instability problem for a synchronous generator that can be characterized as marginally stable in the first place. It is however observed that by controlling the voltage at the DC side of the rectifier it is able to achieve a more stable system. This is believed to be more related to the reduced switching cycle of the thyristors compared with the diodes, more than it is related to the rectifier itself.

Based on the fact that the increased damping by the inertia constant and the damper windings has yielded good result in relation to the system stability, it was believed that a PSS might give a similar result. The introduction of a PSS to the system has not yielded a satisfactory result and further work on this solution is recommended.

To make the system stable it is evident that the damping of the synchronous generator has to be enhanced in some way or the other. Increasing the inertia constant or adding an additional damper winding requires a severe redesign of the system and might not be applicable.

As a closing remark it should be noted that when designing systems where a synchronous generator is operating with a rectifier in an islanded system, a fair amount of attention should be directed to the synchronous generator and its internal parameters to ensure that a stable operation is achieved when the system is commissioned.

10 Further work

- More work related to the implementation of the power system stabilizer.

- Laboratory experiments to verify the findings.

- Take a closer look into generator design based on the findings from the parameters study in [2].

11 Bibliography

[1] T. H. Helland, "Dynamic analysis of the stability of a diode bridge rectifier connected synchronous generator with high synchronous reactances," Trondheim, 2014.

[2] T. H. Helland, "Stability Analysis of Diode Bridge Rectifier-Loaded Synchronous Generators Characterized with High Values of Reactances," Trondheim, 2015.

[3] BASLER, "DC grid system test report," singapore, 2014.

[4] J. Kirkeluten, "Stability of Synchronous Generators," Trondheim, 2015.

[5] M. Weiming, H. An, L. Dezhi and Z. Gaifan, "Stability of a Synchronous Generator with Diode-Bridge Rectifier and Back-EMF Load," 2000.

[6] H. Auinger and G. Nagel, "Vom trnsienten Betriebsverhalten herrührende Schwinungen bei einem ûber Gleichrichter belasteten Syncrongenrator," Siemens co. Ltd., 1980.

[7] M. J. Hoeijmakers, "The (in)stability of a synchronous machine with diode rectifier," The Netherlands.

[8] "http://www.herzo-agenda21.de/_ilse/wind/wind5e.html," [Online].

[9] J. Machowski, J. W. Bialek and J. R. Bumby, Power System Dynamics, West Sussex, United Kingdom: John Wiley & Sons Ltd, 2012.

[10] King Saud University, " King Saud University," [Online]. Available: http://faculty.ksu.edu.sa/eltamaly/Documents/Courses/EE%20339/Alternator.pdf. [Accessed March 2016].

[11] N. Mohan, T. M. Undeland and W. P. Robbins, Power Electronics, John Wiley & Sons, 2003.

[12] B. Pal and C. Balarko, Robust control in power systems, USA: Springer science, 2005.

[13] A. Hammer, "Analysis of IEEE power system stabilizer models," NTNU, Trondheim, 2011.

[14] N. Martins and L. T. G. Lima, "Eigenvalue and Frequency domain analysis of small signal electromechanical stability problems," 1989.

[15] O. Ruhle, "Eigenvalue Analysis – All Information on power system oscillation behavior rapidly analyzed," Siemens, 2006.

[16] DIgSILENT GmbH, "DigSILENT PowerFactory User Manual Version 15," DIgSILENT GmbH, Gomaringen, Germany, 2015.

[17] M. Eslami, H. Shareef, A. Mohamed and S. P. Ghoshal, "Tuning of power system stabilizers using particle swarm optimization with passive congregation," 2010.

12 Appendices

12.1 Appendix A

AC1A AVR block diagram

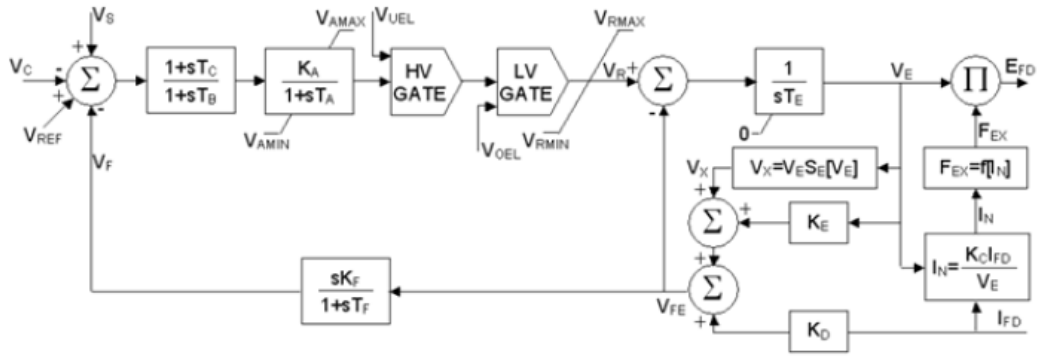

Figure 50: Block diagram AC1A AVR

AC1A AVR parameters

Table 9: AVR AC1A parameters:

Parameter	Symbol	Value	Unit
Lead time constant	TC	0	s
Lag time constant	TB	0	s
Regulator gain	KA	40	pu
Regulator time constant	TA	0.02	s
Maximum regulator internal voltage	VAMAX	5	pu
Minimum regulator internal voltage	VAMIN	-5	pu
Maximum regulator output	VRMAX	6	pu
Minimum regulator output	VRMIN	-5	pu
Rate feedback gain	KF	0.03	pu
Rate feedback time constant	TF	1	s
Exciter time constant	TE	0.8	s
Exciter constant related to field	KE	1	pu
Field circuit commutating reactance	KC	0.2	pu
Demagnitizing factor	KD	0.38	pu
Saturation at VE1	SE(VE1)	0.1	pu
Exciter voltage for SE1	VE1	4.18	pu
Saturation at VE2	SE(VE2)	0.03	pu
Exciter voltage for SE2	VE2	3.14	pu

12.2 Appendix B

Two-stroke diesel engine:

Table 10: Diesel engine parameters

Parameter	Symbol	Value	Unit
Engine rating	Sm	2	MW
Machine rating		2	MVA
Machine rated speed	Wm	3600	rpm
Gear box efficiency	n	0.98	Pu
Gear ratio		1	

Governor:

Table 11: Governor parameters

Parameter	Symbol	Value	Unit
Proportional gain	K	20	pu
Integral time constant	T1	0.01	s
Maximum limit	MAX	10	pu
Minimum limit	MIN	-10	Pu

12.3 Appendix C

Load plots without the battery

Load = 1 MW

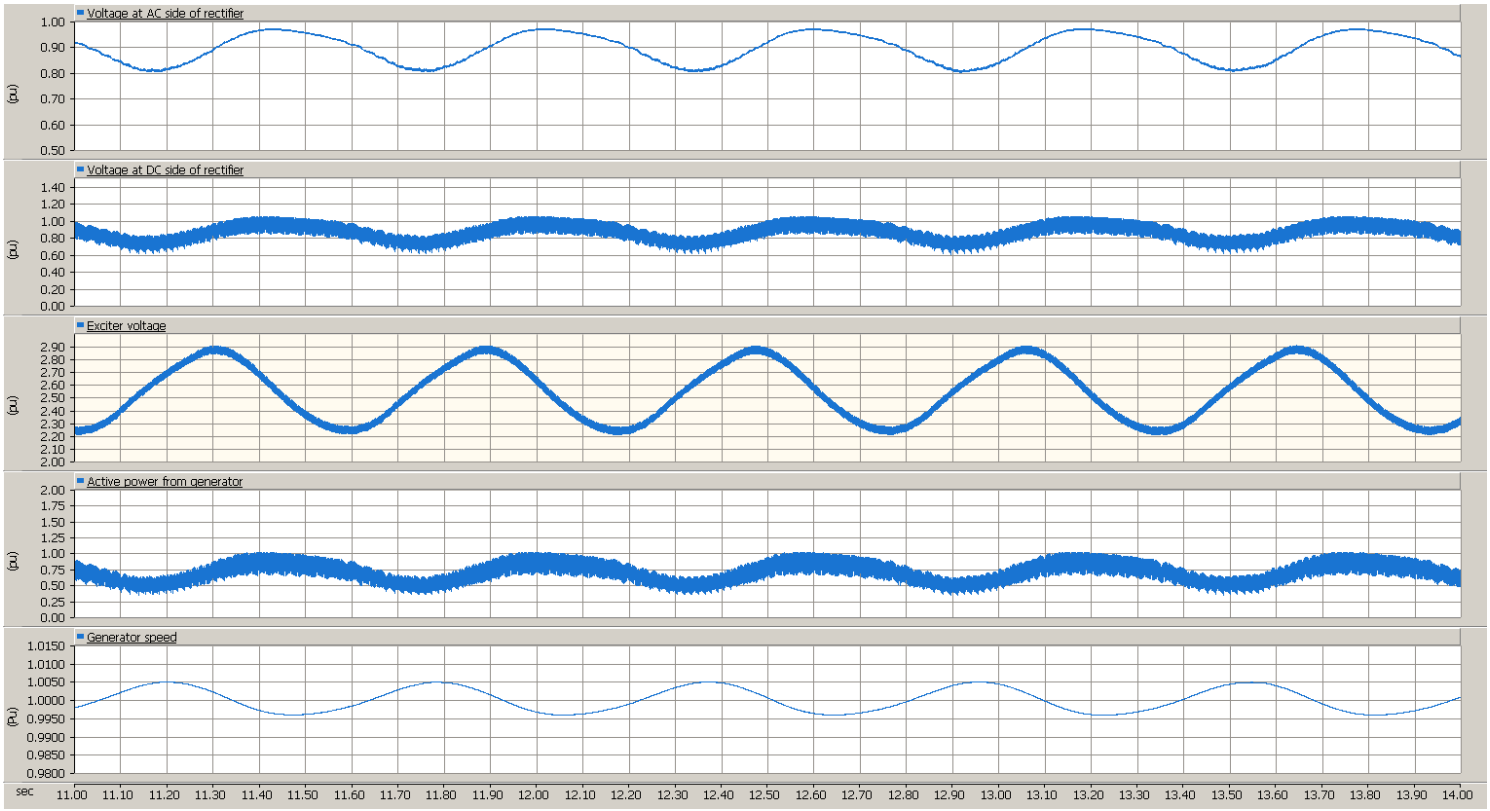

Figure 51: Synchronous generator supplying a load of 1 MW through a rectifier. Voltage at AC side of rectifier, voltage at DC side of rectifier, exciter voltage, active power from the synchronous generator and the speed of the synchronous generator.

Load = 1.9 MW

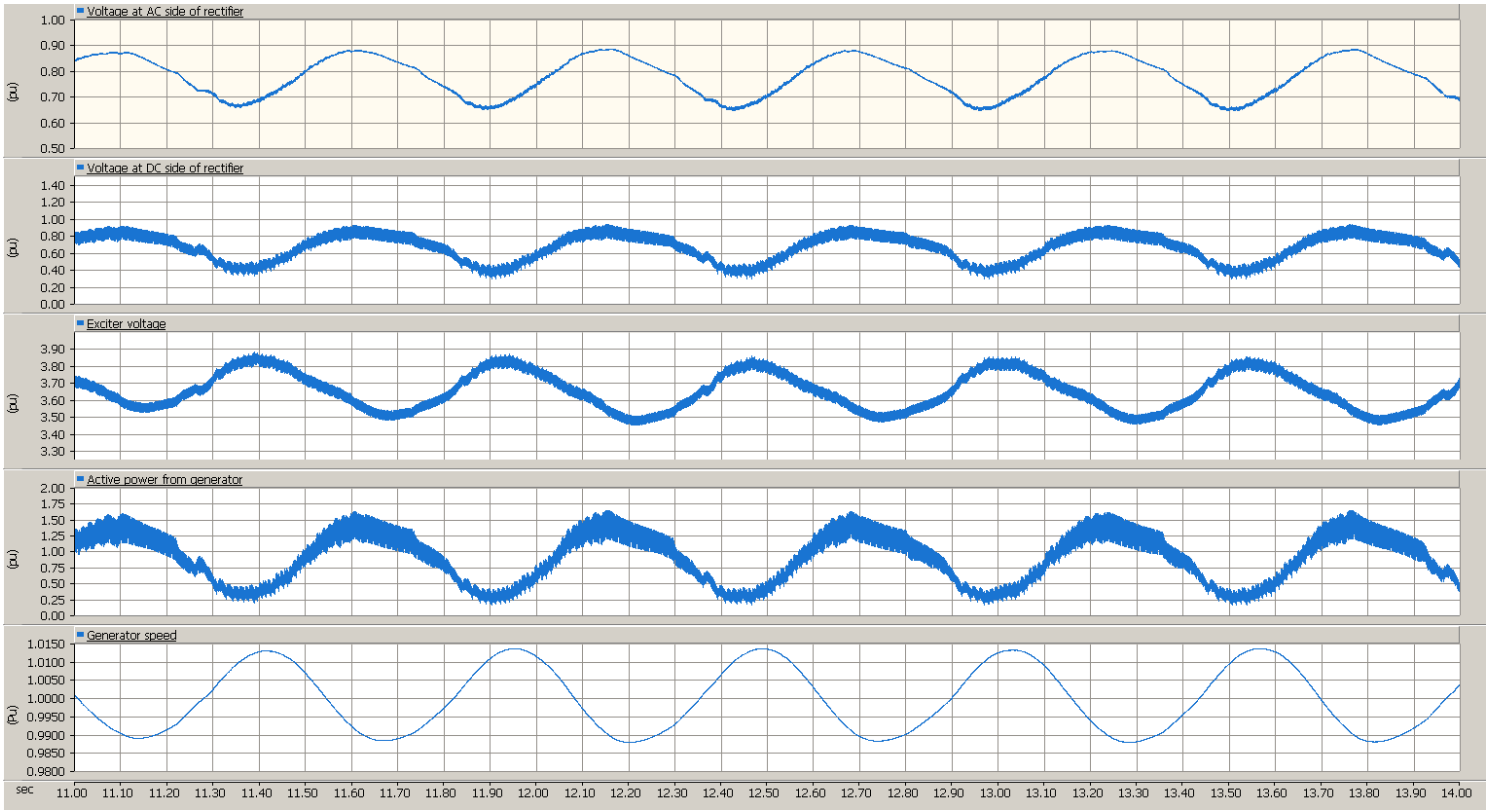

Figure 52: Synchronous generator supplying a load of 1.9 MW through a rectifier with a load of 1.9 MW. Voltage at AC side of rectifier, voltage at DC side of rectifier, exciter voltage, active power from the synchronous generator and the speed of the synchronous generator.

12.4 Appendix D

Load plots with the battery

Load = 1 MW:

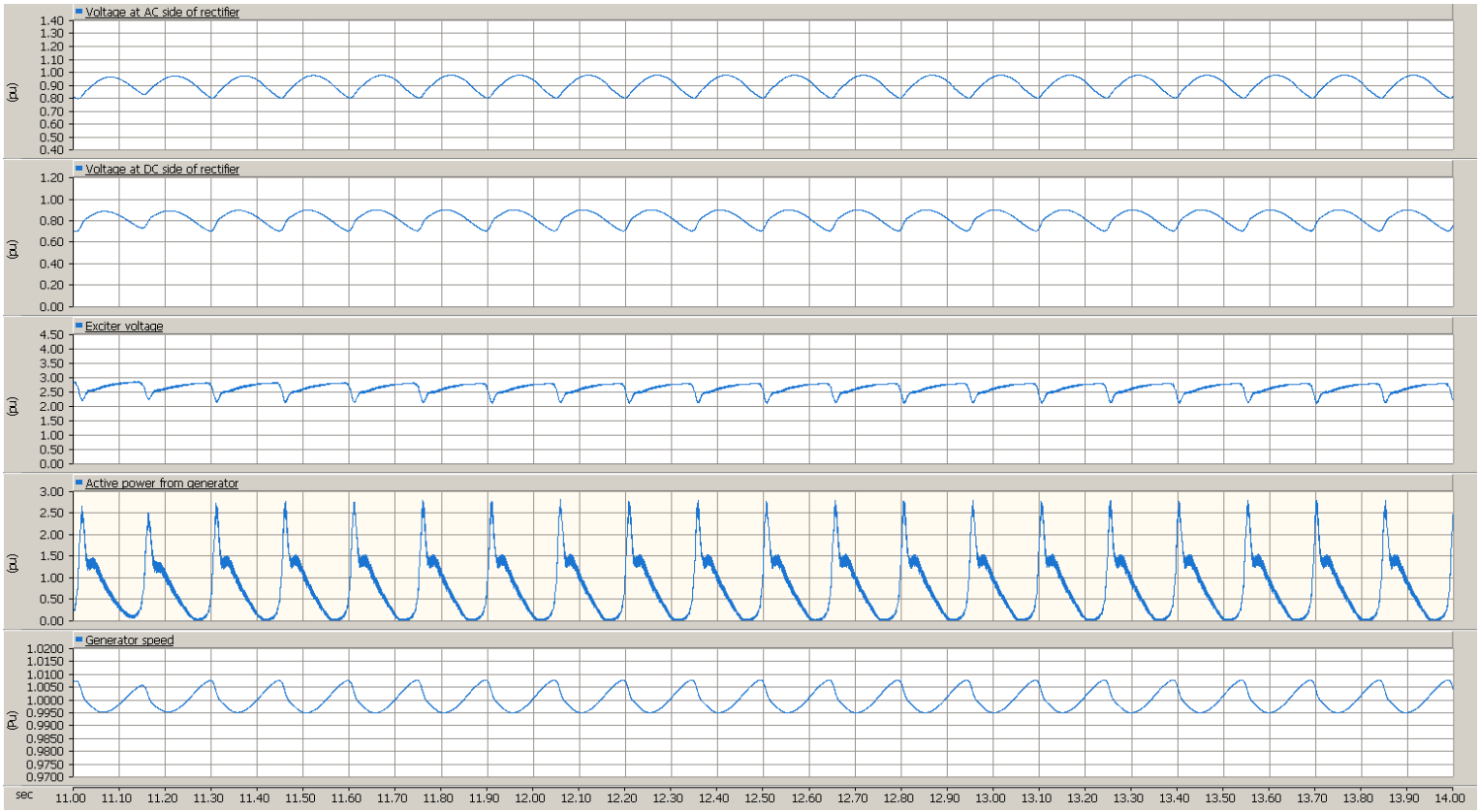

Figure 53: Synchronous generator supplying a load of 1 MW through a rectifier with a battery connected at the DC terminal.. Voltage at AC side of rectifier, voltage at DC side of rectifier, exciter voltage, active power from the synchronous generator and the speed of the synchronous generator.

12.5 Appendix E

Inertia constant

H = 0.1 s:

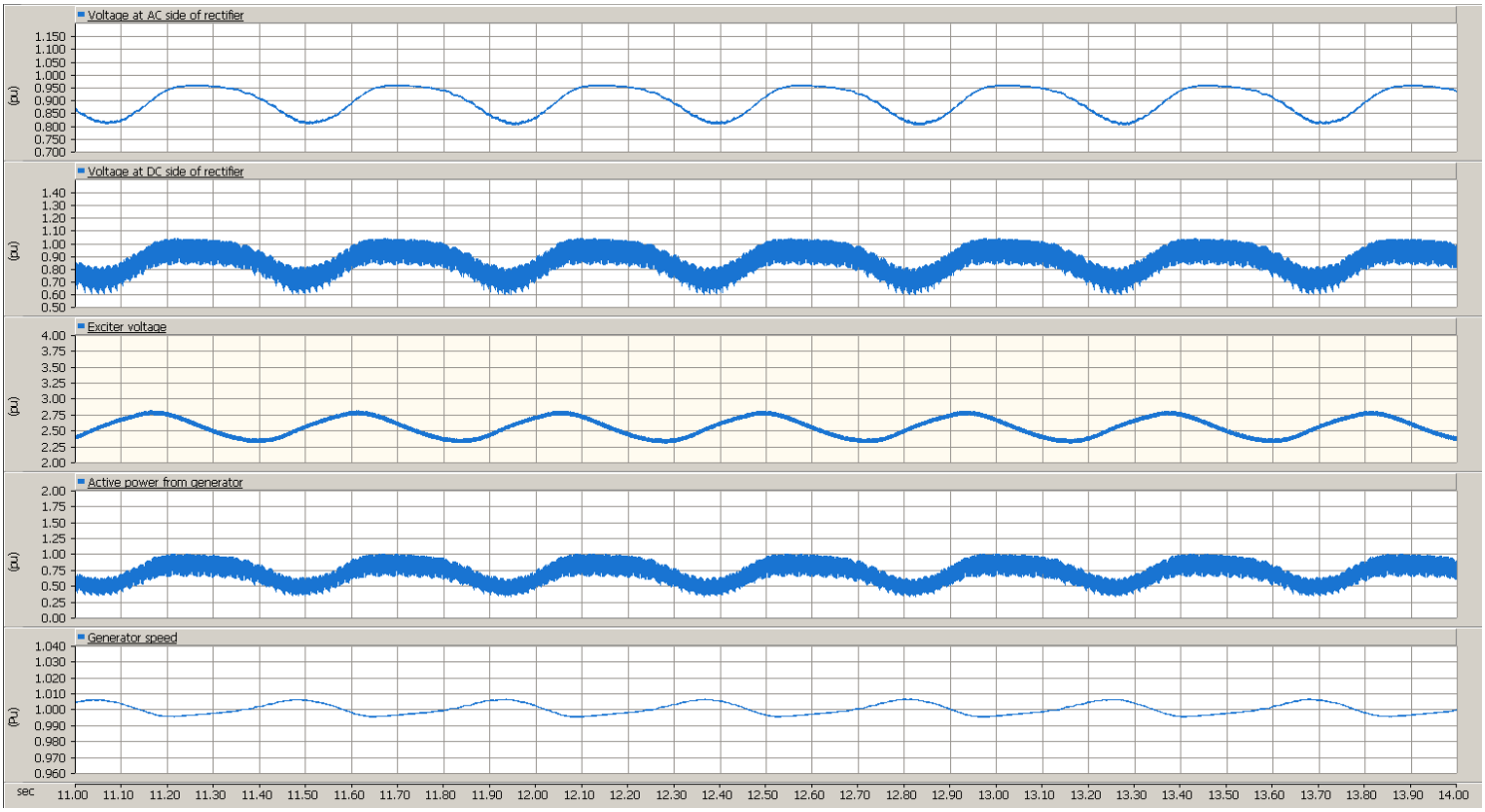

Figure 54: Synchronous generator supplying a load of 1 MW through a rectifier with H = 0.1 s. Voltage at AC side of rectifier, voltage at DC side of rectifier, exciter voltage, active power from the synchronous generator and the speed of the synchronous generator

H = 1 s:

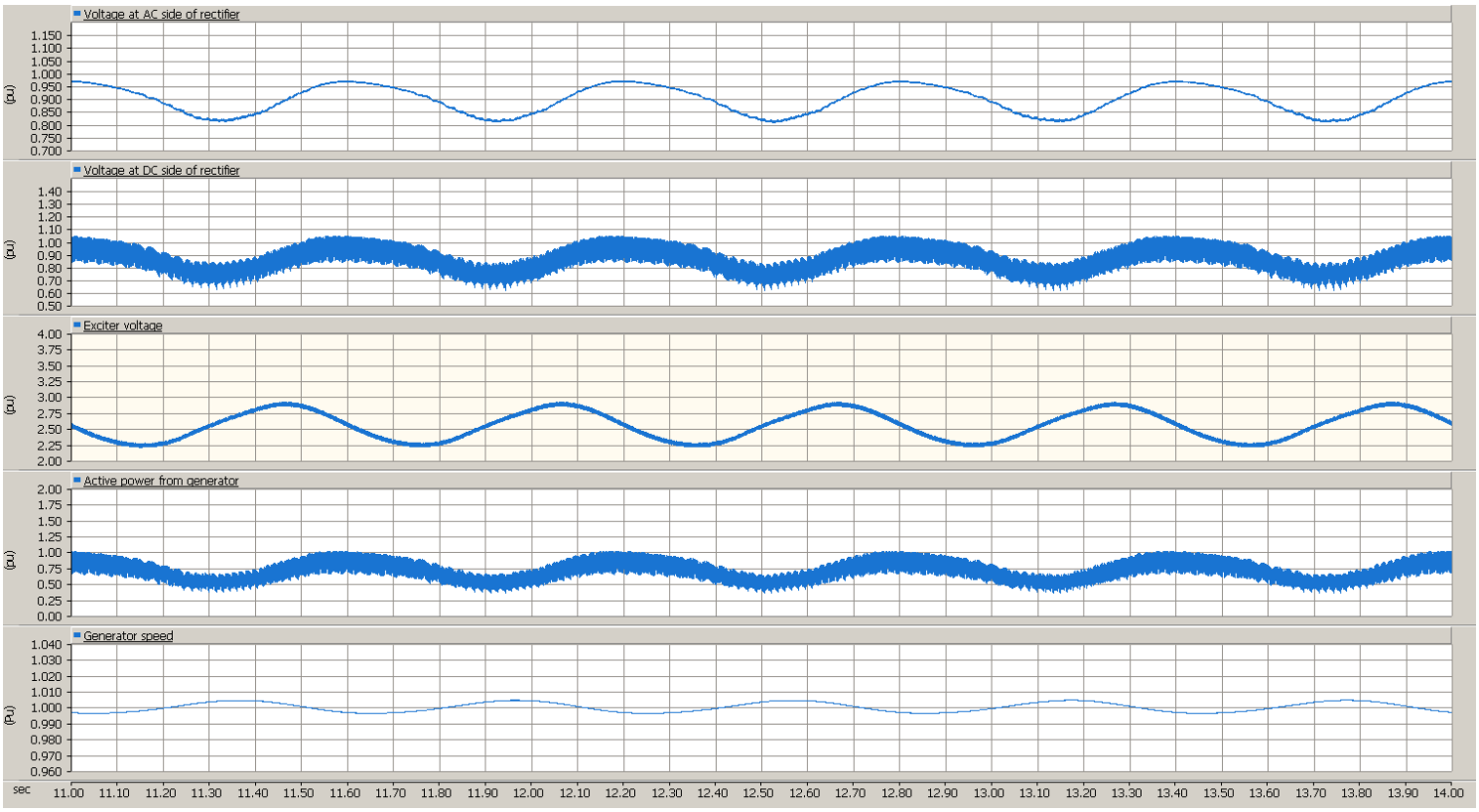

Figure 55: Synchronous generator supplying a load of 1 MW through a rectifier with H = 1 s. Voltage at AC side of rectifier, voltage at DC side of rectifier, exciter voltage, active power from the synchronous generator and the speed of the synchronous generator

H = 2 s:

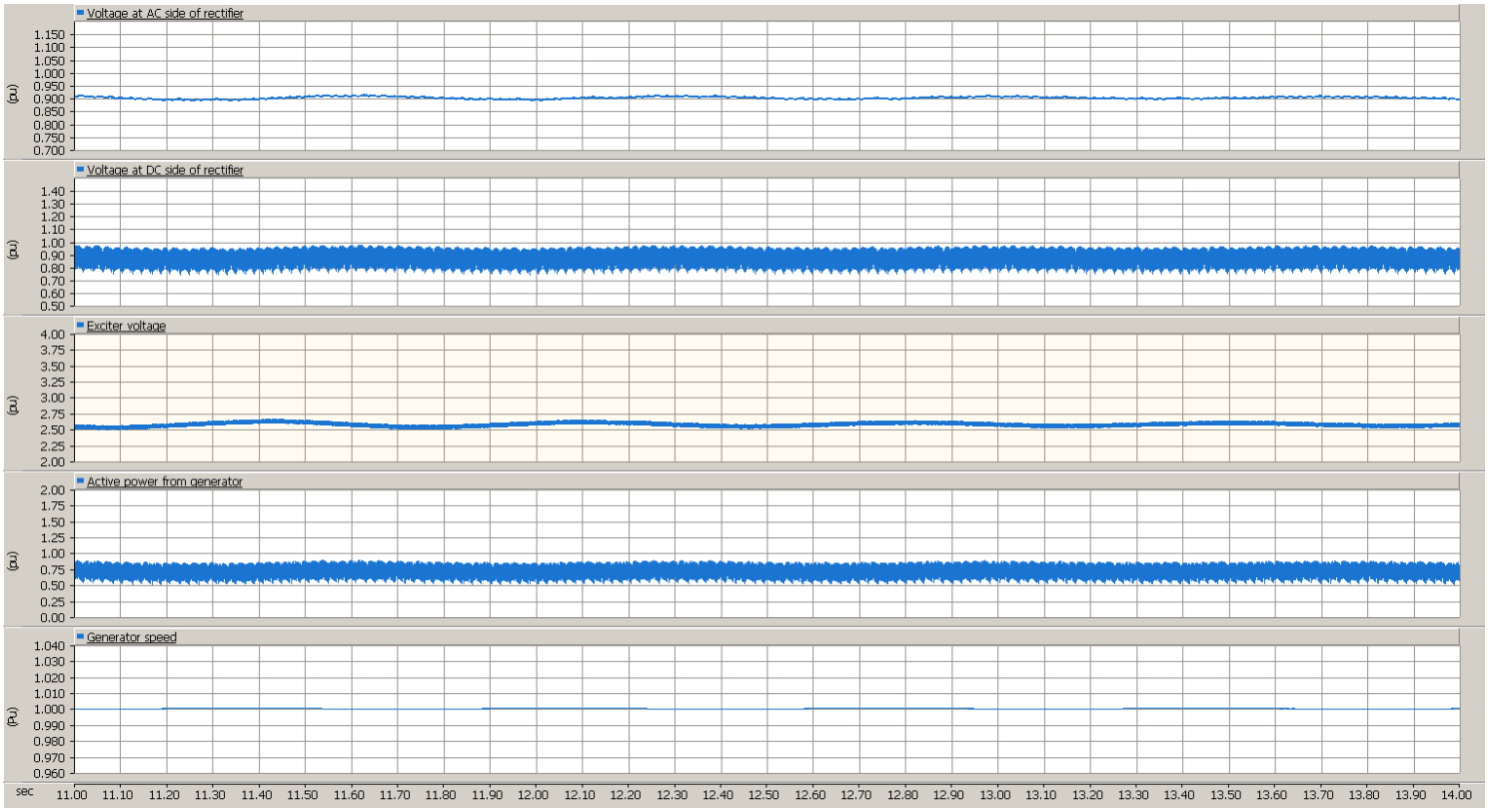

Figure 56: Synchronous generator supplying a load of 1 MW through a rectifier with H = 2 s. Voltage at AC side of rectifier, voltage at DC side of rectifier, exciter voltage, active power from the synchronous generator and the speed of the synchronous generator

12.6 Appendix F

Parameters for the new synchronous generator.

Table 12: New generator parameters

Parameter	**Symbol**	**Value**	**Unit**
Apparent power	Sn	2	MVA
Voltage	Un	0.8	Kv
Frequency	f	65	Hz
Armature resistance	ra	0.0122	pu
Leakage reactance	Xl	0.25	pu
Direct axis synchronous reactance	X_d	3.1	pu
Direct axis transient reactance	X'_d	0.662	pu
Direct axis sub transient reactance	X''_d	0.389	pu
Quadrature axis synchronous reactance	X_q	2.02	pu
Quadrature axis sub synchronous reactance	X''_q	0.377	pu
Direct axis open-circuit transient time constant	T'_{d0}	4.85	s
Direct axis short-circuit sub transient time constant	T''_d	0.0306	s
Quadrature axis short-circuit sub transient time constant	T''_q	0.1715	s

12.7 Appendix G

Powerfactory Model

Governor:

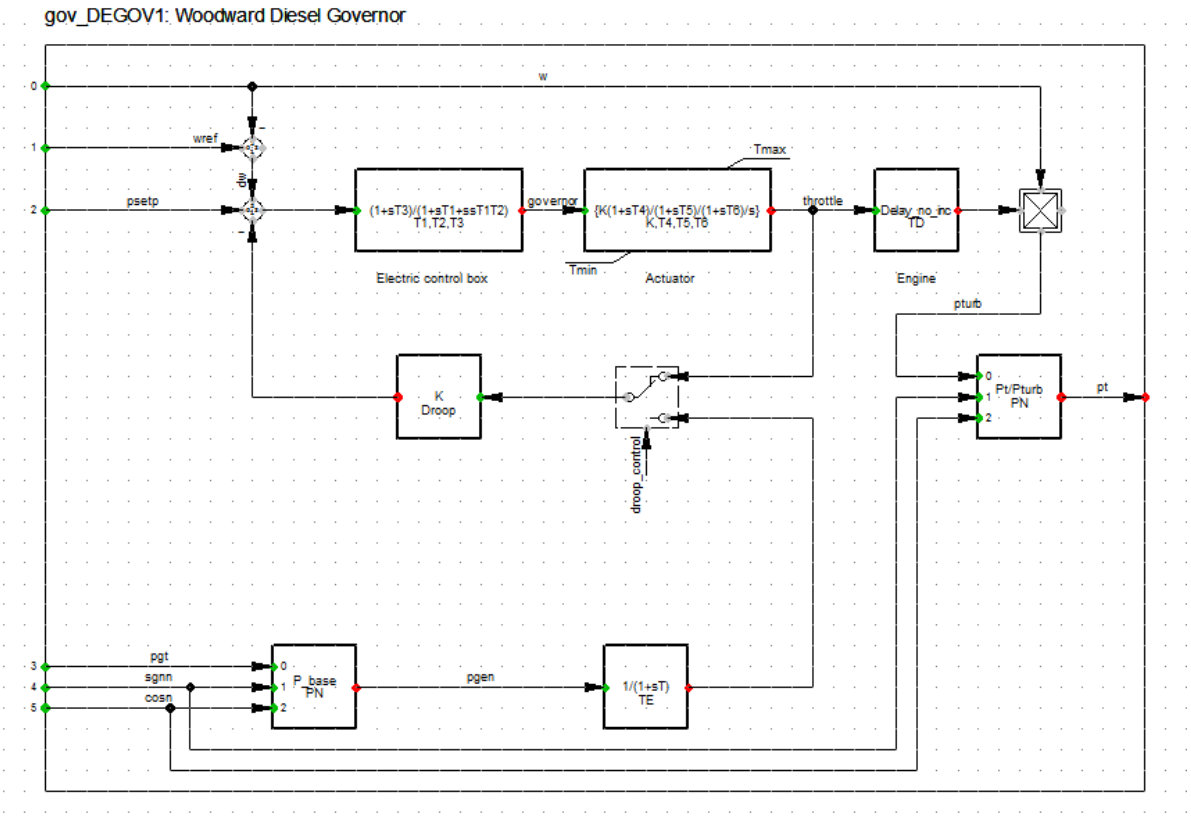

Figure 57: Block diagram for the governor

Table 13: Diesel governor parameters

Name	Value	Unit	Description
K	20	[pu/pu]	Actuator Gain
T4	0,6	[s]	Actuator derivative time constant
T5	0,2	[s]	Actuator first time constant
T6	0,2	[s]	Actuator second time constant
TD	0,01	[s]	Combustion Delay
Droop	0,1	[pu]	
TE	0,1	[s]	Time const. Power fdbk
T1	0,2	[s]	Electric control box first time constant
T2	0,1	[s]	Electric control box second time constant
T3	0,5	[s]	Electric control box derivative time constant
Droop_Contr	0		(0=Throttle fdbk, 1=Elec. Power fdbk)
PN	2	[MW]	Prime Mover Rated Power(=0->PN=Pgnn)
Tmin	0	[pu]	Min. Throttle
Tmax	1,5	[pu]	Max. Throttle

AVR:

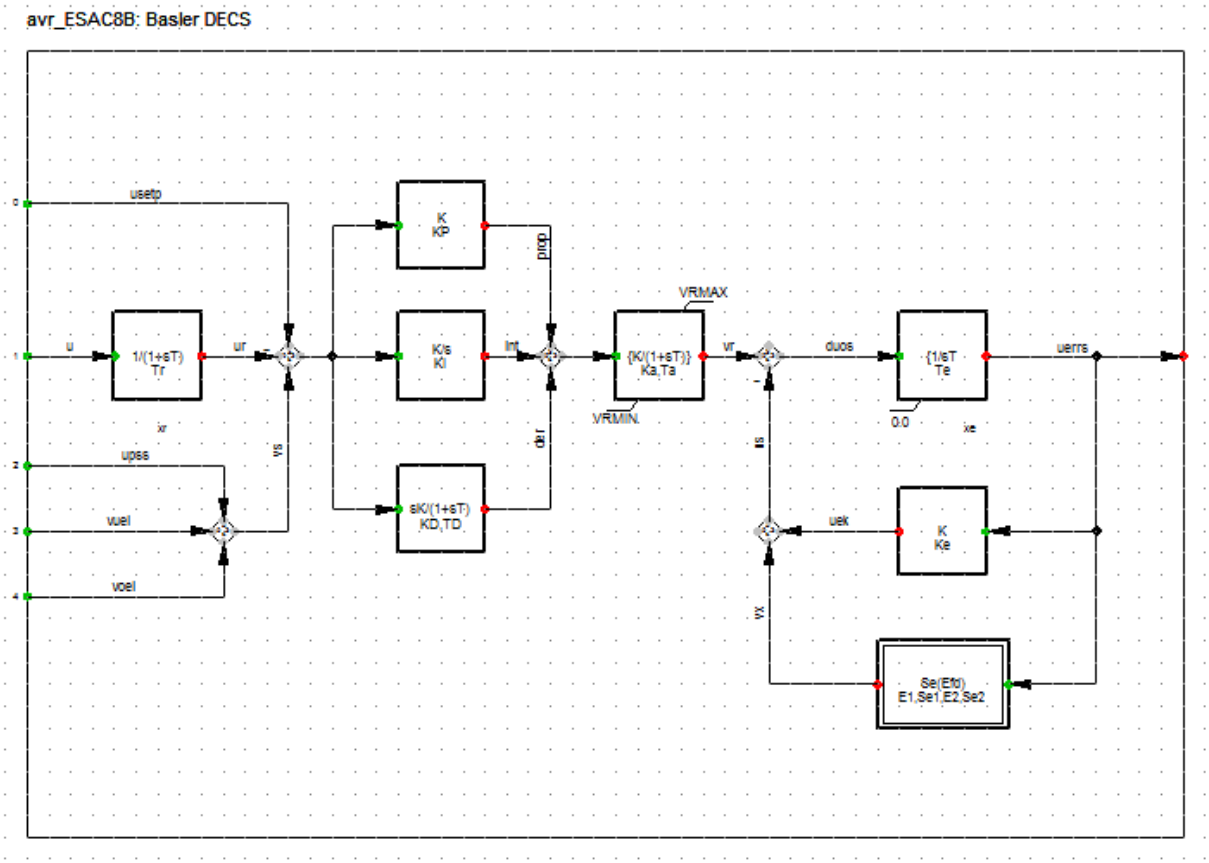

Figure 58: BLock diagram for the PID AVR ESAC8B

Table 14: EASC8B AVR parameters

Name	Value	Unit	Description
Tr	0,01	[s]	Measurement Time const
KP	120	[pu]	Proportional Gain
Ka	40	[pu]	Controller Gain
Ta	0,5	[s]	Controller Time Constant
Ke	0,5	[pu]	Exciter Constant
KI	200	[pu]	Integral Gain
Te	0,5	[s]	Exciter Time Constant
E1	3,9	[pu]	Saturation Factor 1
Se1	0,1	[pu]	Saturation Factor 2
E2	5,2	[pu]	Saturation Factor 3
Se2	0,5	[pu]	Saturation Factor 4
KD	20	[pu]	Derivative Gain
TD	0,01	[s]	Time Const. Derivative Action
VRMIN	0	[pu]	Controller Minimum Output
VRMAX	35	[pu]	Controller Maximum Output

PSS:

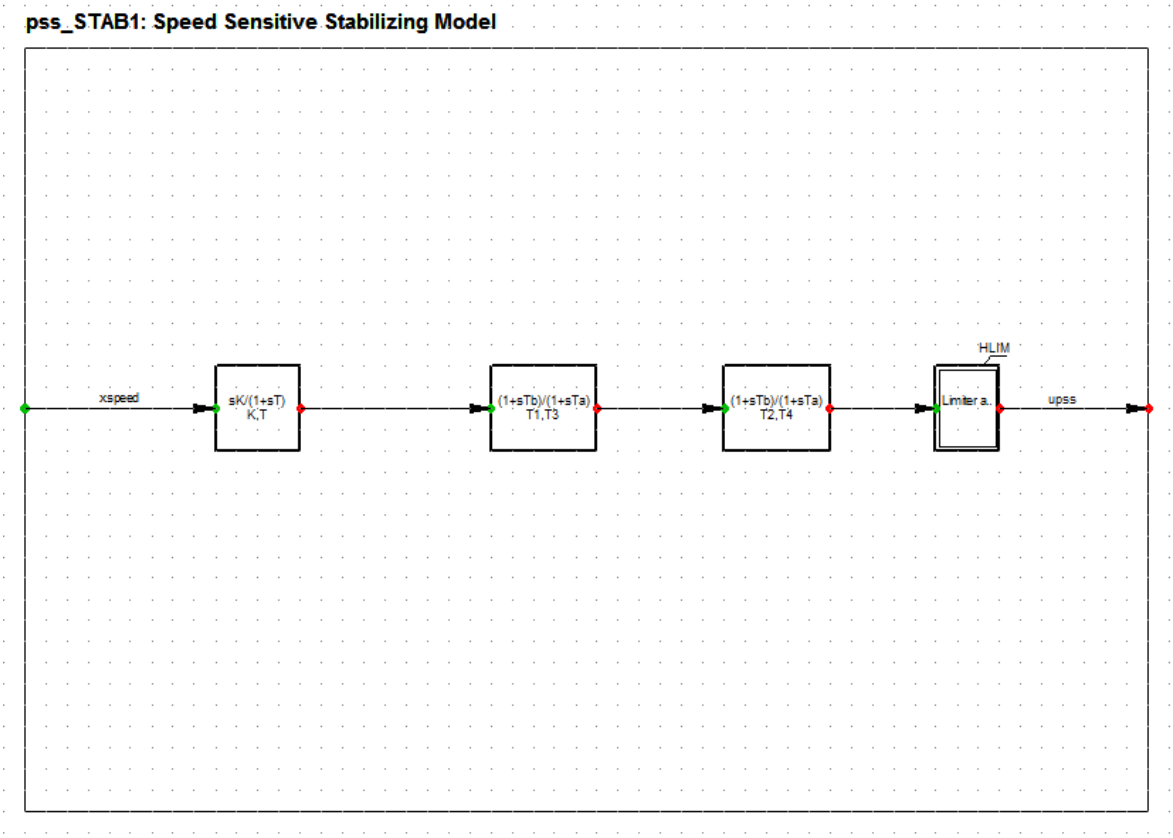

Figure 59: Block diagram for the power system stabilizer

12.8 Appendix H

Initial condition:

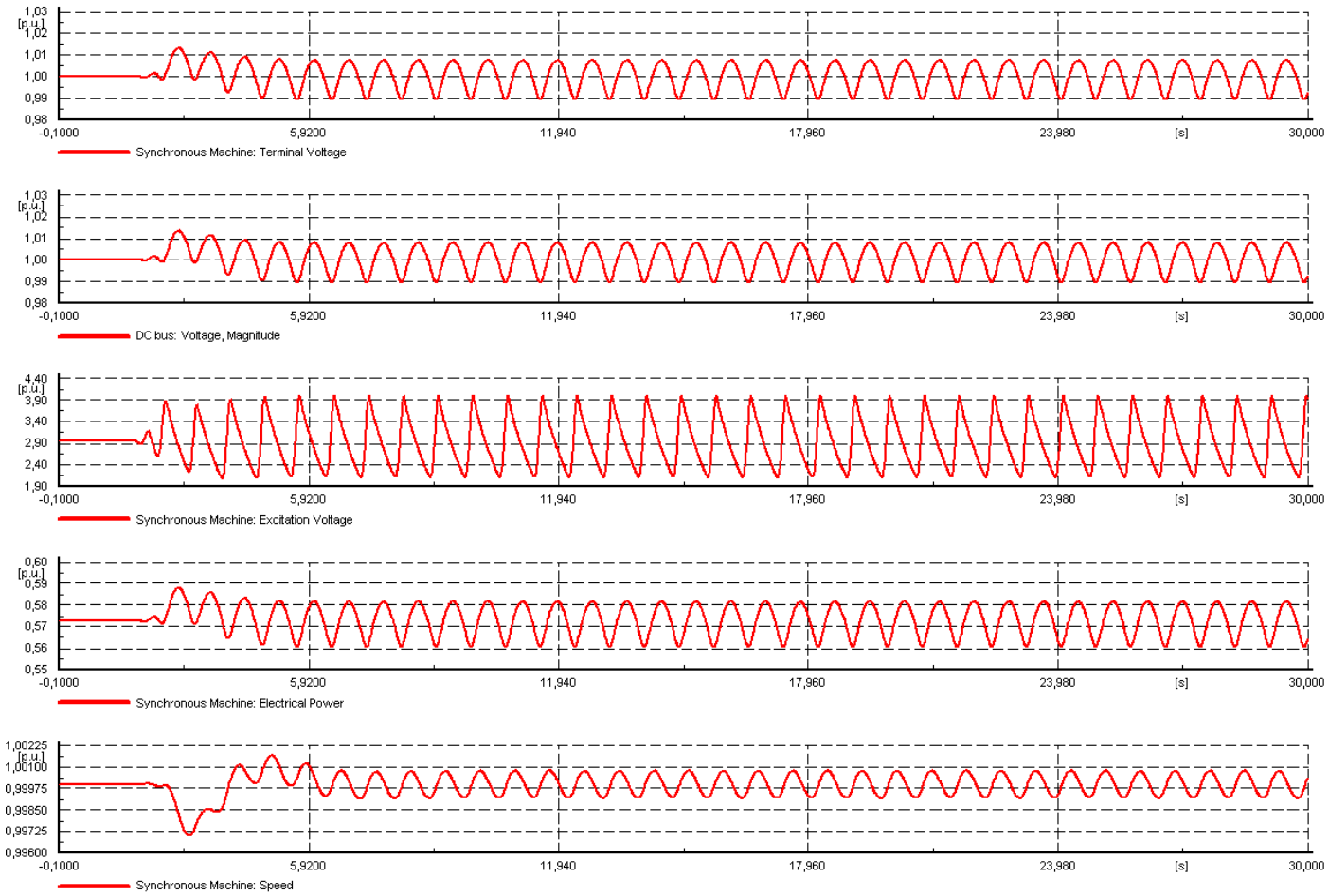

Figure 60: Initial oscillations observed in the Powerfactory model

Table 15: Initial eigenvalues for the instable system

Name	Real part	Imaginary part	Magnitude	Angle	Damped Frequency	Period	Damping
Unit	1/s	rad/s	1/s	deg	Hz	s	1/s
Mode 00001	0	0	0	0	0	0	0
Mode 00002	-153,7511382	0	153,7511382	180	0	0	153,7511382
Mode 00003	-100,6782354	15,05739499	101,7979972	171,4939147	2,396458842	0,417282359	100,6782354
Mode 00004	-100,6782354	-15,05739499	101,7979972	-171,4939147	2,396458842	0,417282359	100,6782354
Mode 00005	6,13521469	16,6221711	17,71827958	69,74098337	2,645500695	0,378000279	-6,13521469
Mode 00006	6,13521469	-16,6221711	17,71827958	-69,74098337	2,645500695	0,378000279	-6,13521469
Mode 00007	-20,1428361	0	20,1428361	180	0	0	20,1428361
Mode 00008	-10	0	10	180	0	0	10
Mode 00009	-3,237979285	6,361390921	7,138053257	116,9763179	1,01244681	0,987706208	3,237979285
Mode 00010	-3,237979285	-6,361390921	7,138053257	-116,9763179	1,01244681	0,987706208	3,237979285
Mode 00011	-3,132446782	0	3,132446782	180	0	0	3,132446782
Mode 00012	-1,484084741	1,633113042	2,206709252	132,2628634	0,259918013	3,847367052	1,484084741
Mode 00013	-1,484084741	-1,633113042	2,206709252	-132,2628634	0,259918013	3,847367052	1,484084741
Mode 00014	-0,391594648	0	0,391594648	180	0	0	0,391594648
Mode 00015	0,306928745	0	0,306928745	0	0	0	-0,306928745
Mode 00016	-10	0	10	180	0	0	10

12.9 Appendix I

AVR test:

Table 16: Eigenvalues for the system with the AVR gain, Kg, equal to 40

Name	Real part	Imaginary part	Magnitude	Angle	Damped Frequency	Period	Damping
Unit	1/s	rad/s	1/s	deg	Hz	s	1/s
Mode 00001	0	0	0	0	0	0	0
Mode 00002	-153,7511382	0	153,7511382	180	0	0	153,7511382
Mode 00003	-100,6782354	15,05739499	101,7979972	171,4939147	2,396458842	0,417282359	100,6782354
Mode 00004	-100,6782354	-15,05739499	101,7979972	-171,4939147	2,396458842	0,417282359	100,6782354
Mode 00005	6,13521469	16,6221711	17,71827958	69,74098337	2,645500695	0,378000279	-6,13521469
Mode 00006	6,13521469	-16,6221711	17,71827958	-69,74098337	2,645500695	0,378000279	-6,13521469
Mode 00007	-20,1428361	0	20,1428361	180	0	0	20,1428361
Mode 00008	-10	0	10	180	0	0	10
Mode 00009	-3,237979285	6,361390921	7,138053257	116,9763179	1,01244681	0,987706208	3,237979285
Mode 00010	-3,237979285	-6,361390921	7,138053257	-116,9763179	1,01244681	0,987706208	3,237979285
Mode 00011	-3,132446782	0	3,132446782	180	0	0	3,132446782
Mode 00012	-1,484084741	1,633113042	2,206709252	132,2628634	0,259918013	3,847367052	1,484084741
Mode 00013	-1,484084741	-1,633113042	2,206709252	-132,2628634	0,259918013	3,847367052	1,484084741
Mode 00014	-0,391594648	0	0,391594648	180	0	0	0,391594648
Mode 00015	0,306928745	0	0,306928745	0	0	0	-0,306928745
Mode 00016	-10	0	10	180	0	0	10

Table 17: Eigenvalues for the system with the AVR gain, Kg, equal to 30

Name	Real part	Imaginary part	Magnitude	Angle	Damped Frequency	Period	Damping
Unit	1/s	rad/s	1/s	deg	Hz	s	1/s
Mode 00001	0	0	0	0	0	0	0
Mode 00002	-153,4855273	0	153,4855273	180	0	0	153,4855273
Mode 00003	-100,5111789	13,11815507	101,3636182	172,5641073	2,087819224	0,478968671	100,5111789
Mode 00004	-100,5111789	-13,11815507	101,3636182	-172,5641073	2,087819224	0,478968671	100,5111789
Mode 00005	5,265005797	14,9744112	15,87303616	70,62831615	2,383251563	0,419594816	-5,265005797
Mode 00006	5,265005797	-14,9744112	15,87303616	-70,62831615	2,383251563	0,419594816	-5,265005797
Mode 00007	-18,9997659	0	18,9997659	180	0	0	18,9997659
Mode 00008	-10	0	10	180	0	0	10
Mode 00009	-3,237979285	6,361390921	7,138053257	116,9763179	1,01244681	0,987706208	3,237979285
Mode 00010	-3,237979285	-6,361390921	7,138053257	-116,9763179	1,01244681	0,987706208	3,237979285
Mode 00011	-3,132446782	0	3,132446782	180	0	0	3,132446782
Mode 00012	-1,485261908	1,633598206	2,207860057	132,2770039	0,259995229	3,846224418	1,485261908
Mode 00013	-1,485261908	-1,633598206	2,207860057	-132,2770039	0,259995229	3,846224418	1,485261908
Mode 00014	-0,391594648	0	0,391594648	180	0	0	0,391594648
Mode 00015	0,306906862	0	0,306906862	0	0	0	-0,306906862
Mode 00016	-10	0	10	180	0	0	10

Table 18: Eigenvalues for the system with the AVR gain, Kg, equal to 20

Name	Real part	Imaginary part	Magnitude	Angle	Damped Frequency	Period	Damping
Unit	1/s	rad/s	1/s	deg	Hz	s	1/s
Mode 00001	0	0	0	0	0	0	0
Mode 00002	-153,2107416	0	153,2107416	180	0	0	153,2107416
Mode 00003	-100,3423656	10,77681299	100,9194234	173,8699066	1,715183057	0,583028147	100,3423656
Mode 00004	-100,3423656	-10,77681299	100,9194234	-173,8699066	1,715183057	0,583028147	100,3423656
Mode 00005	4,203441328	12,90121786	13,56872659	71,95348894	2,053292594	0,48702265	-4,203441328
Mode 00006	4,203441328	-12,90121786	13,56872659	-71,95348894	2,053292594	0,48702265	-4,203441328
Mode 00007	-17,48426774	0	17,48426774	180	0	0	17,48426774
Mode 00008	-10	0	10	180	0	0	10
Mode 00009	-3,237979285	6,361390921	7,138053257	116,9763179	1,01244681	0,987706208	3,237979285
Mode 00010	-3,237979285	-6,361390921	7,138053257	-116,9763179	1,01244681	0,987706208	3,237979285
Mode 00011	-3,132446782	0	3,132446782	180	0	0	3,132446782
Mode 00012	-1,487630887	1,634558698	2,210164653	132,305693	0,260148097	3,843964315	1,487630887
Mode 00013	-1,487630887	-1,634558698	2,210164653	-132,305693	0,260148097	3,843964315	1,487630887
Mode 00014	-0,391594648	0	0,391594648	180	0	0	0,391594648
Mode 00015	0,306863122	0	0,306863122	0	0	0	-0,306863122
Mode 00016	-10	0	10	180	0	0	10

Table 19: Eigenvalues for the system with the AVR gain, Kg, equal to 10

Name	Real part	Imaginary part	Magnitude	Angle	Damped Freque	Period	Damping
Unit	1/s	rad/s	1/s	deg	Hz	s	1/s
Mode 00001	0	0	0	0	0	0	0
Mode 00002	-152,9260062	0	152,9260062	180	0	0	152,9260062
Mode 00003	-100,1719168	7,66855969	100,4650174	175,6223181	1,220489181	0,819343601	100,1719168
Mode 00004	-100,1719168	-7,66855969	100,4650174	-175,6223181	1,220489181	0,819343601	100,1719168
Mode 00005	-15,20757257	0	15,20757257	180	0	0	15,20757257
Mode 00006	2,759566795	9,937650179	10,31368508	74,48066136	1,581626149	0,632260665	-2,759566795
Mode 00007	2,759566795	-9,937650179	10,31368508	-74,48066136	1,581626149	0,632260665	-2,759566795
Mode 00008	-10	0	10	180	0	0	10
Mode 00009	-3,237979285	6,361390921	7,138053257	116,9763179	1,01244681	0,987706208	3,237979285
Mode 00010	-3,237979285	-6,361390921	7,138053257	-116,9763179	1,01244681	0,987706208	3,237979285
Mode 00011	-3,132446782	0	3,132446782	180	0	0	3,132446782
Mode 00012	-1,494854842	1,637357434	2,217099539	132,3950773	0,260593529	3,837393825	1,494854842
Mode 00013	-1,494854842	-1,637357434	2,217099539	-132,3950773	0,260593529	3,837393825	1,494854842
Mode 00014	-0,391594648	0	0,391594648	180	0	0	0,391594648
Mode 00015	0,306732109	0	0,306732109	0	0	0	-0,306732109
Mode 00016	-10	0	10	180	0	0	10

Table 20: Eigenvalues for the system with the AVR gain, Kg, equal to 1

Name	Real part	Imaginary part	Magnitude	Angle	Damped Frequency	Period	Damping
Unit	1/s	rad/s	1/s	deg	Hz	s	1/s
Mode 00001	0	0	0	0	0	0	0
Mode 00002	-152,6605085	0	152,6605085	180	0	0	152,6605085
Mode 00003	-100,0172518	2,439195798	100,0469907	178,6029617	0,388210068	2,575924948	100,0172518
Mode 00004	-100,0172518	-2,439195798	100,0469907	-178,6029617	0,388210068	2,575924948	100,0172518
Mode 00005	-10,62900881	0	10,62900881	180	0	0	10,62900881
Mode 00006	-10	0	10	180	0	0	10
Mode 00007	-3,237979285	6,361390921	7,138053257	116,9763179	1,01244681	0,987706208	3,237979285
Mode 00008	-3,237979285	-6,361390921	7,138053257	-116,9763179	1,01244681	0,987706208	3,237979285
Mode 00009	0,336973976	3,72374399	3,73895985	84,82919834	0,592652263	1,687330097	-0,336973976
Mode 00010	0,336973976	-3,72374399	3,73895985	-84,82919834	0,592652263	1,687330097	-0,336973976
Mode 00011	-3,132446782	0	3,132446782	180	0	0	3,132446782
Mode 00012	-1,647804262	1,652651427	2,333777115	134,9158535	0,263027644	3,801881755	1,647804262
Mode 00013	-1,647804262	-1,652651427	2,333777115	-134,9158535	0,263027644	3,801881755	1,647804262
Mode 00014	-0,391594648	0	0,391594648	180	0	0	0,391594648
Mode 00015	0,304425088	0	0,304425088	0	0	0	-0,304425088
Mode 00016	-10	0	10	180	0	0	10

12.10 Appendix J

Rectifier:

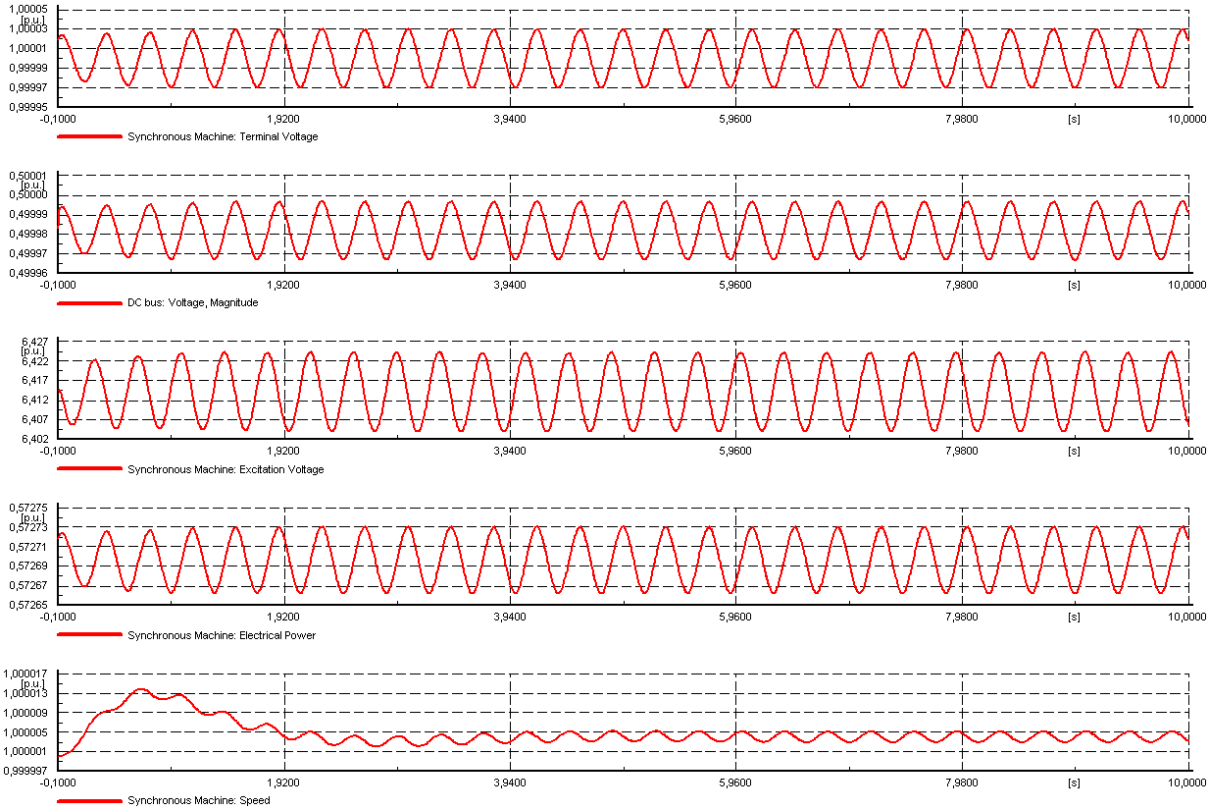

Figure 61: Oscillations with the rectifiers DC voltage reduced to 0.5 p.u.

Table 21: Eigenvalues for the situatuion with the thyristors rectifier voltage equal to 0.5 p.u.

Name	Real part	Imaginary part	Magnitude	Angle	Damped Frequency	Period	Damping
Unit	1/s	rad/s	1/s	deg	Hz	s	1/s
Mode 00001	0	0	0	0	0	0	0
Mode 00002	-165,2159681	0	165,2159681	180	0	0	165,2159681
Mode 00003	-102,2851281	18,97957169	104,0311087	169,4880084	3,020692653	0,3310499	102,2851281
Mode 00004	-102,2851281	-18,97957169	104,0311087	-169,4880084	3,020692653	0,3310499	102,2851281
Mode 00005	-29,71805285	0	29,71805285	180	0	0	29,71805285
Mode 00006	-0,84835409	16,23395481	16,25610634	92,991442	2,583714154	0,387039719	0,84835409
Mode 00007	-0,84835409	-16,23395481	16,25610634	-92,991442	2,583714154	0,387039719	0,84835409
Mode 00008	-10	0	10	180	0	0	10
Mode 00009	-3,237979285	6,361390921	7,138053257	116,9763179	1,01244681	0,987706208	3,237979285
Mode 00010	-3,237979285	-6,361390921	7,138053257	-116,9763179	1,01244681	0,987706208	3,237979285
Mode 00011	-3,132446782	0	3,132446782	180	0	0	3,132446782
Mode 00012	-1,457160623	1,673850542	2,219254991	131,0410066	0,266401588	3,753731382	1,457160623
Mode 00013	-1,457160623	-1,673850542	2,219254991	-131,0410066	0,266401588	3,753731382	1,457160623
Mode 00014	-0,391594648	0	0,391594648	180	0	0	0,391594648
Mode 00015	0,313070216	0	0,313070216	0	0	0	-0,313070216
Mode 00016	-10	0	10	180	0	0	10

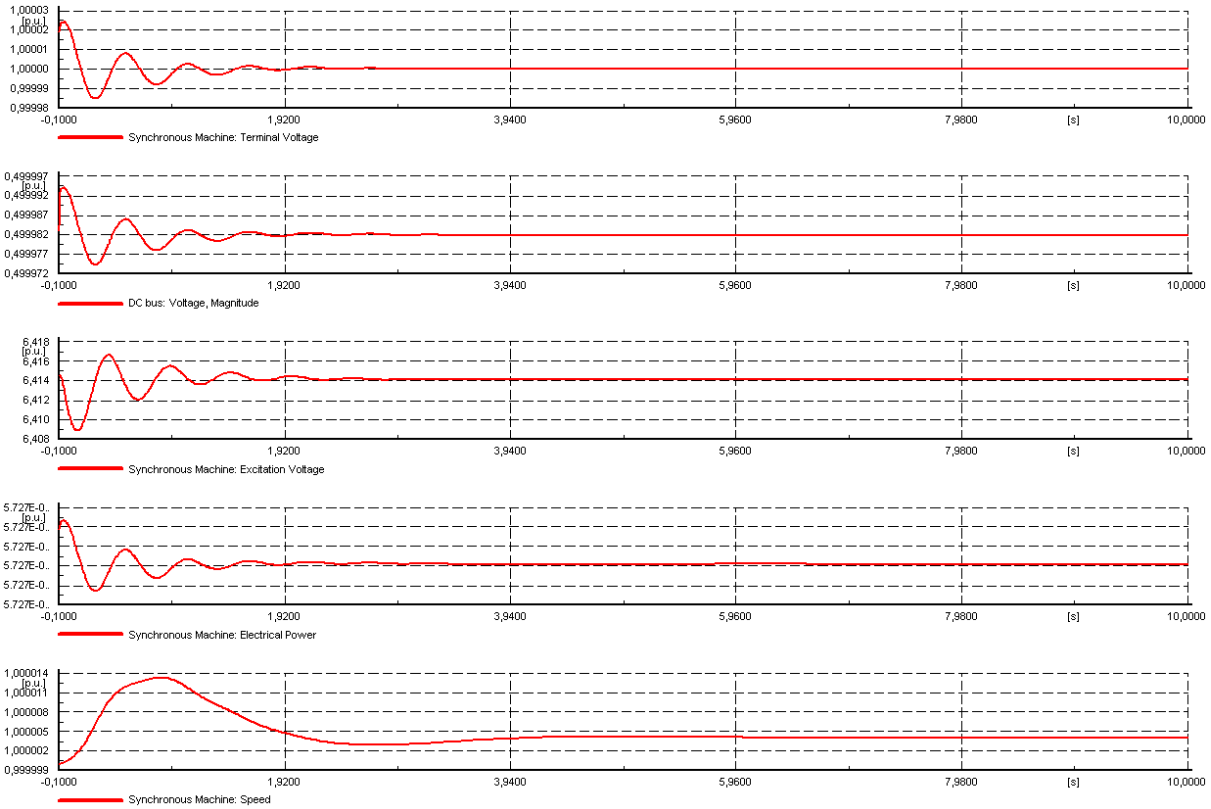

Figure 62: Oscillations with the rectifiers DC voltage reduced to 0.5 p.u. and the AVR gain set to 20

Table 22: Eigenvalues for the situatuion with the thyristors rectifier voltage equal to 0.5 p.u. and the AVR gain set to 20

Name	Real part	Imaginary part	Magnitude	Angle	Damped Frequency	Period	Damping
Unit	1/s	rad/s	1/s	deg	Hz	s	1/s
Mode 00001	0	0	0	0	0	0	0
Mode 00002	-164,7437011	0	164,7437011	180	0	0	164,7437011
Mode 00003	-101,2282771	13,76573687	102,1599706	172,2560168	2,190885068	0,45643654	101,2282771
Mode 00004	-101,2282771	-13,76573687	102,1599706	-172,2560168	2,190885068	0,45643654	101,2282771
Mode 00005	-29,25181564	0	29,25181564	180	0	0	29,25181564
Mode 00006	-2,4031892	11,50423721	11,75256535	101,7991832	1,830956219	0,546162704	2,4031892
Mode 00007	-2,4031892	-11,50423721	11,75256535	-101,7991832	1,830956219	0,546162704	2,4031892
Mode 00008	-10	0	10	180	0	0	10
Mode 00009	-3,237979285	6,361390921	7,138053257	116,9763179	1,01244681	0,987706208	3,237979285
Mode 00010	-3,237979285	-6,361390921	7,138053257	-116,9763179	1,01244681	0,987706208	3,237979285
Mode 00011	-3,132446782	0	3,132446782	180	0	0	3,132446782
Mode 00012	-1,428041211	1,717770729	2,233839291	129,7378993	0,273391703	3,657755485	1,428041211
Mode 00013	-1,428041211	-1,717770729	2,233839291	-129,7378993	0,273391703	3,657755485	1,428041211
Mode 00014	-0,391594648	0	0,391594648	180	0	0	0,391594648
Mode 00015	0,312295474	0	0,312295474	0	0	0	-0,312295474
Mode 00016	-10	0	10	180	0	0	10

12.11 Appendix K

Table 23: Eigenvalues for the system without a PSS added

Name	Real part	Imaginary part	Magnitude	Angle	Damped Frequency	Period	Damping
Unit	1/s	rad/s	1/s	deg	Hz	s	1/s
Mode 00001	0	0	0	0	0	0	0
Mode 00002	-153,7511382	0	153,7511382	180	0	0	153,7511382
Mode 00003	-100,6782354	15,05739499	101,7979972	171,4939147	2,396458842	0,417282359	100,6782354
Mode 00004	-100,6782354	-15,05739499	101,7979972	-171,4939147	2,396458842	0,417282359	100,6782354
Mode 00005	6,13521469	16,6221711	17,71827958	69,74098337	2,645500695	0,378000279	-6,13521469
Mode 00006	6,13521469	-16,6221711	17,71827958	-69,74098337	2,645500695	0,378000279	-6,13521469
Mode 00007	-20,1428361	0	20,1428361	180	0	0	20,1428361
Mode 00008	-8,243084568	0	8,243084568	180	0	0	8,243084568
Mode 00009	-4,029601268	5,604637347	6,902872313	125,7152389	0,892005738	1,121069022	4,029601268
Mode 00010	-4,029601268	-5,604637347	6,902872313	-125,7152389	0,892005738	1,121069022	4,029601268
Mode 00011	-3,516723843	0	3,516723843	180	0	0	3,516723843
Mode 00012	-1,484084741	1,633113042	2,206709252	132,2628634	0,259918013	3,847367052	1,484084741
Mode 00013	-1,484084741	-1,633113042	2,206709252	-132,2628634	0,259918013	3,847367052	1,484084741
Mode 00014	-0,180989053	0	0,180989053	180	0	0	0,180989053
Mode 00015	0,306928745	0	0,306928745	0	0	0	-0,306928745
Mode 00016	-10	0	10	180	0	0	10

Table 24: Eigenvalues for the system with a PSS added

Name	Real part	Imaginary part	Magnitude	Angle	Damped Frequency	Period	Damping
Unit	1/s	rad/s	1/s	deg	Hz	s	1/s
Mode 00001	0	0	0	0	0	0	0
Mode 00002	-1416,430595	0	1416,430595	180	0	0	1416,430595
Mode 00003	-153,7729767	0	153,7729767	180	0	0	153,7729767
Mode 00004	-100,6167647	15,07543857	101,7398751	171,4787446	2,399330567	0,41678292	100,6167647
Mode 00005	-100,6167647	-15,07543857	101,7398751	-171,4787446	2,399330567	0,41678292	100,6167647
Mode 00006	8,227591236	17,08557811	18,96339202	64,28677465	2,719254211	0,367747891	-8,227591236
Mode 00007	8,227591236	-17,08557811	18,96339202	-64,28677465	2,719254211	0,367747891	-8,227591236
Mode 00008	-18,92026048	0	18,92026048	180	0	0	18,92026048
Mode 00009	-4,029601268	5,604637347	6,902872313	125,7152389	0,892005738	1,121069022	4,029601268
Mode 00010	-4,029601268	-5,604637347	6,902872313	-125,7152389	0,892005738	1,121069022	4,029601268
Mode 00011	-8,243084568	0	8,243084568	180	0	0	8,243084568
Mode 00012	-6,253426511	0	6,253426511	180	0	0	6,253426511
Mode 00013	-4,347826087	0	4,347826087	180	0	0	4,347826087
Mode 00014	-3,516723843	0	3,516723843	180	0	0	3,516723843
Mode 00015	-1,481037717	1,630436516	2,202679267	132,2510293	0,259492031	3,853682891	1,481037717
Mode 00016	-1,481037717	-1,630436516	2,202679267	-132,2510293	0,259492031	3,853682891	1,481037717
Mode 00017	-0,180989053	0	0,180989053	180	0	0	0,180989053
Mode 00018	0,04582961	0	0,04582961	0	0	0	-0,04582961
Mode 00019	-10	0	10	180	0	0	10